UNIVERSITÀ DEGLI STUDI DI UDINE
hic sunt futura
www.uniud.it

UNIVERSITY OF UDINE

Ph.D. course in Biomedical Science and Biotechnology

XXX Cycle

The Knock-out of HDAC7 in MCF10A cells negatively impacts on proliferation, stem cells maintenance and neoplastic transformation.

Ph.D. Student:
Valentina Cutano

Tutor:
Professor Claudio Brancolini

Supervisor:
Dott. Eros Di Giorgio, PhD

Accademic Year 2017/2018

ABSTRACT

The mammary gland is a complex tissue which undergoes different morphological changes during women's life. In this thesis, we wanted to clarify the involvement of HDAC7 in the regulation of cell proliferation, stemness and neoplastic transformation that occurs in mammary epithelial cells, using the MCF10A cell line as a model.

Histone deacetylases are important modifiers of the epigenetic status in response to developmental and environmental cues. The subfamily class IIa HDACs comprises four deacetylases (HDAC4, HDAC5, HDAC7 and HDAC9) which are characterized by: poor activity against acetyl-lysine, nuclear-cytoplasmic shuttling and the ability to bind MEF2 transcription factors. In particular, it was demonstrated that HDAC7 is the most expressed member in MCF10A cells, pointing to an important role in the homeostasis of these cells. With the aim to investigate the involvement of HDAC7 in mammary epithelial homeostasis, morphogenesis and proliferation we knocked out HDAC7 in MCF10A cells with the CRISPR/Cas9 system. MCF10A HDAC7$^{-/-}$ cells show an inhibition of cell cycle progression, through p21 up regulation. This data confirms the role of HDAC7 as a repressor of the p21 expression in MCF10A.

Through microarray analysis we described the gene expression profile of MCF10A lacking HDAC7 to reveal the genes directly regulated by the HDAC7 expression.

Moreover, we investigated the HDAC7 involvement in stem cells growth and maintenance by applying the mammosphere assay and FACS analysis. Hence, we propose a double role of HDAC7 in the regulation of stemness. First, an intrinsic role of HDAC7 was verified in stem cells growth, demonstrating the reduced ability of MCF10A-HDAC7$^{-/-}$ cells to form spheres in ultra-low adhesion conditions. This could be explained by a reduced presence of progenitors in a population where HDAC7 is absent. Second, an extrinsic role, was proved by the ability of HDAC7 to release factors important for the stem cells renewal. In fact, conditioned medium by the MCF10A WT cells increases the number of mammospheres, confirming that HDAC7 could play a fundamental role in the regulation of factors released by the mammary stem cell niches.

Finally, we also investigated the contribution of HDAC7 in neoplastic transformation. We obtained MCF10A HDAC7$^{-/-}$ transformed with the RAS oncogene. We discovered that the knock-out of HDAC7 negatively impacts on the RAS transformed phenotype. This observation opens new hypothesis on the cooperation between HDAC7 and oncogenes in promoting proliferation, invasiveness and altered morphogenic processes. Moreover, we described that HDAC7 loss can impact on stemness also in transformed cells. All these findings consolidate a pro-oncogenic role of HDAC7 in mammary epithelial cells, promoting the identification of new therapeutic strategies to target HDAC7 in breast cancer.

Table of contents

ABSTRACT 2
AIM OF THE STUDY 4
1. INTRODUCTION 5
1.1. Histone Deacetylases (HDACs). 5
1.1.1. Class IIa HDACs. 6
1.1.2. MEF2 TFs as class IIa HDACs binding partners. 8
1.1.3. HDAC7. 10
1.1.4. Class IIa HDAC7 in cancer: an oncogene or a tumour-suppressor? 14
1.1.5. Class IIa HDACs in stemness. 16
1.2. Human mammary gland. 17
1.2.1. Breast anatomy. 17
1.2.2. Mammary gland cellular composition 18
1.2.3. Breast cancer. 19
1.3. Stem cells. 22
1.3.1. Mammary stem cells. 22
1.3.2. Breast cancer stem cells. 24
1.4. The stem cells niche. 26
1.4.1. Molecular pathway associated with niche functions. 27
2. MATERIALS AND METHODS 30
3. RESULTS 35
3.1. CRISPR/Cas9 -mediated HDAC7 knockout in MCF10A cells. 35
3.2. Characterisation of the MCF10A HDAC7-/- clones. 37
3.3. HDAC7 WT re-expression in KO rescues the phenotype. 39
3.4. HDAC7 contribution in stemness in MCF10A cells. 41
3.5. Gene expression profiles under HDAC7 influence. 44
3.6. HDAC7 participates in the maintenance of the stem cell niche environment. 52
3.7. HDAC7 loss in MCF10A-HRAS negatively impacts on cell proliferation, migration and acini morphology/invasiveness under 3D culture. 53
4. DISCUSSION 57
5. BIBLIOGRAPHY 63
6. ACKNOWLEDGMENTS 74

AIM OF THE STUDY

This PhD thesis aims to: a) investigate the role of the neglected epigenetic regulator HDAC7 in normal breast development; b) clarify the impact of HDAC7 mutations/amplifications during breast cancer progression. We therefore knocked out HDAC7 in normal mammary epithelial cells MCF10A using the CRISPR/Cas9 technology. The MCF10A HDAC7$^{-/-}$ cells demonstrate the importance of HDAC7 in the cell cycle progression in 2D and 3D cultures. Furthermore, we proposed a role of HDAC7 in stem cell self-renewal indicating that HDAC7 is important for the growth of progenitor stem cells in a cellular population. Moreover, we hypothesized a new role of HDAC7 in stem factors release.

Finally, we supposed a participation of HDAC7 in neoplastic transformation. To investigate this, we transformed MCF10A WT and MCF10A-HDAC7$^{-/-}$ cells with HRAS12V. The obtained data show that HDAC7$^{-/-}$ negatively impact on the RAS transformed phenotype of MCF10A cells. Our results justify the opportunities to consider HDAC7 as a new therapeutic target for the treatment of many breast related pathologies.

1. INTRODUCTION

1.1. Histone Deacetylases (HDACs).

Acetylation is one of the most recurrent post-translational modifications. It regulates several cellular functions including the epigenetic state of the chromatin, from which depends DNA replication, DNA repair, heterochromatin silencing and gene transcription (Drazic et al., 2016). Lysine acetylation is a reversible and tightly regulated histones modification (Martin et al., 2007). The main actors of this epigenetic regulation are the histone acetyltransferases (HATs) and the histone deacetylases (HDACs), which have opposite functions. HDACs are proteins involved in the formation of a compact chromatin structure devoted to transcriptional repression (Delcuve et al., 2012).

In mammals, we can count eighteen HDACs, which are divided into four classes based on their characteristics and sequences homology (Figure 1). The class I, II and IV are Zn^{2+}-dependent proteins instead of the class III groups NAD^{+}- dependent enzymes (Gregoretti et al., 2004).

Class I: HDAC1, 2, 3 and 8.

They show a high degree of sequence similarity with the yeast transcriptional regulator Rpd3. They are ubiquitously expressed and are located in the nucleus (Martin et al., 2007).

Class II: HDAC4, 5, 6, 7, 9 and 10.

They are grouped by their homology with Hda1 (*Saccharomyces cerevisiae*). The expression of these proteins is tissue specific. This class comprise the class IIa formed by HDAC4, 5, 7 and 9 characterised by nucleus-cytoplasm shuttling, which regulates their activity and the class IIb, formed by HDAC6 and 10. The main difference between these two subclasses is that the class IIa HDACs, differently form class IIb lacks of the enzymatic activity (Fischle et al., 2002).

Class III: SIRT1, 2, 3, 4, 5, 6, and 7.

It is a very different class respect to the other HDACs. They are NAD^{+}- dependent proteins and they are homologous to the yeast Sir2. Class III are expressed in different cellular compartments including nucleus, cytoplasm and mitochondria (Haigis and Guatente, 2006).

Class IV: HDAC11

HDAC11 has a sequence similar to the HDACs of classes I and II. In literature, few information about the HDAC11 functions are available. Some data point to a role of HDAC7 in the decision between immune activation and immune tolerance (Gao et al., 2002; Delcuve et al., 2012).

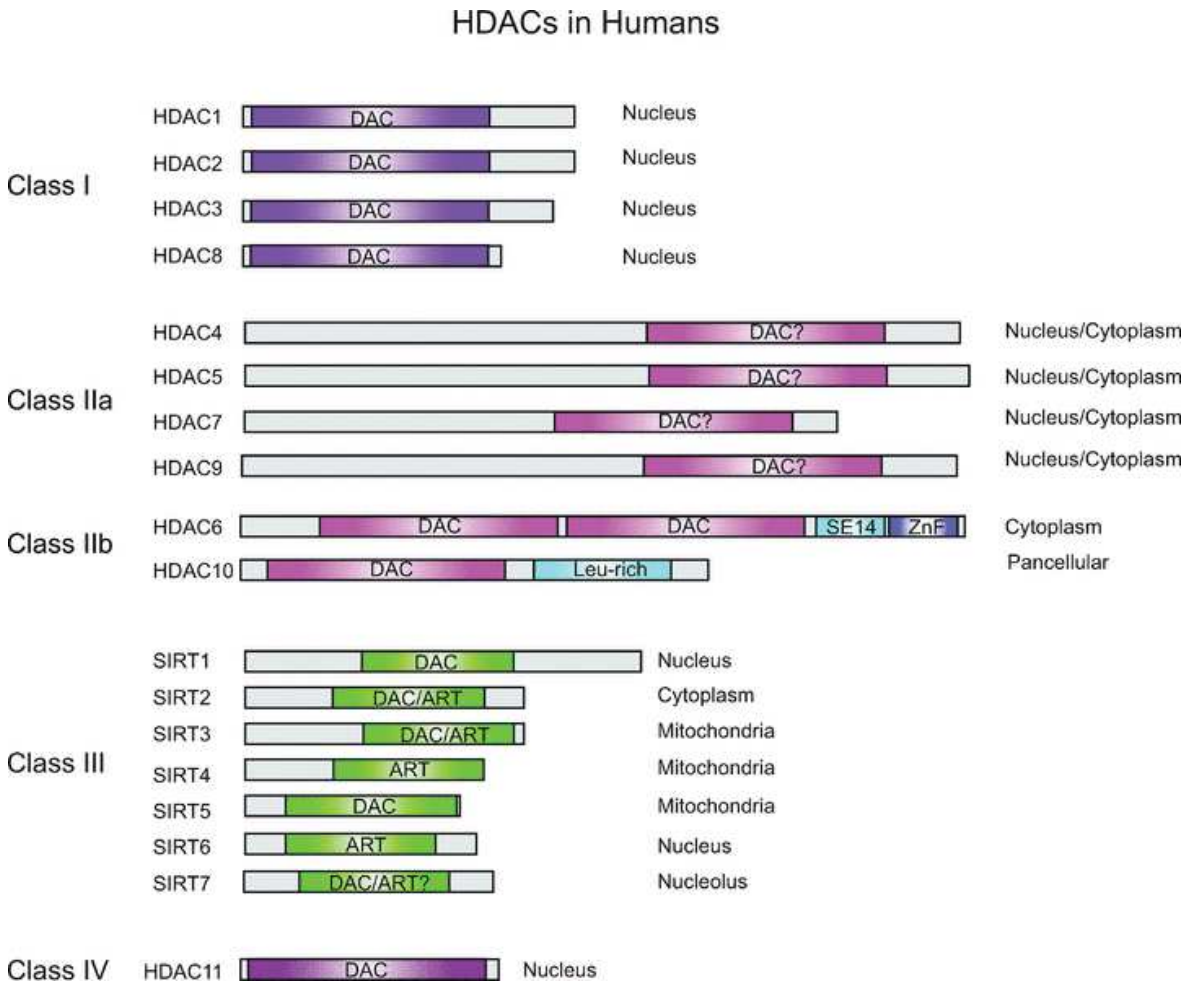

Figure 1: The HDACs world.
Representation of the main characteristics of the 18 HDACs found in mammals and indication of their sub-cellular localization (from Clocchiatti et al, 2011).

1.1.1. Class IIa HDACs.

HDAC 4, 5, 7 and 9 compose the class IIa HDACs subfamily. Since the early 2000s researchers have employed a lot of efforts to understand their biological functions (Parra, 2015). The first discrepancy between class IIa HDACs and class I, is the presence of a long N-terminal domain (absent in class I enzymes) important to regulate HDACs functions (Yang and Gre, 2005). Within the N-terminal domain are located some regions necessary for the interaction with transcription factors. One of the most described interaction, which takes place at the N-terminus of the class IIa involves the binding to MEF2 (Myocyte Enhancer Factor) transcription factors family members (Miska et al., 1999). In fact, all class IIa HDACs contain the MEF2 binding domain.

Class IIa HDACs can shuttle from the nucleus to the cytoplasm, a mechanism important to influence their repressive activity on the chromatin. The translocation from the nucleus to the

cytoplasm is monitored by serine/threonine phosphorylation and involves highly conserved residues present into the N-terminal region (Figure 2). The phosphorylation of these residues allows the interaction with the 14-3-3 proteins. 14-3-3 proteins are the main responsible for class IIa subcellular localisation (Tzivion et al., 2001). Class IIa HDACs shuttle continuously between the nucleus and the cytoplasm. Within the nucleus, they operate as negative regulators of gene transcription. When they are into the cytoplasm their repressive influence is abrogated. This shuttling is supervised by the NLS and NES sequences. In particular, the binding with the 14-3-3 proteins can hide the NLS sequence and can prevent the interaction with the importin-α. This strategy is used by the cells to impede the localisation of class IIa HDACs in the nucleus (Grozinger and Schreiber, 2000). The NES sequence is located close to the C-terminus. After the conformational change that occurs with the 14-3-3 binding, the NES sequence exposition triggers the export of the class IIa HDACs from the nucleus to the cytoplasm (Clocchiatti et al., 2011). Experimental evidences show how mutations of serine residues into alanine can prevent the nuclear export. Mutations of these fundamental residues result in the generation of a super-repressive forms of class IIa HDACs (Clocchiatti et al., 2015; Zhang et al., 2002).

The main regulators of the class IIa HDACs sub-localisation are phosphatases and kinases. Various serine/threonine kinases are involved in the HDACs shuttling. Among them, there are the calcium/calmodulin-dependent protein kinase family (CaMK) and in particular CaMK I and CaMK IV (McKinsey et al., 2000). Other kinases are involved in the class IIa HDACs localisation. These kinases are for example MAPT/tau (MARK1), MARK2 and Serine/threonine-protein kinase D1, AMPK (Hanks, 2003). Indeed, two studies proved that protein kinase D1 (PKD1) phosphorylates HDAC5 and HDAC7 at their 14-3-3 binding sites (Parra et al., 2005).

Phosphorylation is not the only post-translational modification investing class IIa HDACs. HDAC4 and HDAC7 can be subjected to proteolytic cleavage (Paroni et al., 2004), to sumoylation and ubiquitylation (Martin et al., 2007).

The main discovered functions of this class of proteins occur into the nucleus, where they can act on the chromatin. It is important to underline that class IIa HDACs are not able to directly bind the DNA. To interact with nucleic acids, they must bind co-factors and transcription factors (Madjzadeh et al., 2009).

To the N-terminus of the class IIa HDACs is associated the ability to inhibit the transcription factors activity; this attitude is partially due to the presence of the binding site for the co-repressor CtBP (C-terminal binding protein) and a coiled coil region rich in glutamine both absent in HDAC7 (Martin et al., 2007).

Even if they are called histone deacetylases, in vertebrate class IIa HDACs lack of a measurable enzymatic activity. Class IIa HDACs are characterised by the presence of a highly conserved HDAC domain at the C-terminus, however this domain is “inactive” or at least inactive on

acetyl-lysine (Di Giorgio and Brancolini, 2016). The HDAC domain at the C-terminus is important for binding HDAC3. This class I enzyme can provide robust deacetylase activity when in complex with others co-repressor SMRT (Silencing mediator for retinoid and thyroid receptors) and N-CoR (Nuclear-receptor corepressor 1), which are recruited together with HDAC3 by the HDAC domain of class IIa (Fischle et al., 2002). It has been proposed that class IIa HDACs may not be real enzymes but rather, they could act as adaptors for the assembling of super-repressors complexes (Parra, 2015). In the HDAC active site, to permit the enzymatic activity and the substrate binding, a central motif of conserved residues coordinates a Zn ion and is complemented by a second group of highly conserved residues involved in the catalysis. Overall the enzymatic domain of class IIa HDACs is similar to the domain of class I HDACs. As explained above, with Vertebrates class IIa loose the lysine-deacetylase activity. The molecular reason is the substitution of a tyrosine residue that acts as a transition-state stabilizer with a histidine, which is shorter and oriented in a different position, thus compromising the enzymatic activity (Lahm et al., 2007) (Bradner et al., 2010).

Figure 2: Domain organization of classical HDACs from yeast and humans.
In mammals, class IIa HDAC subfamily includes HDAC4, 5, 7, 9, which are related to yeast Hda1. The total number of amino acid residues in each deacetylase is shown on the right. Additional isoforms of the deacetylases can arise from alternative splicing; for simplicity, the number of amino acids refers to the longest isoform. The homologies of the deacetylase domain with Hda1 (identity/similarity: 26/57%) are shown. Myocyte enhancer factor-2 (MEF2)-binding motifs are depicted as short green cylinders, whereas 14-3-3 binding motifs are shown as short blue cylinders labelled with 'S' (for Ser) (from Yang and Seto, 2008).

1.1.2. MEF2 TFs as class IIa HDACs binding partners.

Class IIa HDACs reveal their repressive influence on transcription when they reside into the nucleus. Class IIa HDACs binding partners, as reported by the literature, include different transcription factors (Martin et al., 2007). In this chapter, we will focus the attention on the members of the MEF2 family.

MEF2s are the best characterised partners and this interaction has been studied since 1999 (Wang et al., 1999). MEF2 proteins are conserved among species. A single MEF2 protein is present in *Drosophila melanogaster* and *Caenorhabditis elegans*. Instead four members:

MEF2-A, -B, -C and –D are present in vertebrates (Miska et al., 1999). The MEF2 factors share high homology within the amino-terminal MADS-box and MEF2 domains. MEF2 is a 29 amino acids (AA) motif exclusive of the MEF2 factors. These domains are responsible for homo- and hetero-dimerization of MEF2 proteins and the interactions with transcriptional co-factors and co-regulators, including repressors. Furthermore, the MADS-box/MEF2 domain permit the binding to the conserved A-T rich DNA consensus sequences (YTA(A/T)4TAR) to elicit transcriptional activity on gene promoters and enhancers (Black and Olson, 1998; McKinsey et al., 2002). If the N-terminal domain is well conserved among the MEF2 members, the carboxyl-terminal regions are highly divergent. The C-terminal is represented by the transcription activation domains (TADs) and by the NLS sequence. Moreover this region is susceptible to splicing events (Potthoff and Olson, 2007;Lu et al., 2000).

It is well known that through an autoregulatory loop, MEF2 family members can maintain their own expression (Ramakrishnan et al., 2002; Cripps et al., 2004).

Initially discovered as key regulators of muscle differentiation, Myocyte enhancer factor-2 family members promote the expression of target genes involved in different biological functions. It is important to mention that their function is not just related to muscle tissue. For example, MEF2C is important also for neural differentiation,as confirmed by the generation of specific *Mef2C* KO mice, which evidenced less mature neurons (Li et al., 2008). MEF2s are also involved in the hematopoietic cells differentiation and MEF2A, C, and D regulate apoptosis and EMT processes (Canté-Barrett et al., 2013; Pon and Marra, 2016; Zhuang et al., 2013). The importance of these proteins is proved by the generation of KO mice. *Mef2A* and *Mef2C* null mice exhibited respectively, neonatal death, because of lethal cardiac arrhythmias (80% of newborns) and embryonic lethality at E10.5, due to cardiovascular defects (Lin et al., 1997; Canté-Barrett et al., 2013; Pon and Marra, 2016; Zhuang et al., 2013). Curiously, *Mef2B* or *Mef2D* KO mice survive and do not present abnormalities. An absence of overt phenotype that can be justified with the compensation phenomenon from others MEF2 members (Pon and Marra, 2016).

There are evidences that MEF2s regulate cell cycle progression by activating the transcription of *CDKN1A*. The CDK inhibitor p21 (*CDKN1A*) is a well-known negative regulator of cell cycle progression, under the control of multiple signals (Besson et al., 2008; Karimian et al., 2016). It was demonstrated that MEF2D down-regulation was coupled with the reduction of CDKN1A levels, an increase in DNA synthesis and augmented cell proliferation. mRNA levels of MEF2 target genes and of CDKN1A were reduced in cells with impaired MEF2D expression (Di Giorgio et al., 2015). In particular, ChIP experiments demonstrated that MEF2D binds the CDKN1A promoter at +2.1 and +1.5 kb from the TSS (Clocchiatti et al., 2015).

1.1.3. HDAC7.

Identification of histone deacetylase 7 (HDAC7) dates back to 2000 (Kao et al., 2000). The carboxy-terminal of the HDAC7 shows high homology with the other class IIa HDACs and the N-terminus show similarities with HDAC4, 5 and hMITR. It can bind and repress MEF2 transcription, however it lacks the Glu rich domain, presents in HDAC4/5/9. The longest HDAC7 isoform contains 952 residues and it is encoded by *HDAC7* gene, located into the chromosome 12q13.1 minus strand. The *HDAC7* promoter has the minimal PDGF-BB-responsive element, which contains one binding site for the transcription factor Sp1. Mutation of the Sp1 binding site abolished PDGF-BB-induced HDAC7 activity (Zhang et al., 2010). In *silico* predictions confirmed byEncode data suggest that HDAC7 expression could be regulated by some proto-oncogenes acting as transcription factors on the *HDAC7* promoter. Among these proto-oncogenes JUN, FOS and MYC can be found (Di Giorgio and Brancolini, 2016).

Regulation of HDAC7 activity

Like others class IIa HDACs, HDAC7 can shuttle in and out from the nucleus by the 14-3-3 binding. Unlike to HDAC4, 5 and 9, HDAC7 has four serine residues (positions 155, 181, 321, 446) that through phosphorylation, allow the binding with 14-3-3 proteins (Grozinger and Schreiber, 2000;Dequiedt et al., 2005). As a consequence the HDAC7 quadruple mutant, in which the four serine residues are replaced by alanine residues (S155A, S181A, S321A, S446A), is not efficiently exported from the nucleus to the cytoplasm, confirming the importance of these serines into the nucleo-cytoplasm shuttling (Clocchiatti et al., 2015; Dequiedt et al., 2003).

Different kinases are responsible for these phosphorylations. An example is represented the PKD1 that acts on HDAC7, mediating the repression of Nur77 expression (Dequiedt et al., 2005). Moreover, HDAC7 phosphorylation by PKD1 is supervised by VEGF concentration, thus linking HDAC7 activities to RTK signalling (Chang et al., 2008).

Additional 14-3-3 binding sites or phosphorylation-independent mechanisms that mediate the export of HDAC7 could exist as the cytoplasmic accumulation of HDAC7 phospho-mutants is some circumstances is reported(Gao et al., 2006).

On the contrary phosphatases are involved in the nuclear accumulation of HDAC7. One of them is PP2A that directly dephosphorylates the 14-3-3 binding sites in HDAC7, thus preventing the association of 14-3-3 proteins (Martin et al., 2008).

In thymocytes, where HDAC7 is highly expressed, the myosin phosphatase complex (PP1β and MYPT1) dephosphorylates HDAC7 and permits its translocation into the nucleus. This regulation is mandatory for the inhibition of the apoptosis in $CD4^+/CD8^+$ cells (Parra et al., 2007). Also the Rho-Kinase (ROCK) is involved in this pathway. In fact, ROCK acts through phosphorylation of the Myosin Phosphatase, specifically targeting subunit 1 (MYPT1). ROCK

activity leads to the inhibition of the myosin light chain phosphatase (MLCP). As we already mentioned, MYPT1 and the catalytic subunit of MLCP (PP1β) interact specifically with HDAC7 dephosphorylating it. Hence, ROCK, thought re-localising HDAC7, induces the down-regulation of NR4A1 expression, a member of the nuclear orphan receptors. The final output is the promotion of the T cell tolerance by the induction of apoptosis in thymocytes (Kasler et al., 2011). Compagnucci et al., demonstrated that phosphorylation levels of MYPT1 increase in parallel with ROCK activity. Hence, as a consequence, HDAC7 phosphorylation also increases. Moreover, they demonstrated that low levels of ROCK activity correspond to an increase in the MYPT1/MLCP-dependent de-phosphorylation of HDAC7, thus promoting its nuclear export (Compagnucci et al., 2015).

Until now, two different splicing variants of HDAC7 have been characterised. The most common spliced isoform is made up of 25 exons (HDAC7s), whereas the second one is an isoform that conserves the first intron after the first ATG (HDAC7u) (Di Giorgio and Brancolini, 2016). A manuscript reported that this splicing event is fundamental in smooth muscle cells (SMC) proliferation both in mice and humans. HDAC7 is normally maintained as an unspliced isoform in the cytoplasm, where it binds β-catenin to mantain SMCs in a quiescent state. PDGF (Platelet-derived growth factor) stimulation triggers HDAC7 splicing, which allows β-catenin release. In this way β-catenin translocates into the nucleus and binds TCF transcription factors to activate the expression of genes required for entry the S phase of the cell cycle (Zhou et al., 2011).

miRNAs also play a relevant role in the regulation of the HDACs activities. In particular, two miRNAs are able to target HDAC7: miR140-5p and miR34.

Over-expression of miR140-5p reduces HDAC7 expression and the expression of others target genes in Cal27 cells (human tongue squamous carcinoma cell line). This regulation causes a reduction in cell migration (Kai et al., 2014). In breast cancer, miR34 has key roles favouring cell-survival and therapy resistance. Among genes regulated by this miRNA there are HDAC1 and HDAC7 (Wu et al., 2014).

Finally, HDAC7 is also subjected to proteolytic cleavage. For example, HDAC7 undergoes proteolysis during caspase-8 mediated apoptosis. In CD4/CD8 positive thymocytes HDAC7 is cleaved by caspase-8. This processing influences HDAC7 subcellular localisation and consents the establishing of the Nur77-dependent gene expression response (Scott et al., 2008).

HDAC7 tissue specific expression

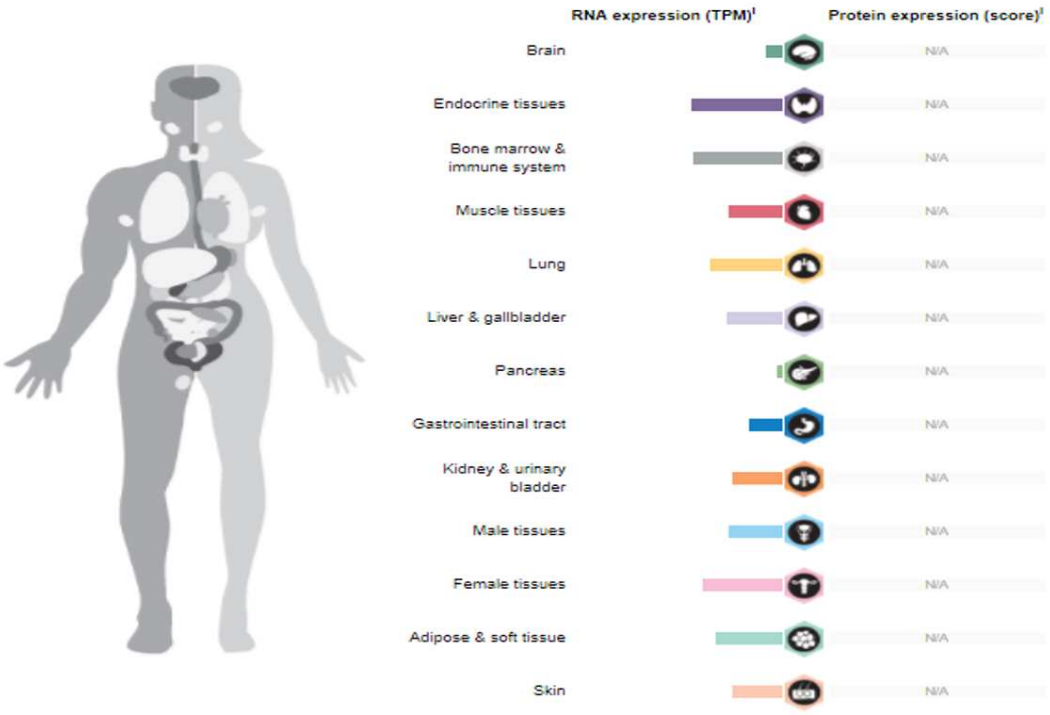

Figure 2: HDAC7 expression in Human tissues.

The image represents the expression of HDAC7 in human tissue. It is possible to appreciate the high levels of HDAC7 in the endocrine tissues and in the immune system (from proteinatlas.org)

As the other class IIa HDACs, HDAC7 shows a heterogeneous tissue expression (Figure 2). HDAC7 is highly expressed in heart, thymus, lung, $CD4^+/CD8^+$ thymocytes and in vascular endothelium (Clocchiatti et al., 2011). Importantly, HDAC7 is more abundant in human thymus compared to HDAC4 and HDAC5. Interestingly, HDAC7 expression is modulated during thymocytes maturation. In primary human thymocytes, sorted by flow cytometry based on the differentiation markers CD3, CD4 and CD8, HDAC7 is abundant. On the other hand, low levels of HDAC7 mRNA were observed in immature triple-negative thymocytes (TN, $CD3^-CD4^-CD8^-$). HDAC7 expression was highly and transiently increased during the CD4+CD8+ DP stage and returned to lower levels in mature Single Positive T cells (SP4 or SP8). Regulation of HDAC7 expression is important to modulate MEF2D transcription, which is able to induce Nur77 expression and thus triggering apoptosis. For this reason, during the maturation of Double Positive T cells, signals emanating from the TCR lead to the displacement of HDAC7 from MEF2 and its re-localization into the cytoplasm. The displacement of HDAC7 from the Nur77 promoter and other promoters, regulated in a similar manner, leads to the MEF2-dependent activation of Nur77 and apoptosis (Verdin et al., 2004). HDAC7 has a role also in the

development of B cells. In B cells progenitors HDAC7 interacts with MEF2C and represses a set of genes involved in the establishment of the B cells identity and development (Azagra et al., 2016).

The embryonic lethality of *HDAC7* null-mice arises from defects in the adhesion of endothelial cells. This deficit causes a defective angiogenesis and impairs vessels integrity. Indeed, HDAC7 mutant embryos show an increasing expression of the MMP10 in the vascular endothelium, and a consequent down regulation of the tissue inhibitor of metalloproteinase 1 (TIMP1). This observation confirms that HDAC7 inhibits MMP10 transcription through the association with MEF2C, an activator of MMP10 expression (Chang et al., 2006).

VEGF plays a pivotal effect in angiogenesis by regulating the proliferation, migration, and survival of endothelial cells. As we already mentioned, VEGF can control HDAC7 phosphorylation via PKD. It was demonstrated that HDAC7 regulates VEGF-Induced expression of RCAN2 and Nur77 genes, which are implicated in angiogenesis (Wang et al., 2008). Furthermore, HDAC7 can sustain cell motility and angiogenesis, by regulating *PDGF-B/PDGFR*-β genes expression (Mottet et al., 2007).

A single manuscript reported that in different cell lines and in particular in prostate cancer cell lines, HDAC7 is sequestered into the mitochondria where it is processed at the N-terminal domain. After the "mitochondrial cleavage" the resulting HDAC7 is a protein of 80 KDa that is located within the inner membrane space and released into the cytoplasm after pro-apoptotic signals (Bakin and Jung, 2004).

A negative impact of HDAC7 was proposed for cartilage formation and regeneration. A study reported that HDAC7 binds β-catenin in proliferating chondrocytes inhibiting its function. During chondrocytes maturation, HDAC7 is degraded by the ubiquitin-proteasome system into the cytoplasm. HDAC7 degradation increases β-catenin activity and enhances post-natal chondrocyte proliferation (Bradley et al., 2015).

Not only in chondrocytes but also in osteoblasts HDAC7 is important for maturation. Jensen and co-authors described, by applying a RNAi approach, a repressive activity of HDAC7 on RUNX2 until the moment when osteoblasts undergo maturation. During the osteoblast differentiation process, BMP2 acts as a signal to trigger the osteoblast maturation. BMP2 transiently impacts on HDAC7 nuclear localization and permits to switch-on RUNX2-dependent gene expression (Jensen et al., 2008).

Finally, class IIa HDACs are historically known to negatively regulate myogenesis by inhibiting MEF2. When HDAC7 translocates into the cytoplasm, muscle differentiation starts through MEF2 activation (Dressel et al., 2001)(Lu et al., 2000).

HDAC7 in breast

In our laboratory, we are investigating the importance of HDAC7 in breast tissue. The morphogenetic processes that control the mammary gland development is very complex and not completely defined. To study the influence of the MEF2-HDACs axis on mammary epithelial morphogenesis and maintenance, we initially compared expressed sequence tag (EST) profiles for class IIa HDACs, MEF2A, MEF2C and MEF2D within different tissues. We discovered that in breast tissue, MEF2A, MEF2D and HDAC7 are the most expressed proteins (Clocchiatti et al., 2015).

Gene Set Enrichment Analysis (GSEA), using a signature of putative MEF2-target genes, suggested that MEF2-dependent transcription was positively modulated during MCF10A acinar morphogenesis. With the consciousness that expression of HDAC7 in this cell line could be related to some mechanism of mammary gland development, we decided to investigate the HDAC7 role in breast using the MCF10A cell line as experimental model. Experimental evidences demonstrated that HDAC7 changed its expression during acini formation. At day 4, HDAC7 is abundantly expressed but at the day sixteen its expression is reduced by post-transcriptional mechanisms. This phenomenon seems to be independent from proteasome-mediated degradation or lysosome- and autophagy-mediated degradation (Clocchiatti et al, 2015).

During the acinar morphogenesis, the regulation of the cell cycle exit is very important. Class IIa HDACs are involved in the regulation of transcription of CDKN1A (p21), a negative regulator of the cell cycle progression (Wilson et al., 2008). With ChIP experiments, we explained that HDAC7 binds the p21 promoter preferentially to the region containing the MEF2-binding site at +1.5 kb from the transcription start site (TSS).

We generated MCF10A cells expressing a conditionally super-repressive form of HDAC7 (HDAC7/SA-ER), fused to the ligand binding domain of the oestrogen receptor (Dequiedt et al., 2003). Upon treatment with 4-OHT, this chimera accumulates into the nucleus and represses MEF2-dependent transcription. When grown in 3D conditions MCF10A expressing HDAC7/SA-ER formed acini bigger than the control at all time points analysed. The increasing in size depends on an increase in the number of nuclei per acinus. These data indicate that HDAC7 can stimulate epithelial cell proliferation (Clocchiatti et al., 2015).

1.1.4. Class IIa HDAC7 in cancer: an oncogene or a tumour-suppressor?

To date, the role of HDAC7 in the neoplastic transformation is controversial. There are evidences claiming for a tumour suppressive role and others that demonstrate an oncogenic activity for HDAC7.

We already discussed about the importance of HDAC7 in endothelial cells (EC) and the relation between HDAC7 and β-catenin. Margariti et al., in 2010, demonstrated that the knockdown of HDAC7 promotes the endothelial cells proliferation causing hypertrophy (Margariti et al., 2010).

Recent results in Pro-B acute lymphoblastic leukaemia (pro-B-ALL) and Burkitt lymphoma, evidenced a down-regulation of HDAC7 in these two cancer types. In addition, an inducible expression of HDAC7 in lymphoma and leukaemia cell lines reduced their viability (Barneda-Zahonero et al., 2015). Although the anti-proliferative contribution of HDAC7 in this study is unclear, taking together these data shed light on new highly specific therapies for the treatment of pro-B-ALL and B-cell lymphoma (Barneda-Zahonero et al., 2015).

Despite these results, the idea that class IIa HDACs are aberrantly overexpressed in cancer, is still prevalent. A genomic screening conducted on 154 glioma patients, demonstrated a strong positive correlation between STAT3 down-regulation and HDAC7 expression, strictly related to a poor clinical outcome. In glioma, it has been demonstrated that HDAC7 has a strong role in angiogenic pathways activation. In fact, STAT3 can induce anti-angiogenic genes when HDAC7 is not present. Considering that glioblastoma cells are addicted to angiogenesis, a down-regulation of HDAC7 should inhibit the uptake of oxygen and nutrients, required for the cancer growth. Unfortunately, to date, no specific inhibitors does exist for HDAC7, making its targeting extremely difficult in glioblastoma (Peixoto et al., 2016).

The crucial role of HDAC7 in cancer proliferation was also confirmed in HeLa cells. In this cell line, HDAC7 activates the c-Myc transcription. When HDAC7 in knocked down, there is a support of the expression of some regulators of the cell cycle such as p21 and p27. ChIP assay was carried out to better understand the histone acetylation of *c-Myc* gene. As expected the HDAC7 silencing promotes a strong decrease of histone H3/H4 acetylation compared with the control (Zhu et al., 2011).

In pancreatic adenocarcinoma (PA), HDAC7 has a crucial role in proliferation. It has been demonstrated by a screening on PA patients, that HDAC7 is overexpressed and its expression is linked to a poor clinical outcome (Ouaïssi et al., 2014).

Furthermore, the oncogenic activity of HDAC7 was also revealed in breast cancer. There are evidences that HDAC7 is highly expressed in the triple negative breast cancer cells, with a peak in the BRCA1-mutated HCC1937 cells (Clocchiatti et al., 2013) . In oestrogen receptor (ER)-positive tumours cells, the HDACs-MEF2 axis is compromised by on over expression of class IIa HDACs causing a strong repression of putative MEF2-target genes (Clocchiatti et al., 2015).

All these evidences could be explained with a dual role of HDAC7, related to a specific tissue/lineage context. Understanding these specificities will help researchers to better define the influence of HDAC7 in tumour progression.

1.1.5. Class IIa HDACs in stemness.

In literature, evidences suggest that class IIa HDACs could be involved in different stem pathways. It is well demonstrated that the activation of the epithelial/mesenchymal transition (EMT), in non-transformed epithelial cells, promotes stemness (Fabregat et al., 2016).

Not surprisingly epigenetic changes are critical for the EMT and it is possible to impede the EMT plasticity using the HDACs inhibitors. In 2015, Ruscetti published that the treatment with the histone deacetylase inhibitor LBH589 inhibit EMT plasticity and stemness activities in prostatic cancer cells (Ruscetti et al., 2015, 2016).

It is also true that the available information about the involvement of HDACs in stemness is still not well defined and controversial. As a matter of fact, in 2010 it was published that OCT3/4, a crucial transcription factors in stem cells re-programming, binds the first intron of *HDAC4* gene, interfering with splicing maturation. This interaction down-regulates HDAC4 transcription in embryonic stem cells (Addis et al., 2010).

On the contrary, it was demonstrated that, in glioblastoma (GLB), HDAC4 could have a crucial role in regulating stem potential. Importantly, the presence of GLB cancer stem cells can induce radio-resistance in patients treated with radiotherapy. Researchers investigated the ability of GLB stem-like cells (GSLC) and adherent not stem-like cells, to form CD133-and Nestin-positive neurospheres after HDAC4 or HDAC6 silencing. They confirmed that HDAC4 or HDAC6 knockdown counteracts the ability to generate neurospheres. Moreover, in GSLCs obtained from neurospheres, the levels of nuclear HDAC4 and HDAC6 proteins were augmented. These results suggest that HDAC4 and 6 could be involved in stem pathways within these cells (Marampon et al., 2017).

Recent discoveries demonstrated an important role of HDAC7 in stem regulation in breast and ovarian tissue. A correlation between high HDAC7 protein expression and CSC markers in breast and ovarian cancer cell lines was observed. To better understand the role of HDAC7 in maintaining cancer stem phenotype, the authors knocked-down the expression of HDAC7. The resulting data proved that HDAC7 depletion decreases CSC markers expression and inhibits mammospheres formation. These data were confirmed by HDAC7 over-expression in which an up regulation of CSC markers was evident. These findings indicate that HDAC7 is necessary and sufficient to augment the CSC phenotype in breast and ovarian cancer cell lines (Witt et al., 2017).

1.2. Human mammary gland.

1.2.1. Breast anatomy.

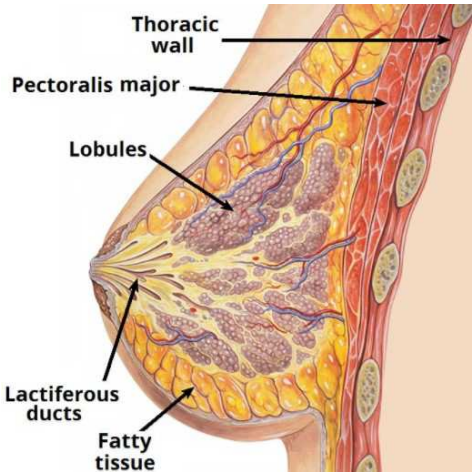

Figure 4: Human breast.
Representation of the anatomy of human breast with the indication of the single component (from Wikipedia).

Breast in humans is an organ that plays a fundamental role in lactation (Figure 4). Breast is present in both males and females, but they become more prominent in females during puberty. Among the mammalian species, breasts number depends from the average number newborns at birth (http://teachmeanatomy.info/thorax/organs/breasts/).

Anatomically, breast presents at the centre the nipples, which are surrounded by a pigmented area of skin called areolae. The areolae contain little glands called Montgomery glands, responsible of the lipoid fluid secretion. This secretion acts as a protective lubricant, important during breastfeeding and its smell attracts for the infant.

The breast contains the mammary glands, the key structures responsible in all the functions in which this organ is involved.

A mature mammary gland is composed by alveoli and ducts (Macias and Hinck, 2013) (Gudjonsson et al., 2009). Alveoli gather together to develop structures known as lobules (Fig. 4). Each lobule is connected with the lactiferous ducts. Ducts are structures that connect the lobules with the nipples (Love and Barsky, 2004). Under the oxytocin stimulation, the ducts through contraction support the milk flow from alveolar units to the nipples (Haaksma et al., 2011).

Humans normally have two mammary glands, one in each breast. Every mammary gland consists of 10/20 simple lobules and each lobule is formed by 10/100 alveoli. All these structures are sustained by the stroma, connective tissue principally composed by collagen and elastin (Campbell and Watson, 2009). In addition to the connective tissue, breasts are

supported by the presence of adipose tissue that surrounds the mammary gland. Furthermore, in breast there is a diffuse presence of blood and lymphatic vessels. Both type of vessels play a key role in cancer because of the spreading of cancer cells from breast to lymph nodes and other tissues, supporting the formation of metastasis.

1.2.2. Mammary gland cellular composition.

As we described above, the ductal network terminates in lobular units commonly known as the terminal duct lobular units (TDLUs) (Yang et al., 2012). The TDLU structure represents the basic mammary gland unit.

The entire mammary gland is constituted by two main mammary epithelial cell (MEC) subtypes: an external layer of basal MECs (myoepithelial cells) and an inner layer of luminal MECs (Loeffler and Roeder, 2002).

Myoepithelial (or basal) cells are present on the perimeter of the lobules and of the ducts, where they establish contacts with the extracellular matrix, by hemi-desmosomes and to the adjacent luminal epithelial cells to desmosomes (Gusterson et al., 1982). The myoepithelial layer that surrounds the ducts, represented by spindle-shaped cells, is a continuous layer (Gudjonsson et al., 2009). On the contrary, the myoepithelial cells surrounding the lobular structures, create an irregular layer, permitting the interaction between the luminal epithelial cells and the basement membrane (Glukhova et al., 1995).

There are a set of cytokeratins expressed by myoepithelial cells such as CK5, 14 and 17, which are crucial for the mammary cytoarchitecture (Dairkee and Heid, 1993). The myoepithelial cell cytoplasm is filled with actin and myosin, which are responsible of the contractile phenotype mediated by oxytocin stimuli during lactation (Murrell, 1995). The contractile phenotype is supported by the expression of the α-smooth muscle actin (α-sm actin) and of the heavy chain-myosin (hc-myosin) (Lazard et al., 1993). Beside the contractile properties, this cell layer has the peculiarity to contribute to the basement membrane production, through the secretion of fibronectin, collagen IV and laminins (Gudjonsson et al., 2009). The strong connection between the extracellular matrix and myoepithelial cells is guarantee by the expression of β4 and α1 integrins (Lambert et al., 2012).

Strong evidences demonstrate that, among the myoepithelial cells there are cells that lack typical characteristics of the myoepithelial lineage, which can be considered progenitor cells. (Oakes et al., 2014) (Joshi et al., 2012).

A single layer of luminal epithelial cells delimits the lumen of lobules and ducts. The luminal lineage can be further subdivided into ductal and alveolar luminal cells (Visvader and Stingl, 2014). To support the critical changes occurring during puberty and pregnancy, the epithelium

of the mammary gland must be extremely dynamic. This requirement can explain the heterogeneous composition of this tissue, made by early stage stem cells, progenitors and differentiated cells (Twigger et al., 2015).

The alveolar epithelial cells are in prevalence $ER^{+/-}$,$CD29^{low}$, $CD49f^{+}$, $CD24^{+}$, $CD61^{-}$ and express CK7 and CK19 (Joshi et al., 2012; Visvader and Stingl, 2014). Alveolar epithelial cells are the only responsible of the milk production and secretion (Taylor-Papadimitriou et al., 1989). Alveolar cells start to proliferate during late pregnancy to support the final development of the alveolar structures (Kobayashi et al., 2016). Milk production by alveolar MECs is elicited by prolactin and glucocorticoids stimulation at birth (Houdebine et al., 1985).

The ductal epithelial differentiated cells could be ER^{-} or ER^{+}, $EpCam^{+}$, $CD49f^{+}$, $MUCI^{+}$. The main keratins expressed in this layer are the CK7, 8, 18, 19 (Taylor-Papadimitriou et al., 1989). Microscopically, the luminal layer is formed by cuboidal epithelial cells bound together by the tight junctions (TJ), principally composed by one or more types of Claudins (Cldns) (Sasaki et al., 2003). Claudins supervise changes in TJ permeability that occurs during parturition and lactation (Kobayashi et al., 2016). The tight junctions are the principal responsible of the mammary ductal barrier and the main regulators of the polarity of the luminal epithelial cells. The polarization of these cells explains why the myoepithelial side of the epithelial cells have different functions compared with the apical membrane (membrane side of the cell exposed to the alveolar lumen) implicating also a polarization of the organelles of the cells (Roignot et al., 2013).

1.2.3. Breast cancer.

Indeed, breast cancer is a highly heterogeneous disease and can be classified into different categories using specific parameters:

Histopathological: The histopathological classification of breast carcinoma is based on the specific morphological features of different tumours. The most common classification divides the breast carcinoma in

1) The *Ductal Carcinoma In Situ* (DCIS) is one of the most common type, which means that the original site of the disease is within the ducts. DCIS most often occurs at a

single site. In 90% of the cases, DCIS is not palpable and it is discovered through screening mammography. DCIS is more commonly diagnosed in women with the incidence rising steadily after age 40 (Winchester et al., 1972).

2) The *Lobular Carcinoma in situ* (LCIS) is an indolent, non-invasive breast lesion characterized by abnormal changes in the cells that compose the milk-producing lobules. LCIS is a marker indicating that a woman is at increased risk of developing breast cancer. However, most women with LCIS will never develop breast cancer (Makki, 2015).
3) The *Invasive/Infiltrating Ductal Carcinoma* (IDC) is the most common subtype (70–80% of all invasive lesions) (Malhotra et al., 2010). Here cancer cells have penetrated the basement membrane that separates the ductal epithelium from the underlying tissue and invaded the surrounding breast tissue. Cells may then metastasize in other tissues through the bloodstream or lymphatic system (Malhotra et al., 2010).
4) The *Invasive Lobular carcinoma* (ILC) is relatively uncommon, comprising about 5-15% of invasive breast cancers. The prognosis is similar to the invasive ductal carcinoma, but often is more favourable. ILC metastasize later than invasive ductal carcinoma. Compared with invasive ductal carcinoma, patients with ILC are more often prone to bilateral disease. Because of its infiltrative growth pattern, a diagnosis of ILC may be arduous, particularly with dense breast tissue (Guiu et al., 2014; Keshtgar et al., 2010).

Grade: Pathologists also classify breast cancer by grade. The grade is defined according to the appearance of the tissue after biopsy. A lower grade usually means that the cancer grows slower and is less likely to metastasize, whereas a higher grade refers to faster cancer growth with more probability of spreading. Grade 1 means that the cells look most like normal cells and they are well differentiated, while grade 2 means moderately differentiated. Grade 3 refers to poorly differentiated cells that waste their tissue-related characteristics and are identified by accelerated proliferation (Zhang et al., 2012).

Stage: Stage 0 is referred to a not invasive cancer. At stage 1 patients usually have invasive breast cancer, smaller than two centimetres. Spreading to the lymph nodes is observed but not outside the breast tissue. Stage 2 is when the tumour has spread to the auxiliary lymph nodes, which can be from two to five centimetres and remain localized or measure 0.2 to two millimetres of metastasis. Stage 3 describes a more aggressive form of invasive breast cancer. Stage 4 indicates the that the cancer has spread to other organs of the body such as the lungs, the liver, distant lymph nodes, skin or bones. This is the stage with less favourable prognosis (Zhang et al., 2012).

Molecular classification: This classification is one of the most important because of the gene expression component of the cancer cells permits targeted therapy to patients. Gene expression profile studies classify breast cancer as: basal-like, $HER2^{+}$, normal breast like, luminal subtype A, luminal subtype B and claudin low. These breast cancer types are divergent

because of their patterns of gene expression, clinical features, response to treatment and prognosis.

Basal-like (BLBC): They represent the greatest challenge because of the clinically aggressive nature and poorly characterized molecular pathogenesis. BLBC group triple negative breast cancer marked by the lack of the oestrogen (ER) and progesterone (PR) receptors, and the absence of HER2 overexpression (Schnitt, 2010). These peculiarities confer to the cancer cells resistance to specific disease-oriented therapies such as: tamoxifen and aromatase inhibitors or trastuzumab. Generally, cells from basal-like breast cancer evidence expression of cytokeratins 5/6, epidermal growth factor receptor (EGFR), and other basal-related genes (Toft and Cryns, 2011). In addition, many sporadic basal-like breast cancers show BRCA1 dysfunction (Schnitt, 2010).

$HER2^+$: Amplification of the HER2 gene and/or overexpression of the encoded protein have been found in up to 25% to 30% of human breast cancers and have been shown to be associated with poor prognosis. HER2-positive breast cancer are diagnosed by immunohistochemistry (IHC), which identifies overexpression of HER2 and fluorescence in situ hybridization (FISH), which identifies amplification of the HER2 gene (Rena Callahan, 2011). An improvement of patients' outcome has been obtained in the recent years by applying specific therapies such as the monoclonal antibody trastuzumab and the small molecule tyrosine kinase inhibitor lapatinib.

Luminal A and Luminal B: Luminal A tumours express high levels of ER and/or PR and low levels of proliferation related genes. Generally, luminal A tumours have low histological grade and have a good outcome, whereas luminal B cancers have more often higher histological grade, higher proliferation rates and a significantly worse prognosis compared luminal A counterparts (Weigelt et al.). In some cases, Luminal B overexpress HER2 (Schnitt, 2010).

Normal breast-like: Unlike the other four breast cancer subtypes, with well recognizable molecule characteristic pattern, the normal-like subtype is still undefined (Weigelt et al., 2010). This cancer expresses adipose and non-epithelial genes and shares high basal like gene expression patterns. Normal-like tumours have an intermediate prognosis (Toft and Cryns, 2011).

Claudin-low: Less information are available on this breast cancer subtype, in particular concerning the clinical treatment and biological changes. These weaknesses depend on its recent discovery/classification. The claudin-low subgroup comprises tumours which evidence transcriptomic features suggestive of a "cancer stem cell-like" phenotype (Hennessy et al., 2010; Herschkowitz et al., 2007). Claudin-low cells are ER^-, PR^- and $HER2^-$.

1.3. Stem cells.

1.3.1. Mammary stem cells.

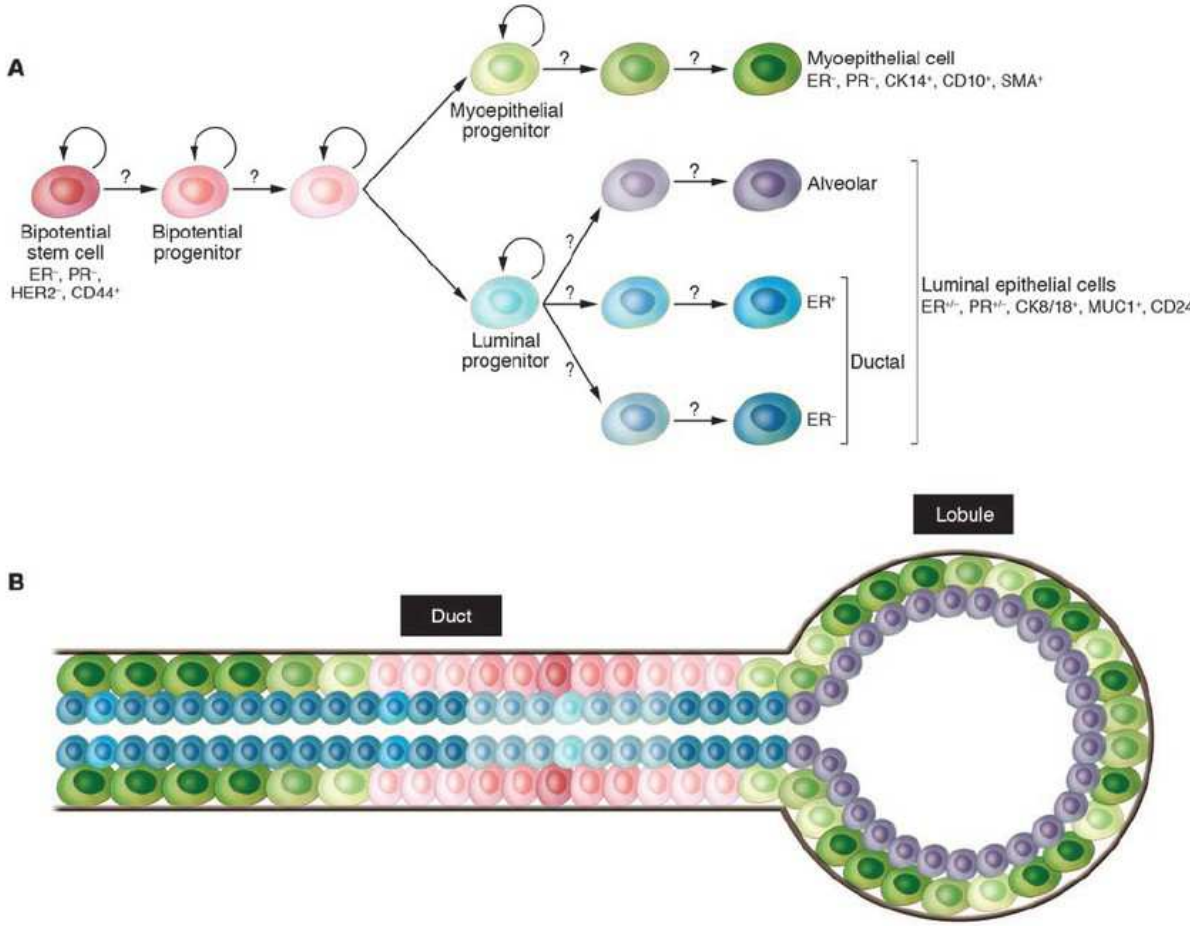

Figure 5: Mammary stem cells.

Hypothetical model of human mammary epithelial stem cell hierarchy and differentiation. (A) Mammary stem cells and their progenitors. A bipotential stem cell gives rise to luminal epithelial and myoepithelial cells, but the intermediary steps and their regulation are largely unknown. (B) Schematic picture of a normal terminal duct lobular unit with the putative location of the various stem and differentiated cells indicated (from Polyak 2007)

Currently scientists strongly affirm the presence of human mammary stem cells (MaCSs) (Figure 5). To support the development, remodelling and differentiation in response to the hormonal signals, the breast tissue must be sustained by the presence of undifferentiated cells. Hence, MaCSs must be considered as multipotent stem cells. These cells have the ability to both self-renew and generate daughter cells that can differentiate in several lineages within the breast tissue.

Stem cells localisation in the mammary gland is still unclear but there are evidences that these cells are mostly located in ducts and alveolar regions. Accordingly, mammary epithelial

fragments extracted from different areas of the mammary gland can give rise to new ductal trees (Fridriksdottir, Agla J.R., et al., 2011).

Different studies tried to prove the mammary stem cells ability to recreate breast tissues. Tissue fragments or dissociated MECs have been introduced into the mouse mammary fat pads of immunocompromised mice but these experiments resulted unsuccessful, presumably because of the lack of an adequate stromal environment (Kuperwasser et al., 2004). These unsuccessful experiments unveiled the key role played by stromal cells in stem cells growth and maintenance. Stem cells are important but their properties will be useless without the stroma-derived signals released by the mammary stem cell niche. The exact nature of these stromal released factors has not yet fully elucidated. In order to form a functional ductal tree, stroma-derived signals should govern both symmetrical and asymmetrical division of the stem cells. It is important to underline that steroid hormones play a pivotal role in directing the fate of the stem cell, probably by acting on the stem cell niche (Fridriksdottir, Agla J.R., et al., 2011). Kuperwasser published in 2004 a work in which they demonstrated that the fat pad injection with human mammary stromal fibroblasts, supported the creation of a humanized stromal environment. The highly activated microenvironment created by these cells was characterized by remodelling of the extracellular matrix proteins of the stroma, including increased collagen synthesis and activation of TGF-β signalling (Kuperwasser et al., 2004). Moreover, in the same study they demonstrated that this chimeric fat pad is essential for the ductal and acinar structures formation after the human MEC organoids injection. These data confirmed the importance of the environment where the MaCSs are located.

More recently, a new model described how fibroblasts and putative mammary stem cells recapitulate the hierarchal nature of the normal human mammary gland. The used model took advantage from engraftments in a collagen plug under the murine kidney capsule (Eirew et al., 2008).

To isolate cells with stem properties, scientists have identified some special molecular markers. In particular cell surface markers have been useful to both identify and characterize mammary stem cells and Cancer Stem Cells (CSCs).

The list of common stem markers includes:

CD44: is a member of a large family of cell adhesion molecules, responsible for the communication and adhesion among adjacent cells and between cell and extracellular matrix (ECM). The *CD44* gene contains 20 exons, which encode ~20 CD44 isoforms (Fox et al., 1994). The non-variant standard isoform, denoted as CD44s, is the smallest and most widely expressed isoform. It is expressed at the surface of many cell types (Louderbough et al., 2011). The longest isoform CD44v (250 KDa) is a well-known marker for normal and cancer stem cells (Witt et al., 2017). Importantly, the expression of specific CD44 isoforms has been detected in advanced stages of cancer. In particular, the overexpression of the variant isoform CD44v6

has been detected in cervical, colorectal and pancreatic carcinomas and correlates with poor prognosis and metastatic potential (Morath et al., 2016).

CD49f/α-6 integrin: ITGA6 is considered a stem marker thanks to studies realized on the epidermal stem cells (Li et al., 1998). In 2006, two groups isolated mouse mammary stem cells *in virtu* of the surface profile marked by $CD24^-$ and $CD49f^+$ (Stingl et al., 2006)(Shackleton et al., 2006). Cells which expressed CD4f in combination with CD44 generate higher number of mammospheres in culture and shown tumorigenesis *in vivo* (Duru et al., 2016).

ALDH1: Aldehyde dehydrogenase 1 (ALDH1) is an intracellular enzyme, frequently selected as a marker of both normal and cancer stem cells (Ginestier et al., 2007). Many studies described the expression of this marker in normal and cancer stem cells. Among the many different ALDH1 isoforms, ALDH1A3 is related to stemness (Qu et al., 2015) and tumorigenesis (Marcato et al., 2011)

CD24: is a glycosylphosphatidylinositol-linked cell membrane adhesion protein expressed in a variety of malignant tumors including ovarian cancer, breast cancer and lung carcinoma (Lim et al., 2014). Its contribution to stemness is still unclear. Cells with stem features show low CD24 expression in combination with CD44 high expression (Qu et al., 2015). $CD44^+/CD24^{-/low}$ breast cancer cells have significant tumorigenic properties and have been identified as a cancer stem cell (CSC) population. Conversely in 2010 Gao et al., (Gao et al., 2010) described how $CD24^+$ ovarian cancer stem cells are enriched for cells at the S phase compared with $CD24^-$ population. Moreover, they described that $CD24^+$ cells preferentially expressed genes, which have an essential role in self-renewal, proliferative capacity and fate determination. Overall these studies suggest that stem cell-like characteristics of $CD24^+$ cells are mediated by multiple signalling pathways, for example, Wnt signaling and Notch signaling pathways. Well known signalling systems involved in the regulation of stem cell function and niche stem cell interactions (Gao et al., 2010).

1.3.2. Breast cancer stem cells.

Tumours are characterised by a strong cellular heterogeneity. A key question that researchers try to answer is: do all the neoplastic cells sustain cancer? or is this feature just restricted to a small population of cells?

In 2003 Dick proposed the cancer stem cells (CSC) theory. This theory could explain why in solid tumours, only a small proportion of the neoplastic cells are able to form colonies in vitro and why a huge number of cells must be transplanted in mice to permit the rising of the neoplastic mass (Dick et al., 2003). Tumours can be heterogeneous tissues governed by a hierarchical organisation. Within the tumour, there is a rare population of cells, called the

tumour initiating cells (T-IC) which are defined as cells with self-renewal ability and tumour-initiating capacity (Zhou et al., 2009). In breast cancer for example, a primitive breast cancer-initiating cell (BrCa-IC) grows and thanks to the self-renewal can maintains the BrCa-IC population and the tumour growth. The same cells, on the other side, can differentiate giving rise to the breast cancer cells that lost the ability to sustain the tumour. Some of these "differentiated" cells can still be considered progenitor cells, but they have lost the ability to sustain the tumour after transplantation (Dick, 2003).

Evidences supporting the CSC theory in breast cancer were published by Al-Hajj in 2003 (Al-Hajj et al., 2003). This work described how in breast cancer, just a distinct population of cells can form tumours in mice. These cells are detectable by the presence of specific markers. For example, $CD44^{+/high}/CD24^{-/low}$ cells from patients with neoplasia, exhibited properties of cancer stem cells (Al-Hajj et al., 2003).

Within a tissue, a CSC can be created *de novo*. This process is characterised by the Epithelial Mesenchymal Transition (EMT), a process that can mark cancer development but also normal morphogenesis of the mammary gland (Nelson et al., 2010).

EMT in cultured cancer cells is characterized by the loss of epithelial markers (E-cadherin and epithelial cytokines) and the gain of mesenchymal markers like SNAIL, TWIST, Vimentin and many others (Turley et al., 2008). These changes in gene expression promote the disruption of the epithelial polarity and establish a mesenchymal phenotype (Cabrera, 2015). EMT results in an increased migratory and invasive potential and in the acquisition of a cell-surface marker profile characteristic of breast CSCs ($CD44^{+/high}/CD24^{-/low}$). The EM transition promotes, in this way, self-renewal properties, and most importantly, tumor-initiating ability to the cells (Marjanovic et al., 2013)

Unfortunately, breast cancer stem cells and normal breast stem cells have very similar characteristics and for this reason it is very difficult to recognise them in a heterogeneous population (Britton et al., 2011).

As discussed above certain markers can be used to recognize breast cancer stem cells. CD44 splice variants seem to have an important role in tumorigenesis. In fact, some studies suggested that variant isoforms expression is linked to an increased metastatic behaviour. For example, transfection of CD44 variants into a non-metastatic rat pancreatic carcinoma cell line, caused a metastatic potential in these cells (Louderbough and Schroeder, 2011).

Beside CD44 and CD24 other markers can be used to identify cancer stem cells in a population. ALDH is a common marker for both normal and malignant stem and progenitor cells. Analysing the expression of ALDH1 in 577 human breast carcinomas, it was proved that the expression of this stem cell marker is a powerful predictor of poor clinical outcome (Ginestier et al., 2007). However, the definition of markers and their use could be not simple to identify a very heterogeneous population like breast cancer stem cells. In fact, a recent paper described the

lack of correlation of stem cells markers in BCSCs. They examined through immunohistochemistry the expression of different cancer stem markers and they affirm that within the same population, the expression of each marker is different. For this reason, each marker identifies a unique sub-population of cancer cells, rather than identifying the same population of cells (Liu et al., 2014).

In 2012 a manuscript described two markers that could help to find cancer stem cells in a population. Among ten markers tested in different human breast cancer cell lines, CD14 and CD90 resulted the most promising. CD90 could be a potential marker of breast CSCs, since $CD90^{+}$ cells represented more than 90% of cells in the Hs578-T cell line, directly correlating with their high tumorigenicity and metastatic potential. On the contrary, the CD14 marker is expressed in a non-tumorigenic cell line. In fact, CD14 is higher than 60% in the non-tumorigenic MCF10-A cell line and less than 15% in the Hs578-T tumorigenic and metastatic cell line (Lobba et al., 2012). These data further stress the need of finding real cancer stem markers in order to bypass the heterogeneity within the cancer stem cells.

1.4. The stem cells niche.

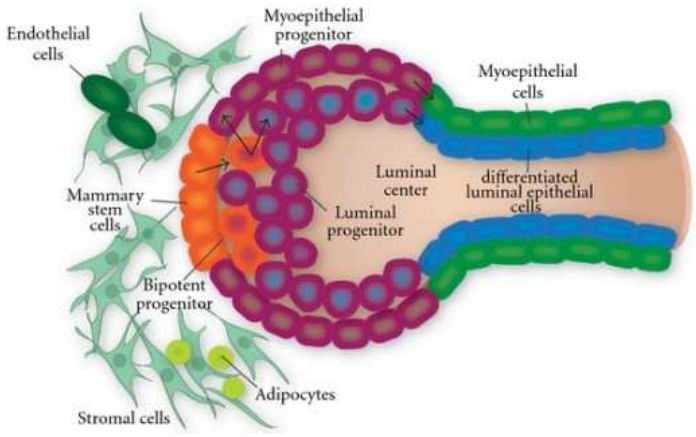

Figure 6: Mammary stem cell niche.

Model of the breast stem cell niche. Key populations of the mammary stem cell niche include mammary stem cells (MSCs), mesenchymal stem cells, endothelial stem cells (ESCs), bi-potent progenitor (BPP), luminal progenitor (LP), myoepithelial progenitor (MEP), myoepithelial cells (MCs), luminal epithelial cells (LCs), and stromal cells (from Tieu et a., 2012).

The stem niche can be defined as the microenvironment where the adult stem cells are maintained (Figure 6). Niches are sites where external signals can influence the stem cells behaviour to permit a quiescent state, the self-renewal or the differentiation.

First demonstration and characterization of niche components was conducted in simplest model organisms such as *Drosophila melanogaster* and *Caenorhabditis elegans* gonads (Xie and Spradling, 1998).

Curiously, in niches from different tissues and organisms, some conserved components can be found. Stromal cells and the extracellular matrix are important players of the niche. Stromal cells are close to the stem cells and secrete factors important for stemness properties, whereas the ECM acts as an anchor for the epithelial cells. Furthermore, the stem niche is supported by blood vessels, which are important for the nutritional support and help the recruitment of circulating stem cells from and to niches (Jones and Wagers, 2008). It is also true that progenitor cells are important in the niche maintenance. The "daughter progenitor cells" send forward signals to the progeny, instrumental to prevent their differentiation. Pardo-Saganta demonstrated that basal stem/progenitor cells regulate the maintenance of their own progeny (Pardo-Saganta et al., 2015).

1.4.1. Molecular pathway associated with niche functions.

Soluble factors and molecules present in the microenvironment are the most important components of stem niches, required to keep active pathways for stem cells maintenance. Different pathways are engaged within the niches including Wnt/β-catenin, Notch, Angiopoietin-1 (Ang-1) bone morphogenetic protein (BMP) and several growth factors, such as fibroblast growth factor (FGF), vascular endothelial growth factor (VEGF), insulin growth factor (IGF), transforming growth factor-alpha (TGF-alpha) and platelet derived growth factor (PDGF) (Ferraro et al., 2010).

IGFs

Among the molecules present in the niche there are the small polypeptides (~7 KDa) known as Insulin Growth Factors (IGF-1 and IGF-2). The expression of IGFs is under the control of the growth hormone. In fact, experimental evidences demonstrate that in the stromal cells the growth hormone (GH) binds the GH receptor and triggers IGF-1 mRNA expression (Kleinberg, 1997). IGFs action takes place thanks to the engagement of the IGF-1R and the IGF-2R (IGF-2 specific receptor) which are tyrosine kinase receptors.

Through different signalling pathways, IGF-1/2R activity is transduced in changes of gene expression aimed to promote survival, self-renewal, and differentiation of MSCs (Youssef et al., 2017).

IGFBPs

To modify the activity of the free IGF-1 ligand there is a class of IGF-binding proteins (IGFBPs, 1-6). Under physiological conditions, IGFs bind IGFBPs with higher affinity than they bind IGF-1R. IGFs and IGFBPs proteins interact through non-covalent binding that resulted important for the protection against their degradation. An increase in their half-life facilitates the delivery to different tissues (Youssef et al., 2017). The IGFBPs family is composed by six members, which are characterised by conserved N and C-terminal domains and variables regions in the middle of the proteins. The N-terminal domain is formed by 80-93 aa and is highly conserved among the IGFBPs. Particularly, at the N-terminus lies a conserved motif (GCGCCxxC), presents in all the IGFBPs, with the exception of IGFBP-6. The real function of this motif is still unclear but researchers suppose that this motif is fundamental for the IGFs binding. Although IGFBP-6 lacks this motif, it shows high binding affinity with the IGFs. The C-terminus domain of the IGFBPs, is well conserved like the N- terminal domain and is involved in the IGFBPs binding between the cell surface and the extracellular matrix (Hwa et al., 1999). The IGFBP (1-6) possess a strong affinity for IGF-1 and IGF-2, but how this class of proteins can release the IGFs? Different strategies are employed to free IGFs. IGFBPs can be subjected of proteolysis, alteration in phosphorylation status and conformational changes (Hwa et al., 1999).

Among the IGFBPs there is another class of protein the IGFBP-rPs (1-9), well known for their less affinity for the IGFs than the IGFBPs. For example, IGFBP-7 (Mac25 or IGFBP-rP1) has binding sites for IGF-1, insulin, VEGFA and activin A and has been described as BMP antagonist. Down regulation of IGFBP7 was associated with unfavourable outcome in breast, lung and pancreatic cancer, demonstrating a correlation between the expression of these proteins and cancer (Bolomsky et al., 2015).

BMP

The bone morphogenic protein belongs to the TGF-β superfamily and has a strong role in the stem regulation. There are more than twenty BMPs, which act through two types of receptors: type 1 and 2.

There are two well-known pathways within BMPs are involved, the first acts through the receptor type I which phosphorylate Smad1, Smad5, or Smad8 (R-Smad). Two phosphorylated R-Smads form a hetero-trimeric complex with a common Smad4 (coSmad). This complex translocates into the nucleus and cooperates with other transcription factors to modulate target gene expression. The second pathway involves the X-linked inhibitor of apoptosis (XIAP) which, after BMP binding can activate the JNK and NF-kB pathways (Zhang and Li, 2005).

Among the BMPs, BMP-2 and BMP-4 are key regulators of the cell fate and differentiation of the human mammary epithelial stem cells. In particular it was demonstrate that BMP-4

prevents the lineage differentiation of the MCF10A cells, by promoting stemness (Clément et al., 2017).

2. MATERIALS AND METHODS

Cell cultures and reagents.

Human normal immortalized epithelial breast cells (MCF-10A), MCF-10A HRasG12V, MCF10A MEF2D VP16 and MCF10A MEF2D ΔDBD were maintained in Ham's F12/DMEM 1:1 medium (Sigma-Aldrich) supplemented with 5% horse serum (Euroclone), penicillin (100U/ml), streptomycin (100µg/ml), L-glutamine (2mM) (Lonza), insulin (0,01mg/ml), hydrocortisone (500ng/ml), cholera toxin (100ng/ml) (Sigma-Aldrich), and epithelial growth factor (EGF) (20ng/ml) (Peprotech). HEK-293T and AMPHO cells were grown in Dulbecco's modified Eagle's medium (DMEM) supplemented with 10% fetal bovine serum (FBS), L-glutamine (2mM), penicillin (100U/ml), and streptomycin (100µg/ml) (Lonza). Cells expressing inducible forms of HDAC7 were grown in complete F12/DMEM medium without phenol red (Sigma-Aldrich) and with 5% charcoal stripped horse serum. 4-hydroxytamoxifen (4-OHT) (Sigma-Aldrich) was used at 1µM.

Three-dimensional morphogenetic assay.

The 3D morphogenetic assays were conducted as described (Debnath et al., 2002). To obtain acini, cells (3x10^4) were plated in a thick layer of ~1-2mm of laminin-rich extra-cellular matrix (Cultrex-Sigma-Aldrich). Cultrex was overlaid with cells grown in DMEM F12 containing 5ng/ml EGF along with 2% v/v Cultrex.
Cells were maintained at 37ºC and 5% CO_2 and the culture medium was changed every four days. Images of acini were collected by using a Leica AF 6000LX microscope. Instead, confocal images with a Leica confocal microscopy SP equipped with a 488 λ Ar laser and a 543 to 633λ HeNe laser. Acinar area measurements were determined using ImageJ software.

Mammosphere assay

Mammospheres were grown in Mammospheres Medium made up Ham's F12/DMEM 1:1 medium (Sigma-Aldrich) serum free, supplemented with B27 (1X) (Gibco) and EGF (20ng/ml) (Peprotech) seeded on Ultra Low Attachment multiwells (Corning). After 30' of trypsin, 1000 cells were seeded in 24 ULA-MW and cultivate at 37ºC and 5% CO2 for ten days, adding new medium every two days (Shaw et al., 2012). For the BMP4 (Thermo fisher) and IGF-1 (Peprotech) treatments, MCF10A cells were pre-treated at a concentration of 15 ng/ml for 2 days, then single cells were seeded onto 24-well ultra-low attachment plates at limiting

dilution (1000 cells/24-plate well) in medium, as described previously. Spheres larger 50 µM were counted.

Conditioned medium was obtained by seeding MCF10A CTRL and MCF10A HDAC7-/- in complete Mammospheres Medium for 2 days in tissue culture plates (Sarstedt) (1.25^105 cells/ml). After 2 days the medium was collected, filtered and diluted 1:1 with fresh Mammospheres Medium and used for the MCF10A CTRL and MCF10A HDAC7-/- seeding.

Images of mammospheres were collected by using a Leica AF 6000LX microscope.

Mammospheres area was determined using Imagej image analysis software.

MCF10A HDAC7$^{-/-}$ achievement

MCF10A HDAC7-/- cells were obtained using the CRISPR/Cas9 technology. With the aim of obtaining different KO clones, three guides were designed targeting different exons. To do this we used the bioinformatics tool "CRISPR design "available from http://crispr.mit.edu/ to design three gRNAs.

gRNA exon 3: 5'CACCGAGCGCTCGGTGGAGCCCATG 3'

gRNA exon 4: 5'CACCGCCGATGCCCGAGTTGCAGG 3'

gRNA exon 5: 5' CACCGGGTCAAGCAGAAGCTACGG 3'

The three guides pair immediately before the PAM sequence (NGG). gRNAs were clone into the lentiviral plasmid pLentiV2 which bring the Cas9 sequence and the gene for the puromycin resistance. CTRL cells were infected with the pLentiV2 lacking the guide. Immediately after the infection cells were selected by puromycin. Monoclonal cultures were obtained seeding single cell in 96 multiwells. Clones were screened by immunoblot. KO clones for HDAC7 were further validated by Sanger sequencing.

Proliferation assay

MCF10A CTRL and HDAC7 KO $1*10^4$ cells/ml were seeded in a 12 multiwell plates. Cells were trypsinized and counted with a solution 0.1% Tripan blue. All experiments were done in triplicate.

Immunofluorescence and immunoblotting

Cells were fixed with 3% paraformaldehyde and permeabilized with 0.1% Triton X-100. The secondary antibodies were Alexa Fluor 488-, 546-, or 633-conjugated anti-mouse and antirabbit (Molecular Probes). Actin was labeled with phalloidin-AF546 (Molecular Probes)

or phalloidin- ATTO 665 (Sigma-Aldrich). Cells were imaged with a Leica confocal microscopy SP equipped with a 488 λ Ar laser and a 543 to 633 λ HeNe laser.
Cell lysates after SDS-PAGE and immunoblotting were incubated with primary antibodies. Secondary antibodies were obtained from Sigma-Aldrich, and blots were developed with Super Signal West Dura (Pierce). For antibody stripping, blots were incubated for 30 min at 60°C in stripping solution containing 100 mM β-mercaptoethanol

Antibody used

The following primary antibodies were used: MEF2D (BD Bioscience), MEF2A (Santa Cruz Biotechnology), p53 and pERK (Cell Signaling Technology), p21, ACTIN and RACK-1 (SigmaAldrich), RAS (Abcam), HDAC4 (Paroni et al., 2004), HDAC5 (Clocchiatti et al., 2015), mouse antiBrdU (Sigma-Aldrich) and secondary antibodies were obtained from Sigma-Aldrich. For HDAC7 antibody production, rabbits were immunized with recombinant histidine-tagged HDAC7 fragment 261-522 purified from Escherichia coli. For anti-HDAC7 antibody purification HDAC7 was fused to glutathione S-transferase (GST) and cross-linked to glutathione-Sepharose as described previously (Paroni et al., 2001).

Plasmid construction, transfection, retroviral and lentiviral infection

To generate pWZL-Hygro-HDAC7 WT-ER, an *Eco*RI fragment of HDAC7 WT was cloned into pWZL-Hygro-ER. MCF-10A cells expressing HDAC7 WT-ER, RAS-V12G, MEF2-VP16 and MEF2ΔDBD transgenes were generated by retroviral infection as described previously (Cernotta et al., 2011). 293T AMPHO packaging cells were transfected 24h after plating by calcium-phosphate precipitation and incubate at 32°C. After 48h the virus-containing medium was filtered and added to target cells.
gRNAs were cloned in pLENTiv2 vector. MCF10A was infected with lentiviral particles. 293T packaging cells were transfected 24h after plating by calcium-phosphate precipitation and incubate at 37°C. After 24h the virus-containing medium was filtered and added to target cells.

RNA extraction and quantitative qRT-PCR.

Cells were lysed using Tri-Reagent (Molecular Research Center). 1 μg of total RNA was retrotranscribed by using 100U of Moloney murine leukemia virus reverse transcriptase (Invitrogen). Quantitative reverse transcription-PCR (qRT-PCR) analyses were performed using Bio-Rad CFX96 and SYBR Green technology. The data were analyzed by use of a comparative

threshold cycle method using HPRT (hypoxanthine phosphoribosyltransferase) as normalizer gene. All reactions were done in triplicate

RNA expression array and data analysis.

Total RNA was isolated with RNeasy (Qiagen). Samples were profiled using Illumina HumanHT12 expression Beadchip v 4.0. The BeadChips were scanned with the Illumina's Beadarray system scanner (Illumina, San Diego, CA, USA). Each array on the BeadChip targets > 47,000 probes derived from the National Center for Biotechnology Information Reference Sequence (NCBI) RefSeq Release 38 (November 7, 2009) and other sources, using 3-µm beads bearing covalently attached 50-base oligonucleotide probes. The raw data images were imported into Illumina Genome Studio, which generated an average intensity of each probe for each sample. The Bead Studio output was then processed with the lumi package (Du et al., 2008) in Bioconductor using the variance stabilizing transform and quantile normalization.
Fold-change and P-values for each probe set were calculated using a moderated t-statistic in the limma package (Ritchie et al., 2015), with the variance estimate being adjusted by incorporating global variation measures for the complete set of probes on the array. The Pvalue data were then corrected for multiple hypotheses testing using the Benjamini and Hochberg. Differentially expressed genes (DEGs) were selected based on fold change >1.5 and <-1.5 fold and P values <0.05.
Gene set enrichment analysis (GSEA) (Subramanian et al., 2005) was used to investigate putative statistical association between genes modulated by HDAC7 and genes perturbed by other signal transduction pathways.

FACS analysis and BrdU assay

For cell cycle FACS analysis, cells were fixed with ethanol (O/N), treated with 10µg Rnase A (Applichem Lifescience) and stained with 10µg propidium iodide (Sigma-Aldrich). Data were analyzed with Flowing Software (http://www.flowingsoftware.com/). Cell surface markers CD44/CD24 have been detected using harvested cells incubated for 30 min on ice with anti-CD44-FITC (Clone G44-26, BD Pharmingen) and anti-CD24-APC (Clone ML5 BioLegend). Cells were processed by the BD FACSCalibur.
For S phase analysis, cells were grown for 3h with 100µM bromodeoxyuridine (BrdU). After fixation, coverslips were treated with 1N HCl (10min, on ice), followed by 20min with 2N HCl at room temperature. Mouse anti-BrdU (Sigma) was used as primary antibody. Nuclei were stained with Hoechst 33258 (Sigma).

Transwell migration assay

For migration assays, cells were plated in the upper well of a transwell chamber separated with a filter containing 0.8 µm pore size (Corning) coated with a solution composed 400 µg/ml cultrex and DMEM/F12 without EGF in the upper part, while in the lower well complete DMEM/F12 was added. After 16h of incubation, cells that migrated through the filter were fixed with 4% PFA. Nuclei were stained with Hoechst 33258 (Sigma) and cells were counted with Leica AF 6000LX microscope and compared with the random motility of the cells.

Statistics

Results were expressed as means ± standard deviations from at least three independent experiments, except for CHIP experiments where standard error was used. Statistical analysis was performed using a Student's t test with the level of significance set at $P < 0.05$. Data from 3D acinar area measurement was determined using ImageJ image analysis software and analyzed using Non-parametric Mann-Whitney test (Prism GraphPad Software). Data were from at least three independent experiments. *$P<0.05$; **$P<0.01$; ***$P<0.005$.

3. RESULTS

3.1. CRISPR/Cas9 -mediated HDAC7 knockout in MCF10A cells.

With the aim of investigating the involvement of HDAC7 in mammary epithelial homeostasis and especially in epithelial morphogenesis and proliferation, we applied the CRISPR/Cas9 system to obtain human breast epithelial MCF10A-HDAC7$^{-/-}$ cells. Our strategy was to target different exons of the *HDAC7* gene (Figure 7A). We designed three guides to employ a precise targeting of the exons 3, 4 and 5. Guides (gRNAs) were designed with the CRISPR/Design software, in order to get guides with the smallest off-targets chance (Figure 7B).

Each single guide was cloned in the lentiCRISRv2 plasmid and, with the packaged lentivirus, three different infections on MCF10A cells were performed. We also used the empty lentiCRISPRv2 to obtain MCF10A-WT cells. After selection, we generated monoclonal cell lines, by seeding a single cell in 96 wells plate. We decided to screen our clones using the immunoblotting technique, to unambiguously demonstrate the abrogation of HDAC7 expression. Hundreds of clones were selected for the analysis and the resulting lysates screened by immunoblotting using an anti-HDAC7 antibody that we have generated.

Curiously, with this preliminary screening we did not found KO clones of MCF10A cells infected with the guides against the exon 3. Moreover, few clones of HDAC7$^{-/-}$ cells were isolated with the gRNAs targeting exon 4 and 5. On the contrary we obtained a higher number of HDAC7$^{+/+}$and some heterozygous HDAC7 $^{-/+}$ clones (data not shown). These results suggest a possible negative selection versus the HDAC7 KO clones. This selection could be justified by the importance of HDAC7 in influencing cell fitness.

Among the resulting HDAC7$^{-/-}$ clones obtained with the guides against the exon 4 and the exon 5, we decided to evaluate the corresponding genomic regions by Sanger sequencing. As expected, DNA sequencing revealed indels introduction and deletions, possibly through *NHEJ,* in which the alterations of the open reading frame resulted in a premature stop codon, thus justifying the absence of the HDAC7 protein (Fig. 7C).

We selected two MCF10A-HDA7$^{-/-}$ clones. The clone 2.65 was obtained using the gRNA against the exon 4. Sequencing proved an insertion of a single nucleotide “A” within the exon 4, three nucleotides before the PAM sequence. Because of this insertion, a premature stop codon is introduced which causes the lack of the protein expression. Concerning the second characterized clone (clone 3b) another insertion is the cause of the HDAC7 loss. In this case, a little indel of four nucleotides “ACCA” was present into the exon 5 of the *HDAC7* gene, thus producing a premature stop codon (Figure 7C).

Both clones were selected for further analyses.

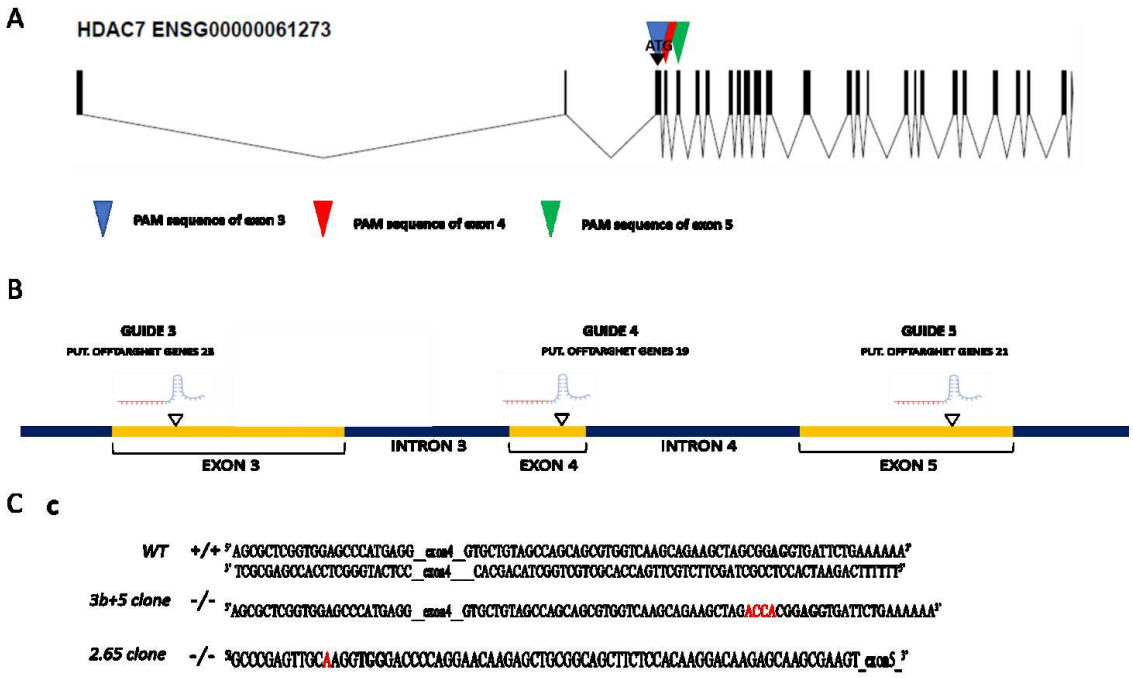

FIGURE 7: Crispr/Cas9 strategy to knock out HDAC7 in MCF10A cells.

A: Representation of the human *HDAC7* gene. The ATG was placed on the first coding exon. In blue, red and green are represented the exons where PAM sequences, are located.

B: Description of the HDAC7 exons selected to be targeted by Cas9 and by the respective gRNAs with the number of putative off-targets genes.

C: Illustration of the HDAC7 $^{+/+}$ and HDAC7 KOs sequences. KO clone sequences are described showing in red the insertion caused by the NHEJ, which promotes the premature STOP codon formation in MCF10A HDAC7$^{-/-}$cells. In bold are represented the PAM sequences.

3.2. Characterisation of the MCF10A HDAC7-/- clones.

To further characterize the generated MCF10A-HDAC7$^{-/-}$ cells, in particular clones 2.65 and 3b, we first analysed the protein levels of HDAC4 and HDAC5 (Figure 8A) in order to exclude compensatory mechanisms among proteins of the same family. These two proteins are the foremost expressed class IIa HDACs in MCF10A, after HDAC7 (Clocchiatti et al., 2015). Immunoblot analysis did not evidence compensatory effects. HDAC4 and HDAC5 maintain the same expression both in KOs and MCF10A WT cells.

MEF2 transcription factors are directly regulated by class IIa HDACs (Zhang et al., 2002). MEF2A and MEF2D are expressed in MCF10A cells. To verify if the absence of HDAC7 could influence their expression, we analysed their levels by immunoblot. No relevant changes can be observed in the expression of both MEF2 between KOs and WT cells (Figure 2A).

Cyclin-dependent kinases (CDKs) are master regulators of cell cycle progression (Besson et al., 2008). The CDK inhibitor 1A (CDKN1A), also named p21, is a well-known negative regulator of proliferation (Lim and Kaldis, 2013). There are evidences that MEF2 and class IIa HDACs could be involved in the regulation of CDKN1A transcription (Clocchiatti et al., 2015; Di Giorgio et al., 2015). To better understand the effect of HDAC7 on the regulation of p21, we analysed CDKN1A protein levels by Western Blotting (Figure 8A). As expected, HDAC7$^{-/-}$ cells showed a strong up-regulation of CDKN1A compared with HDAC7$^{+/+}$ cells. This phenotype could be caused by a diminished activity of class IIa HDACs on the *CDKN1A* promoter where they are recruited by MEF2 family members (Clocchiatti et al., 2015). If *CDKN1A* is up regulated in KOs cells, an impact on the cell cycle progression should be evident. To verify this hypothesis, we performed some experiments to understand the proliferation rate of HDAC7$^{-/-}$ cells.

First, a BrdU assay revealed a smaller percentage of HDAC7 $^{-/-}$ cells in S phase compared with HDAC7$^{+/+}$ cells. The percentage of proliferating cells is similar between the two clones and fluctuates among 20% to 25%, compared to the ~50% of the WT (Figure 8B).

Second, we performed a cytofluorimetric analysis to discriminate differences in the cell cycle between HDAC7$^{+/+}$ and HDAC7$^{-/-}$cells. Not surprisingly, we discovered that the percentage of cells in the G1 phase was higher in KOs compared to the control (Figure 8C). In addition, a proliferation assay was performed to further confirm the previous data. As predicted, both KO cell lines evidenced a significant lower proliferation rates, in comparison with the WT cells (Figure 8D). These results support the idea that HDAC7 influences the proliferation of the MCF10A cells acting as a repressor of the p21 expression through MEF2.

When MCF10A cells are plated on a reconstituted basement membrane matrix (rBM), derived from a special type of mouse tumour, the Engelbreth Holm-Swann (EHS) murine sarcoma, they give rise, through a morphogenetic process, to a 3D acinar structure (Debnath et al., 2002).

To demonstrate whether the impact of HDAC7 on cell cycle progression could influence the growth of MCF10A cells in 3D condition, we performed a three-dimensional morphogenetic assay on MCF10AHDAC7$^{+/+}$ in comparison with HDAC7$^{-/-}$ (clone 3b) (Figure 8E). Every four days images were collected and for each acinus its area was calculated. HDAC7$^{+/+}$ cells did not showed differences in morphology of acini but, from the day 4, a difference in the acinar area was evident. The main differences were revealed after 8 and 12 days in 3D culture. These data confirmed that the HDAC7 $^{-/-}$ cells are less proliferative compared to the control under 2D as well as under 3D culture conditions.

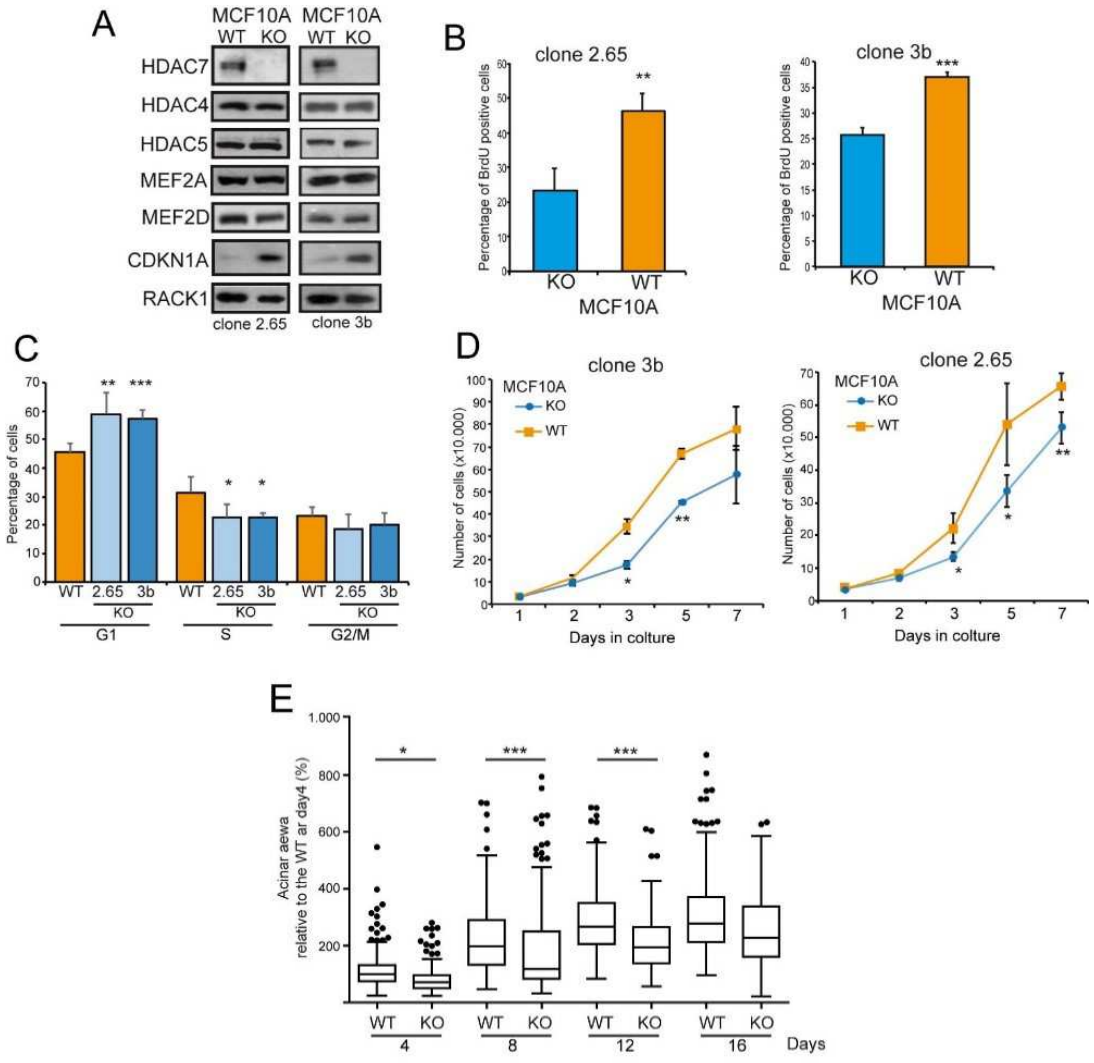

Figure 8: MCF10A HDAC7$^{-/-}$ clones characterization.

A: Immunoblot analysis of HDAC4, HDAC5, MEF2D, MEF2A and CDKN1A expression in MCF10A HDAC7$^{-/-}$ clones (2.65 and 3b) RACK1 was used as loading control.

B: BrdU positive assay was performed with MCF-10A KO clones. After 24h from seeding BrdU was added for 3h. After fixation cells were processed for immunofluorescence to score the percentage of BrdU positive cells

C: FACS analysis of MCF10A HDAC7$^{-/-}$ clones. Cells were fixed with ethanol, treated with Rnase A and stained with propidium iodide.
D: The graph represents the proliferation curves obtained counting the number of cells after 1, 2, 3, 5 and 7 days in culture as indicated. Only alive cells were considered after Trypan blue counting.
E: Acinar size (µm2) of MCF-10A WT and the clone 3b, in 3D culture for 4, 8, 12 and 16 days. Culture medium was changed every 4 days. Data are presented as percentage relative to day 1 WT cells.

3.3. HDAC7 WT re-expression in KO rescues the phenotype.

Today the relevance of the CRISPR/Cas9 technique for genome editing is well affirmed. It is an efficient system, frequently applied *in vitro* experiments, which seems to have promising potentialities for *in vivo* applications, with therapeutic perspectives. Even if the power of this system is confirmed day by day, the off-target effects represent a dark side of this revolutionary technique. The possibility that Cas9 can edit the target gene and other genes is a problem that researchers must climb over. In our specific case, we wanted to prove that the phenotype described previously was directly related to the HDAC7 knock-out. To affirm this, we infected KO cells with the inducible form HDAC7 WT-ER, in order to re-express HDAC7 in MCF10AHDAC7$^{-/-}$ cells. To verify and confirm the stable expression of the HDAC7 protein in KO cells, we performed an immunoblotting and an immunofluorescence analysis, after induction with 4-OHT (Figure 9B and C). After proving the re-expression of HDAC7 in KO cells, we investigated p21 protein levels. In immunoblot analysis, p21 appears strongly down-regulated after HDAC7 re-expression in KO cells (Figure 9C). This down-regulation was confirmed at mRNA level by qRT-PCR analysis (Figure 9E). A BrdU assay was performed to testify the rescue of the proliferative defect in MCF10A KO/HDAC7 WT-ER cells in comparison with the KO/ER cells (Figure 9D).

We further investigated the recovery of the proliferative defect also in 3D culture. After four days from the seeding of WT, KO and KO/HDAC7-ER cells on Cultrex, in cells re-expressing HDAC7 compared to the KO, the acinar size was increased and indistinguishable from WT MCF10A cells (Figure 9A).

All these results confirm a rescue of the phenotype in MCF10A HDAC7 KO cells after the re-expression of HDAC7. In summary, we can exclude that the deficit of proliferation observed in HDAC7 KO cells originate from the off-target activity of Cas9.

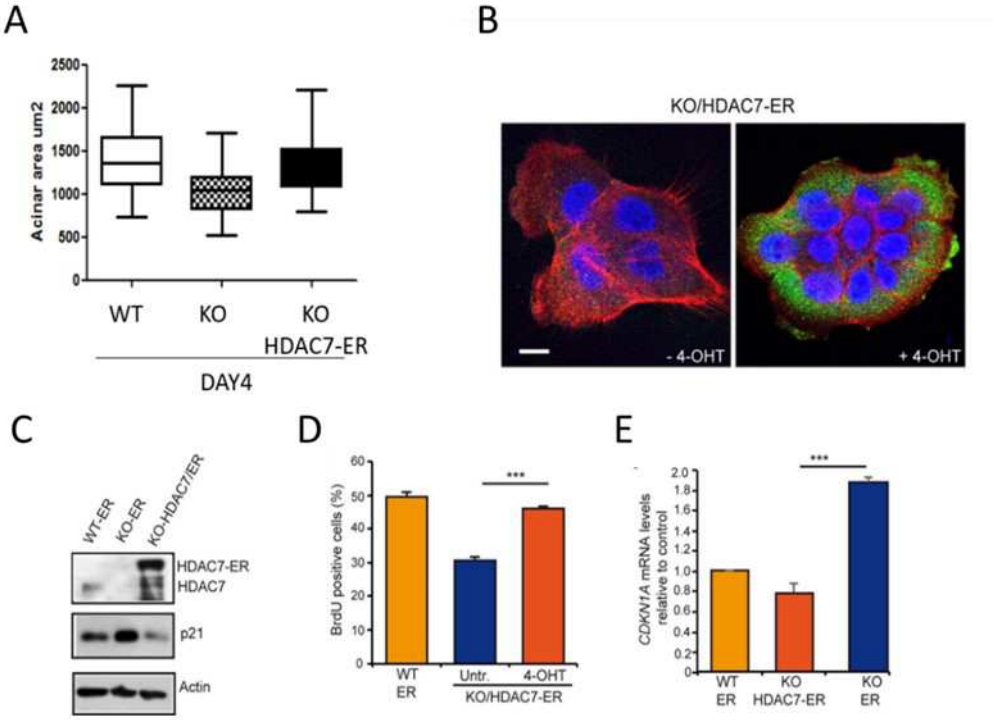

Figure 9: HDAC7 expression in MCF10A HDAC7$^{-/-}$.

A: Acinar size (µm2) of MCF-10A HDAC7$^{+/+}$, HDAC7$^{-/-}$. and HDAC7$^{-/-}$/HDAC7-ER in 3D culture for 4 days. 4-OHT was added in culture medium every two days to induce HDAC7 expression.

B: Confocal pictures of MCF10A cells expressing HDAC7-ER (green). AF546-phalloidin was used to stain F-actin and nuclei were stained with Topro-3. Scale bar, 50 µm.

C: Immunoblot analysis of HDAC7 and p21 in MCF10A HDAC7$^{+/+}$, HDAC7$^{-/-}$. and HDAC7$^{-/-}$/HDAC7-ER cells. Actin was used as loading control.

D: BrdU positive cells percentage of MCF-10A HDAC7$^{+/+}$, HDAC7$^{-/-}$. and HDAC7$^{-/-}$/HDAC7-ER cells. Cells were seeded and after 24h BrdU was added for 3h. After fixation cells were processed for immunofluorescence.

E: mRNA expression levels of the MEF2-target gene CDKN1A were measured by using qRT-PCR in MCF-10AHDAC7$^{+/+}$, HDAC7$^{-/-}$. and HDAC7$^{-/-}$/HDAC7-ER cell. 4-OHT was added to culture medium the day of seeding.

3.4. HDAC7 contribution in stemness in MCF10A cells.

Recent observations have ruled out a possible contribution of HDACs and in particular of HDAC7 in the maintenance of stemness in the breast epithelium, with important impacts on cancer growth (Clément et al., 2017). Hence, we asked if HDAC7 could contribute to stemness also in our experimental model of epithelial mammary cells.

Within a cell population are present some cells that show stem characteristics and play a pivotal role in the stem community maintenance (Joshi et al., 2012). Even if MCF10A cells are considered differentiated cells, among them, are present some progenitors, at very low percentage with stem features (Qu et al., 2015).

We decided to prove the involvement of HDAC7 in the regulation of stem cells by performing a mammospheres assay. This assay is based on the stem cell ability to grow in ultra-low adhesion plates, helping the discrimination with the differentiated cells, which are not able to grow under these conditions. After 10 days in culture, progenitors of the differentiated cells survive and proliferate to generate spheres (in case of mammary stem cells, they are also named mammospheres). Comparing the $HDAC7^{+/+}$ with MCF10A-$HDAC7^{-/-}$ we observed a reduced number of spheres formation in the case of $HDAC7^{-/-}$ cells (Figure 10A and B). The demonstration that HDAC7 is a critical determinant in the regulation of stemness, comes from the experiments with MCF10A KO/HDAC7-ER. When HDAC7 was re-expressed in knocked-out cells, they reacquire the capability of generating spheres (Figure 10D and E).

The reduced number of mammospheres, observed in the absence of HDAC7, suggests for a reduction or for a defect in cells with stem characteristics. Moreover, a smaller area was detected in the few mammosphers derived from KO cells compared to MCF10A WT cells (Figure 10C and E).

Moreover, we used flow cytometric analysis to determine the $CD44^{high}/CD24^{low}$ phenotype in MCF10A WT and $HDAC7^{-/-}$ cells. $CD44^{high}/CD24^{low}$ cells could be considered undifferentiated cells, on the contrary, $CD44^{high}/CD24^{high}$ cells exhibit differentiated properties. We observed that MCF10A $HDAC7^{-/-}$ exhibited a small but significant decrease in the $CD44^{high}/CD24^{low}$ population (5,78$\pm$3.84 versus 8,33$\pm$3,15 p=0,0498) compared with the MCF10A WT, as evidenced in Figure 10F and G. This experiment confirms the role of HDAC7 in sustaining proliferation and argue for an additional contribution in stemness.

BMP4 (bone morphogenetic protein 4) is a protein belonging to the TGF-β super family. Its involvement in the regulation of mammary epithelial stem cells is well known (Clément et al., 2017). To increase the pool of cells with stem characteristics, we pre-treated KO and WT cells with BMP4 in 2D culture. After two days, pre-treated cells were used for sphere assay. After 10 days, the number of mammospheres formed by the WT cells was significantly higher

compared to untreated cells (Figure 10H). Curiously MCF10A/HDAC7 KO cells BMP4-treated, increased the number of spheres, compared with the untreated ones, but they are significantly less compared to WT cells pre-treated with BMP4. These data show that BMP4 treatment can augment the pool of cells with stem features. However, HDAC7 KO cells maintain the original defect in terms of sphere formation efficiency. In addition, the dimension of sphere generated by KO cells treated with BMP4, again appeared smaller compared to WT cells BMP4-treated.

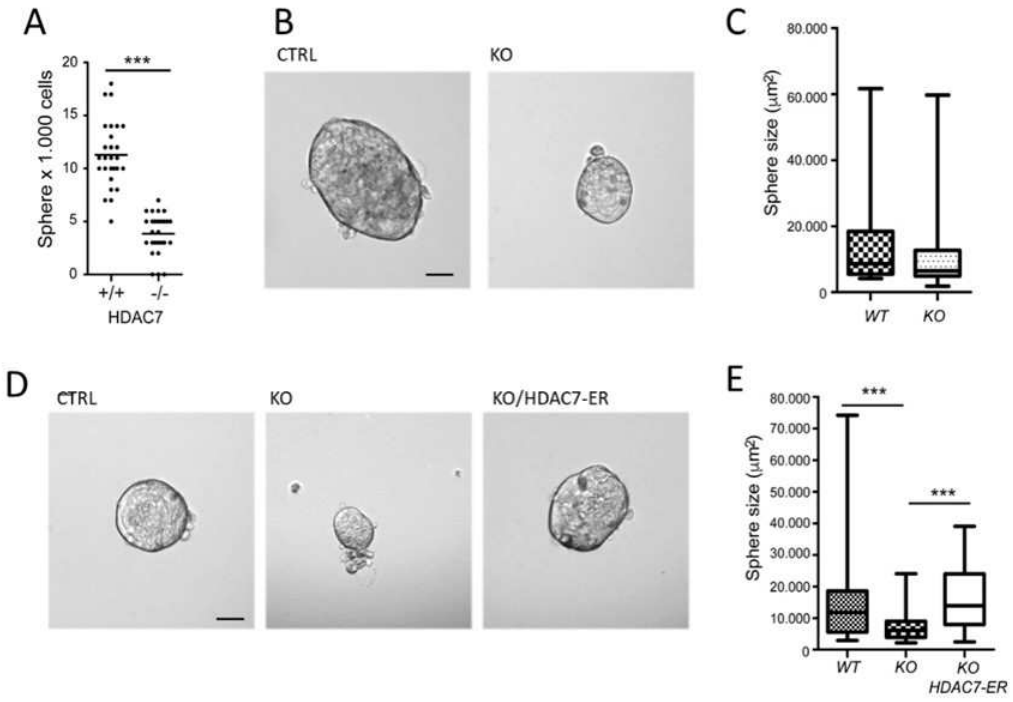

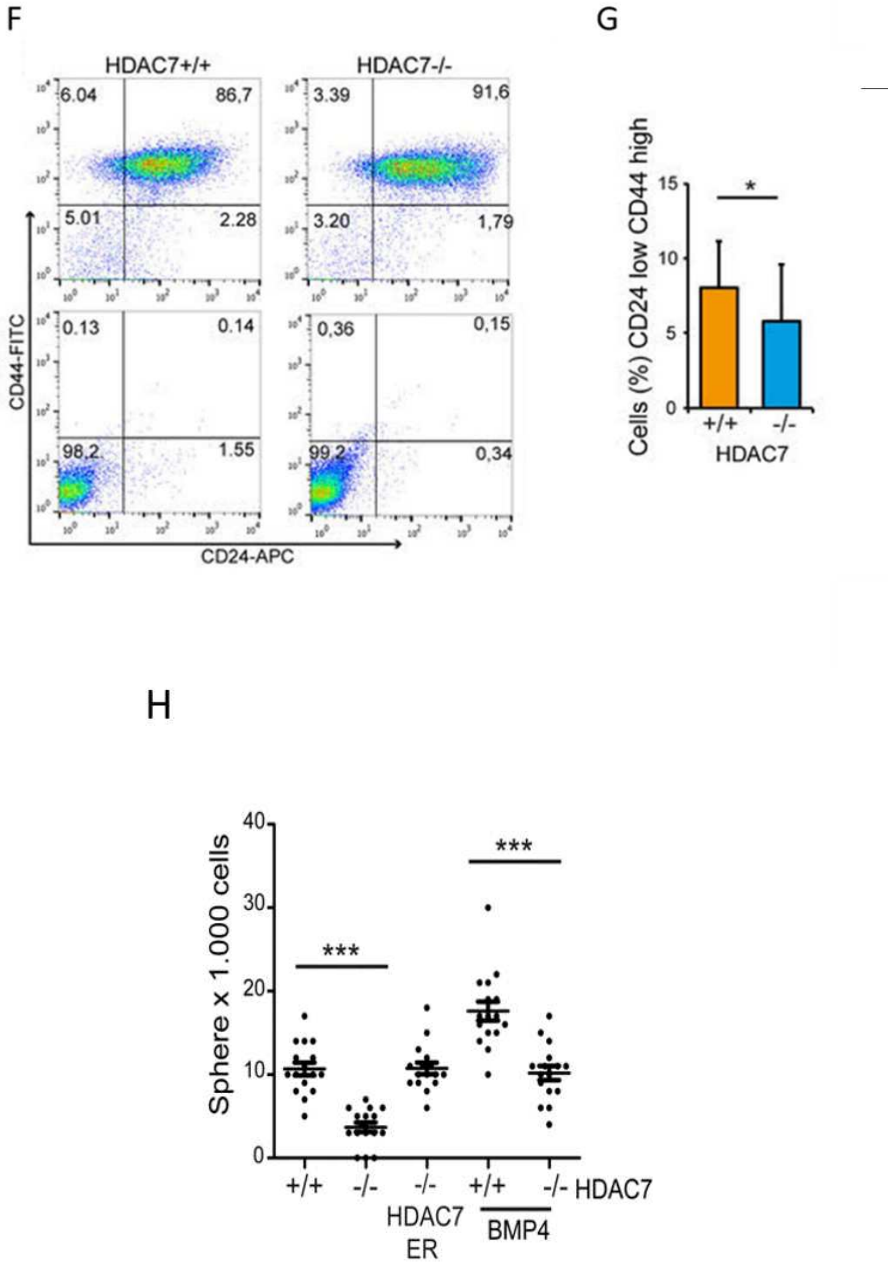

Figure 10: HDAC7 contributes in stemness maintenance in MCF10A cells.
A: Mammosphere assay was performed seeding 1000 cells of each cell line. Spheres with area > 50µm were counted using Leica AF 6000LX microscope after 10 days of culture. Each dot represents an experiment.
B: Images represent mammospheres obtained after 10 days of culture respectively from WT and KO cells. Images were collected using Leica AF 6000LX microscope. Scale bar, 100 µM.
C: Sphere area (µm2) from MCF10A WT and KO plotted as a box plot.
D: Images representing mammosphere resulted from MCF10A WT, KO and KO/HDAC7-ER cells. Images from Leica AF 6000LX microscope. Scale bar, 100 µM
E: Box plot representing the size of spheres generated by WT, HDAC7$^{-/-}$ and MCF10A KO/HDAC7-ER cells as indicated.

F: Representative flow cytometry data from double staining MCF10A WT and HDAC7$^{-/-}$. Cells were incubated with FITC-conjugated CD44 and APC-conjugated CD24 for 30 min in ice at concentrations recommended by the manufacturer. Isotype control double staining for CD44 and CD24 from both cell lines is shown.
G: FACS analysis of the double staining for CD44 and CD24 surface markers. Seven experiments have been collected.
H: The panel shows the results from 3D sphere assays obtained with cells treated with BMP4. MCF10A HDAC7 KO and WT cells were pre-treated 2 days with 15ng/ml of BMP4 and then seeded in Ultra Low Adhesion plates. After 10 days, spheres with an area larger 50µm were counted. Each dot represents an experiment.

3.5. Gene expression profiles under HDAC7 influence.

Microarray analysis of MCF10A and MCF10A-HDAC7$^{-/-}$ cells was performed to unveil changes in gene expression under HDAC7 supervision. To prove that fluctuations in gene expression were a specific consequence of HDAC7 absence, the comparative analysis included the gene expression profile of MCF10A cells re-expressing the inducible version of HDAC7 (KO/HDAC7-ER). The DNA microarray analysis identified 205 genes significantly down-modulated and 272 genes significantly up regulated in HDAC7$^{-/-}$ cells (Figure 11A). If we consider the fold changes of 477 DEGs (differentially expressed genes), IL24, CCL20 and FBOX32 resulted strongly up-regulated in HDAC7$^{-/-}$ cells. On the other hand, SPRR3, SPRR1A and KRTDAP showed the strongest down-regulation (Figure 11B). In a preliminary analysis, we focused our attention on genes up-regulated in HDAC7$^{-/-}$ cells. The Gene Set Enrichment Analysis (GSEA) algorithm was used in conjunction with the Molecular Signatures Database (MSigDb) to confer different biological functions to genes modulated by HDAC7 (Figure 11C). Categories underlined in the hallmark gene set analysis showed the regulation of genes involved in the inflammatory response (interferon α and γ responses), xenobiotic response and extracellular matrix remodelling. Analysing DEGs for the GO biological process identified as the top ranching processes: defence response, response to external stimulus and negative regulation of cell proliferation. Moreover, the top Go-term analysis revealed the up-regulation of the GO-term signal peptide in HDAC7$^{-/-}$ cells. These evidences indicate that HDAC7 profoundly reprogram the expression profile of the secretome, including the inflammatory stress response, cell proliferation, cell adhesion. Overall these studies indicate that HDAC7 could supervise expression of genes involved in the remodelling of the microenvironment.
Another microarray study was performed to better understand the involvement of HDAC7 in the regulation of stemness. The transcriptomes of HDAC7$^{+/+}$ and HDAC7$^{-/-}$ cells treated with BMP4 was compared. This study evidenced the up-regulation of 264 genes in HDAC7$^{-/-}$, 182 in HDAC7$^{+/+}$ cells treated with BMP4 compared to untreated. 75 of these genes were common, between the two cell lines (Figure 11D). As expected, GSEA of the categories “Hallmark gene

set", "KEGG gene set" and "Oncogenic signature gene set", revelled a strong activation of the TGF-β signalling pathway in both cell lines. In addition, HDAC7$^{-/-}$ cells treated with BMP4 showed an up-regulation of genes down-regulated by the KRAS activation (Figure 11E).
Concerning down-regulated genes in HDAC7$^{+/+}$ and HDAC7$^{-/-}$ treated with BMP4, a list of 173 genes resulted down-modulated in HDAC7$^{+/+}$ and 63 in HDAC7$^{-/-}$. Among them 30 are genes commonly regulated in both cell lines (Figure 11F). As illustrated in figure 11F, most of the transcriptional response promoted by BMP4 is common between HDAC7$^{+/+}$ and HDAC7$^{-/-}$ cells (activation of TGFβ signalling, blunting of KRAS signalling and activation of EMT mechanisms). However, a differential response to extracellular stimulation/remodelling after BMP4 treatment could be observed between HDAC7$^{-/-}$ and HDAC7$^{+/+}$ cells by focusing the attention on the 143 genes down-regulated by BMP4 only in HDAC7$^{+/+}$. GSEA analysis groups these genes in categories enriched for the response to oestrogen and in co-culturing MCF10A cells with cancer-associated fibroblasts and among the genes up-regulated in basal subtype of breast cancer samples (Figure 11G).
Radar charts in figure 11H, summarize the microarrays results, underlining the HDAC7-regulated genes in selected pathways and gene families. In fact, among the up-regulated genes we found interleukins (IL1B, IL1A, IL8, IL32), which confirms the activation of the inflammatory response. In particular IL8 is known to be a MEF2 target in LMS cell lines (Di Giorgio et al., 2017). The activation of the inflammatory response in MCF10A HDAC7$^{-/-}$ cells was also confirmed by the up regulation of C-C motif chemokine ligands (CCL5, CCL8, CCL20). Furthermore, a fraction of the up-regulated genes encodes for proteins involved in the inflammatory response mediated by interferon γ and α as proved by the up regulation of IFNA and of the ubiquitin-like protein interferon-stimulated gene 15 (ISG15). Finally, HDAC7 seems to have minor impacts on genes of the (TNF) tumor necrosis factor family, whereas important influences are played on genes of the IGF-1 pathway (IGFBP3, IGFBP6, IGFBP7, IGFL1, IGFL2, IRS1, IRS2), which includes well-known negative regulators of stemness (Farabaugh et al., 2015).
To validate the microarray data, we further confirm the gene expression profile of the up-regulated genes, described before, by RT-PCR (Figure 11I). We analysed the mRNA expression levels of IGFBP6, IGFBP7, IL24, IL8, ERRFI1, FBOX32 and ISG15 and all resulted up-regulated in KO cells. All these experiments included also MCF10A-KO/HDAC7 and WT-ER cells, thus confirming that the fluctuations were specifically caused by HDAC7 absence. Moreover, to exclude genes regulated by tamoxifen, both the microarray analysis and the RT-PCR experiments were performed by comparing also KO cells and the KO-ER cells (treated with 4-OHT). Considering this parameter, we can affirm that genes investigated are directly or indirectly regulated by HDAC7 without tamoxifen influence.

MEF2 family members are the favourite class IIa HDACs binding partners (Di Giorgio and Brancolini, 2016). These proteins act as transcriptional factors and regulate the expression of different genes in different tissues. To estimate if the up-regulation of some genes in HDAC7$^{-/-}$ is influenced by the MEF2-HDACs axis, we analysed the expression of the selected genes in MCF10A cells expressing a conditionally active form of MEF2D fused to the VP16 activation domain of herpes simplex virus (Flavell, 2006) A MEF2D DNA-binding defective mutant (ΔDBD) form was used as control. IL8, IL24, ERRFI1 and FBOX32 resulted up-regulated in MCF10A cells expressing MEF2D-VP16, on the contrary, IGFBP6 and 7 resulted not significantly regulated by MEF2D (Figure 11J). These data prove the important role of MEF2 as target of HDAC7 but also unveil MEF2-independent activities for this class IIa HDAC, particularly on the repression of IGFBP6 and 7 genes.

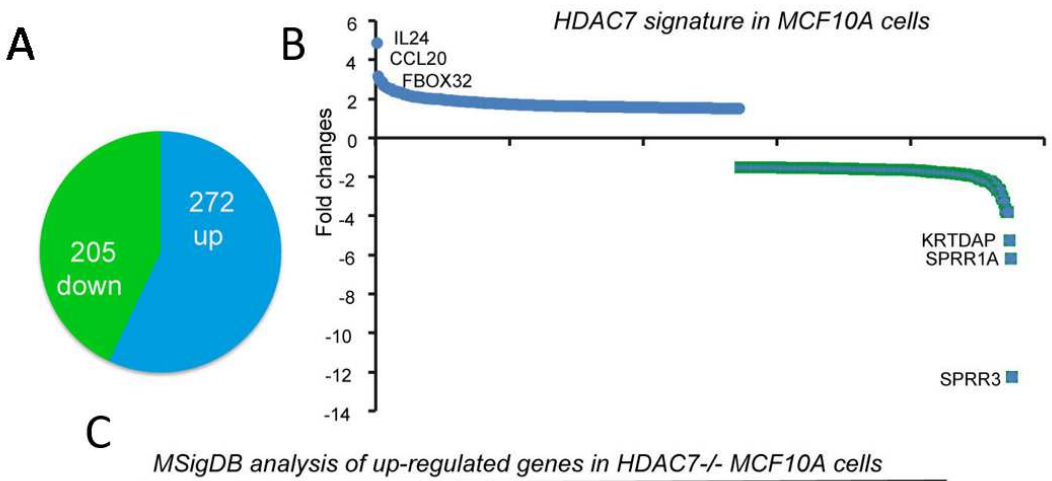

C

MSigDB analysis of up-regulated genes in HDAC7-/- MCF10A cells

Hallmark Gene Set Name	Genes in overlap	% of overlap	p Value	FDR q-value
Interferon-γ response	15	7.5	3,82E-14	1,91E-12
Xenobiotic metabolism	14	7	7,12E-13	1,78E-11
Interferon-α response	10	10.3	3,13E-11	5,21E-10
Epithelial mesenchimal transition	11	5,5	2,81E-9	3,51E-8

MSigDB analysis of up-regulated genes in HDAC7-/- MCF10A cells

GO biological process	Genes in overlap	% of overlap	p Value	FDR q-value
Defense response	41	3.33	2,59E-23	1,15E-19
Response to external stimuls	44	2.42	1,34E-19	2,96E-16
Negative regulation of cell proliferation	25	3.89	5,19E-16	5,75E-13

GO-Terms enrichment analysis for up-regulated genes in HDAC7-/- MCF10A cells

GO-Term	Count	% of overlap	p Value	FDR q-value	Fold enrichment
Signal peptide	90	25.14	8,0E-7	0,0013	1,65
Type I Interferon signalling pathway	10	2.79	1,1E-6	0,0018	9,34
Cell adhesion	22	6.14	3,0E-5	0,0404	2,88

Figure 11: Expression profiles of MCF10A HDAC7$^{-/-}$.

A: Pie-chart indicating the number of genes significantly up and down-regulated in HDAC7$^{-/-}$ compared to HDAC7$^{+/+}$ and HDAC7$^{-/-}$HDAC7-ER MCF10A cells.

B: Histogram representing the HDAC7 signature in MCF10A cells, by comparing HDAC7$^{-/-}$ cells with HDAC7$^{+/+}$ HDAC7$^{-/-}$HDAC7-ER cells. The top regulated genes are highlighted.

C: Enrichment analysis was performed to investigate the biological processes promoted by HDAC7 depletion in MCF10A cells. MSigDB "Hallmarks" and Gene ontology (GO) categories were investigated. The significance of the obtained enrichment for each category is scored as Fold enrichment, p-value and FDR. The percentage of gene calling/overlap for each gene set is shown.

D

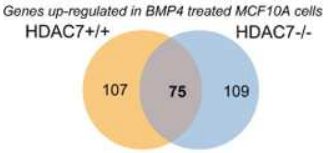

E

Genes up-regulated in BMP4 treated HDAC7+/+ MCF10A cells

Hallmark Gene Set Name	Genes in overlap	p Value	FDR q-value
Genes encoding proteins involved in processing of drugs and other xenobiotics.	11	1,33E-10	6,63E-9
Genes up-regulated in response to TGFB1	7	8,03E-10	2,01E-8

KEGG gene sets	Genes in overlap	p Value	FDR q-value
TGF-beta signaling pathway.	6	5,84E-7	1,09E-4

Oncogenic signatures gene sets	Genes in overlap	p Value	FDR q-value
Genes up-regulated in NCI-60 panel of cell lines with mutated TP53	9	2,91E-8	5,5E-6
Genes up-regulated in a panel of epithelial cell lines by TGFB1	8	3,97E-7	2,92E-5

Genes up-regulated in BMP4 treated HDAC7-/- MCF10A cells

Hallmark Gene Set Name	Genes in overlap	p Value	FDR q-value
Genes down-regulated by KRAS activation.	11	1,73E-10	8,66E-9
Genes up-regulated in response to TGFB1	7	9,55E-10	2,39E-8

KEGG gene sets	Genes in overlap	p Value	FDR q-value
TGF-beta signaling pathway.	6	6,75E-7	8,97E-4

Oncogenic signatures gene sets	Genes in overlap	p Value	FDR q-value
Genes up-regulated in NCI-60 panel of cell lines with mutated TP53	11	1,25E-10	2,36E-8
Genes up-regulated in MCF-7 cells stably over-expressing constitutively acconstitutively active MAP2K1	10	3,97E-7	2,92E-5

F

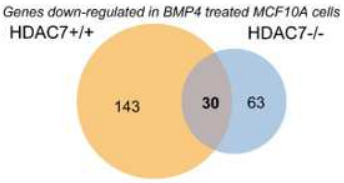

G

Genes down-regulated in BMP4 treated HDAC7+/+ MCF10A cells

Hallmark Gene Set Name	Genes in overlap	p Value	FDR q-value
Genes defining late response to estrogen	12	1,25E-12	6,24E-11
Genes up-regulated by KRAS activation	10	5,93E-10	1,48E-8

Chemical and genetic perturbations	Genes in overlap	p Value	FDR q-value
Genes downregulated in MCF10A cells co-cultured with cancer-associated fibroblasts	24	1,83E-38	6,23E-35
Genes down-regulated in HMLE cells after E-cadhedrin knockdown by RNAi.	34	3,57E-37	6,08E-34

Oncogenic signatures gene sets	Genes in overlap	p Value	FDR q-value
Genes down-regulated in epithelial prostate cancer cell lines over-expressing KRAS.	14	1,74E-17	3,29E-15
Genes down-regulated in epithelial lung cancer cell lines over-expressing KRAS	10	2,50E-11	2,36E-9

Genes down-regulated in BMP4 treated HDAC7-/- MCF10A cells

Hallmark Gene Set Name	Genes in overlap	p Value	FDR q-value
Genes up-regulated by KRAS activation	7	1,67E-8	8,34E-7
Genes defining epithelial-mesenchymal transition, as in wound healing, fibrosis and metastasis	5	1,07E-5	2,67E-4

Chemical and genetic perturbations	Genes in overlap	p Value	FDR q-value
Genes with promoters occupied by SMAD2 or SMAD3 in HaCaT cells	14	1,04E-11	3,54E-8
Genes down-regulated in HMLE cells after E-cadhedrin knockdown by RNAi.	10	1,27E-9	1,71E-6

Oncogenic signatures gene sets	Genes in overlap	p Value	FDR q-value
Genes up-regulated in epithelial cell lines over-expressing an oncogenic form of KRAS	9	3,46E-10	6,53E-8
Genes up-regulated in epithelial lung and breast cancer cell lines over-expressing of KRAS	7	1,79E-9	1,69E-7

Genes down-regulated in BMP4 treated HDAC7+/+ but not in HDAC7-/-MCF10A cells

Hallmark Gene Set Name	Genes in overlap	p Value	FDR q-value
Genes defining late response to estrogen	9	5,26E-10	2,63E-8
Genes defining early response to estrogen	7	2,63E-7	6,59E-6

Chemical and genetic perturbations	Genes in overlap	p Value	FDR q-value
Genes downregulated in MCF10A cells co-cultured with cancer-associated fibroblasts	17	2,12E-27	7,22E-24
Genes up-regulated in basal subtype of breast cancer samles.	21	4,56E-19	7,76E-16

Figure 11: Expression profile of MCF10A HDAC7-/-.

D: The Venn diagram shows genes-up regulated in MCF10A WT and KO cells after BMP4 treatment.

E: Enrichment analysis on genes up-regulated after 15ng/ml BMP4 treatment. “Hallmark”, “KEGG” and “Oncogenic signature” categories were investigated. The significance of the obtained enrichment for each category is scored as genes in overlap, p-value and FDR.

F: The Venn diagram shows genes down-regulated in MCF10A WT and KO after BMP4 treatment.

G: GSEA on gene down-regulated in HDAC7+/+ and HDAC7-/- cells treated with BMP4. “Hallmark”, “Chemical and genetic perturbation” and “Oncogenic signature” gene sets were

used. The significance of the obtained enrichment for each category is scored as genes in overlap p-value and FDR. “Hallmark” and “Chemical and genetic perturbation” gene sets were used to describe the pool of gene down-regulated in MCF10A WT+BMP4.

H

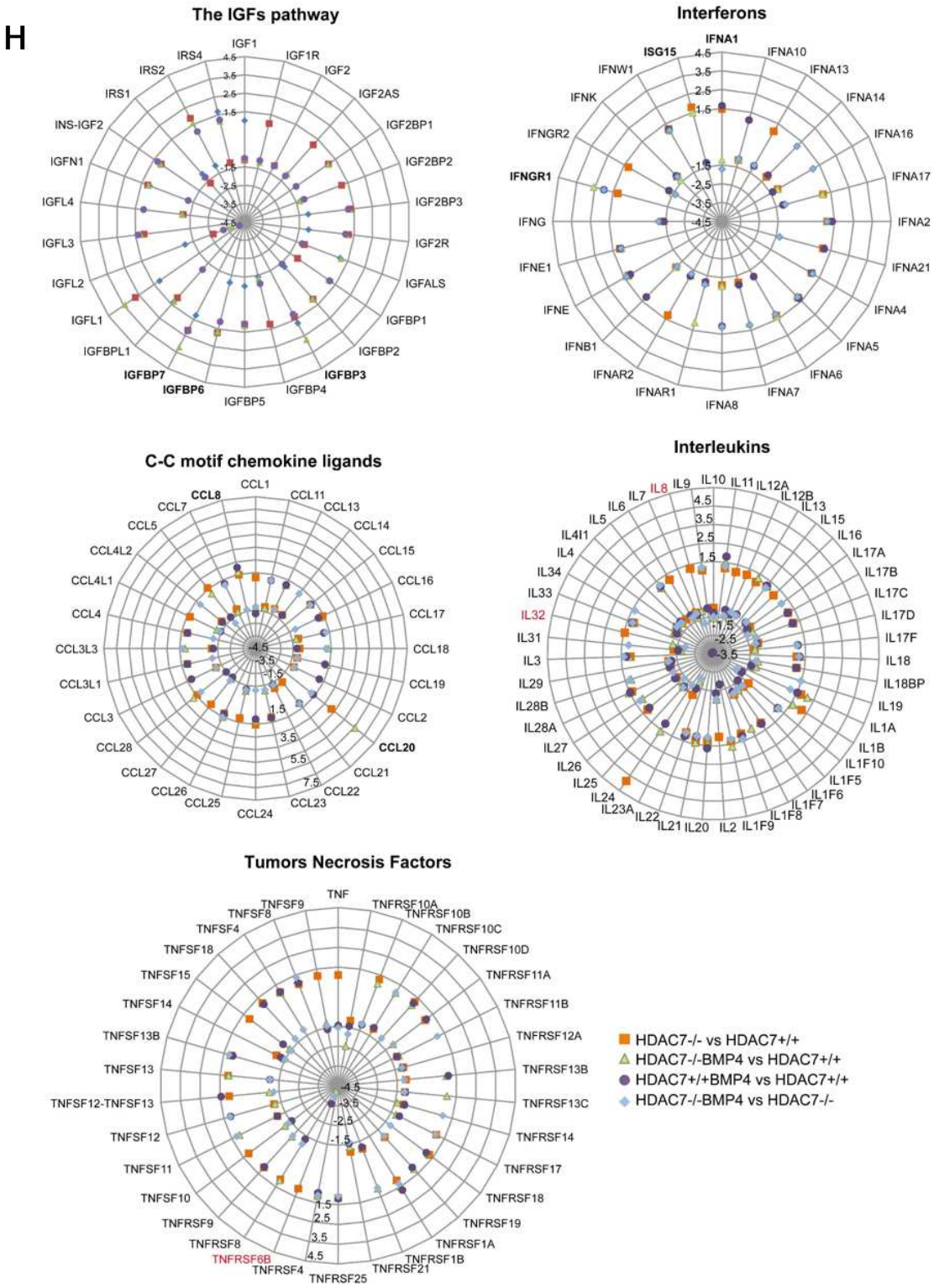

Figure 11H: Radar charts represent gene families and pathways in which HDAC7 is involved.

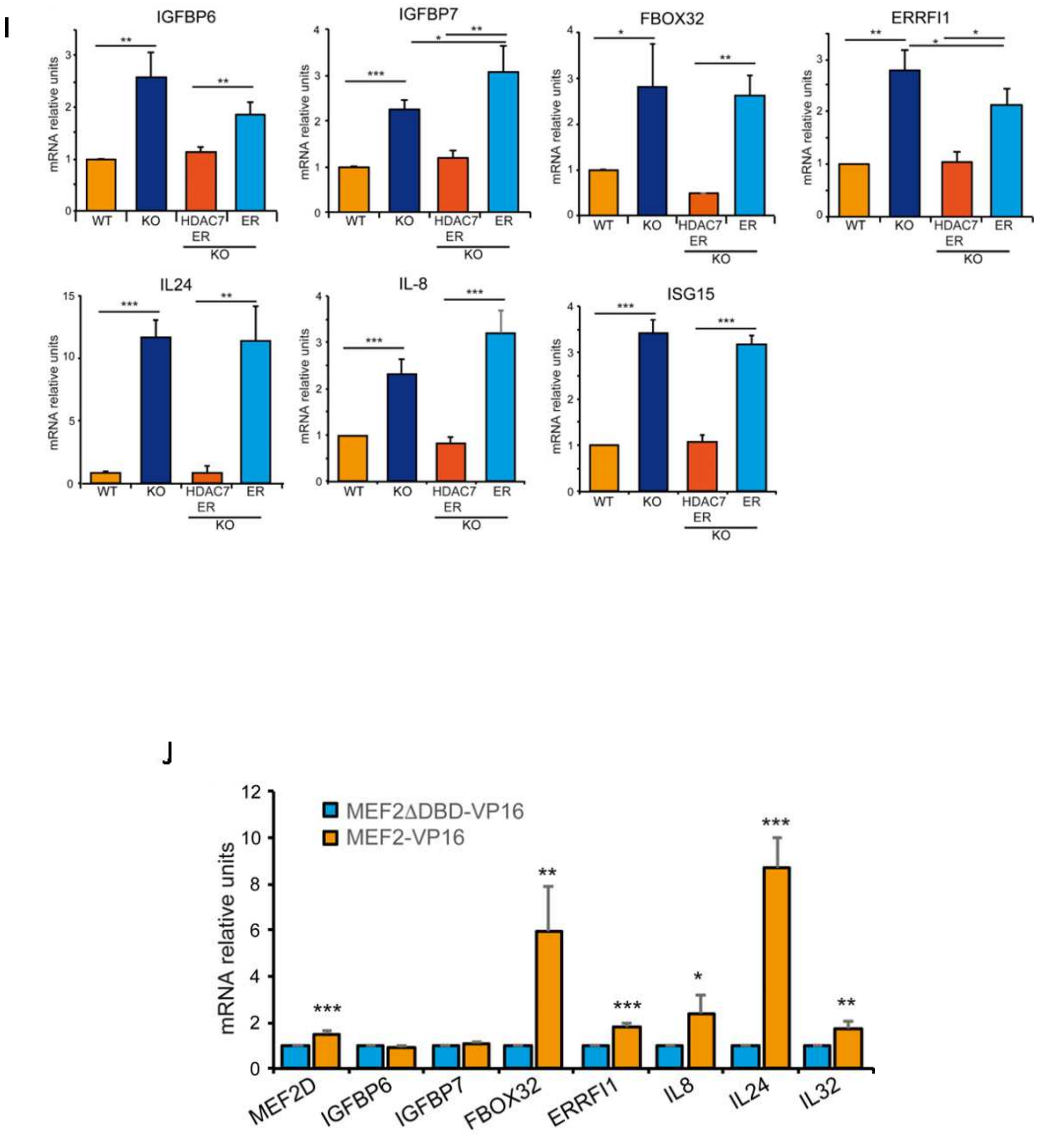

Figure 11: Expression profile of MCF10A HDAC7$^{-/-}$.

I: mRNA expression levels of IGFBP6, IGFBP7, FBOX32, ERRFI1, IL8, IL24 and ISG15 were measured by using qRT-PCR in MCF-10A WT, KO, KO-ER and KO/HDAC7-ER. 4-OHT was added to culture medium the day of seeding.

J: The MEF2 influence on the expression levels of genes up-regulated in MCF10A-KO cells was tested using qRT-PCR. The mRNA expression levels of IGFBP6, IGFBP7, FBOX32, ERRFI1, IL8, IL24 and IL32 in MCF10A expressing MEF2/VP16-ER and MCF10A MEF2/ΔDBD-ER was used as control.

3.6. HDAC7 participates in the maintenance of the stem cell niche environment.

The microarray analysis unveiled, an up-regulation of the IGFBPs in MCF10A-HDAC7$^{-/-}$ cells. Hence, we asked if HDAC7 could have a role in the stem cell niches through the release of niche factors, capable of promoting stemness. IGFBPs interact with IGF-1, causing a reduction of its bio-availability. IGF-1 is considered a factor important for the stem cells renewal and it is released by the stromal cells (Zhao et al., 2017). Considering these evidences, we supposed that HDAC7 represses the transcription of the IGFBPs (in particular IGFBP 3, 6 and 7) to sustain the activation of the IGF-1 pathway in stem cells. We decided to pre-treat WT and KO cells with 15ng/ml of IGF-1 for two days and then we seeded treated cells in ultra-low adhesion plates to allow mammopsheres formation (Figure 12A). After 10 days in culture, we analysed the sphere number. As expected, IGF-1 promoted the formation of mammosphere also in KO cells. However, HDAC7$^{-/-}$ cells pre-treated with IGF-1 still formed less spheres compared to HDAC7$^{-+/+}$ cells. No evident differences were detected between cells pre-treated and cells treated throughout the ULA culture, with 15ng/ml of IGF-1.

It is possible that IGF-1 is less bio-available in KO cells environment and this influences the stem cells growth and renewal.

Since an important fraction of genes under HDAC7 regulation encode for secreted proteins, we supposed that HDAC7 expression can influence the microenvironment by controlling the release of niche factors important for the mammary epithelial stem cells growth/maintenance. In order to investigate this hypothesis, we cultivated HDAC7$^{+/+}$ and HDAC7$^{-/-}$ in ULA condition with different conditioned medium. To perform this experiment, WT and KO cells were seeded in adhesion plates for two days using the mammospheres medium. Conditioned medium was obtained from HDAC7$^{+/+}$ and HDAC7$^{-/-}$ cells and used to cultivate HDAC7$^{+/+}$ and HDAC7$^{-/-}$ mammospheres.

Overall, growing MCF10A in conditioned medium generated higher numbers of mammospheres. Specifically, WT cells plated with the medium conditioned by themself showed a higher number of spheres compared to the WT grown with the conditioned medium from MCF10A KO cells (Figure 12B). The same conditions were repeated with HDAC7$^{-/-}$cells. KO mammospheres grown with the medium conditioned either by the WT and by KO cells generated more spheres respect to HDAC7$^{-/-}$ cells without conditioned medium. In this case the intrinsic nature of the KO is not sufficient to take full advantage from factors released by WT cells in the microenvironment. This experiment proves again the reduced presence of stem progenitors in MCF10A HDAC7 KO cells and the involvement of HDAC7 in the niche factors release. As a matter of fact, the medium conditioned with the WT cells is richer of factors that influence the stem growth compared to the medium conditioned by the KO cells.

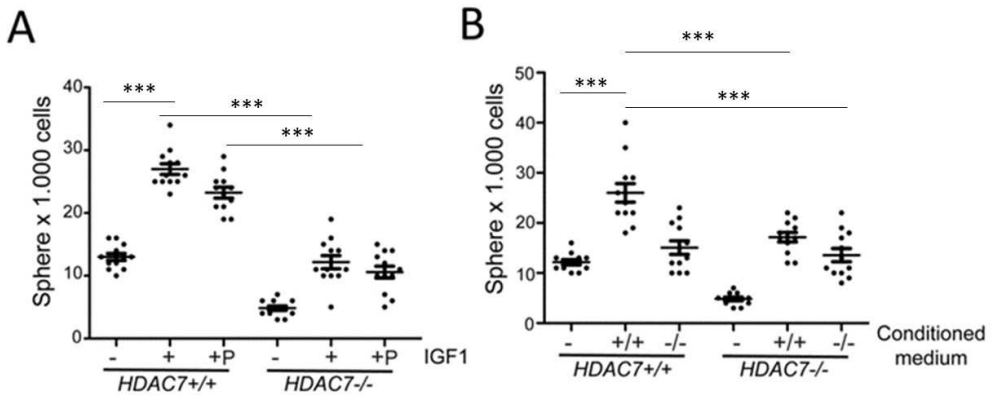

Figure 12: HDAC7 regulates the stem factors releasing inducing stemness maintanence.
A: 3D sphere formation assays was used to demonstrate the IGF-1 effect on MCF10A HDAC7 KO and WT during spheres formation. The plot represents respectively data obtained from WT and KO cells without IGF-1 treatment (-), pre-treatment with 15ng/ml IGF-1 (+) and pre and post seeding treatment (+P). Mammosphere assay was performed seeding 1000 cells for each cell line. After 10 days spheres with > 50µm area were counted using Leica AF 6000LX microscope.
B: 3D sphere formation assay was used to demonstrate the conditioned medium effect on MCF10A WT and KO during spheres formation. The plot represents respectively data obtained from WT and KO cells without conditioned medium (-), conditioned medium with WT (+/+) conditioned medium with KO medium (-/-). Mammosphere assay was performed by seeding 1000 cells for each cell line. After 10 days spheres with > 50µm area were counted using Leica AF 6000LX microscope.

3.7. HDAC7 loss in MCF10A-HRAS negatively impacts on cell proliferation, migration and acini morphology/invasiveness under 3D culture.

Supposing a contribution of HDAC7 in breast cancer progression, normal immortalized breast MCF10A and MCF10A-HDAC7$^{-/-}$ cells were infected with a retroviral vector that promotes a stable expression of HRAS G12V oncogene. First of all, we inspected the RAS expression in WT-HRAS and KO-HRAS cells to verify an equal amount of this protein in both cell lines. Furthermore, we checked the p-ERK levels as marker of RAS activation (Figure 13A). Finally, we evaluated HDAC7 expression. Interestingly we discovered an up-regulation of HDAC7 in RAS-transformed cells (Figure 13A). This data reinforces a hypothetical role of HDAC7 in neoplastic transformation.

In order to test this hypothesis, a BrdU proliferation assay was performed on MCF10A WT, MCF10A-HRASV, MCF10A HDAC7$^{-/-}$ and MCF10A-HRAS-HDAC7$^{-/-}$ (Figure 13B). As expected, RAS expression impacts on cell proliferation. Remarkably, the removal of HDAC7 in a RAS context still strongly impacted on DNA replication. This result makes evident a contribution of HDAC7 to the proliferation also in RAS-transformed cells.

A transwell migration assay was next executed to determine if HDAC7 loss can also influence the migration proprieties of transformed cells. Considering the ratio between the invading cells and their random migration is evident that MCF10A-HRAS-HDAC7$^{-/-}$ cells show less motility compared with the transformed HDAC7 WT cells. This finding reveals that HDAC7 can control the invasiveness of RAS-transformed cells unveiling a role of HDAC7 in cancer cell migration (Figure 13E).

3D culture of RAS-transformed MCF10A cells give rise to acini with an altered morphology, characterized by a stellate shape instead of a spheroid shape (Imbalzano et al., 2009). To investigate a contribution of HDAC7 in this altered morphogenic process, we performed a 3D culture with MCF10A-HRAS and MCF10A-HRAS-HDAC7$^{-/-}$ cells. Acini shape was scored after 8 days and 12 days of culture (Figure 13F). After 8 days on Cultrex, MCF10A-HRAS showed a higher percentage of stellate shaped acini compared to spheroid ones. Opposite results were obtained counting the stellate shaped acini of MCF10A-HRAS-HDAC7$^{-/-}$ cells. At day 12 these results were confirmed, demonstrating an impact of HDAC7 on RAS-transforming capability (Figure 13C and D). Since previous experiments described a role of HDAC7 in stemness, we investigated the involvement of HDAC7 on cancer stem cells growth. To this end, we cultivated in ULA condition MCF10A-WT; MCF10A-HRAS and MCF10A-HRAS-HDAC7$^{-/-}$ cells (Figure 13G). After 10 days in culture mammospheres were counted and analysed. RAS oncogene did not increase the number of generated mammosphere. Interestingly MCF10A-HRAS-HDAC7$^{-/-}$ cells generated a very small number of spheres compared with MCF10A-HRAS cells. This result demonstrates that HDAC7 can control the stem cells potential also in RAS-transformed cells.

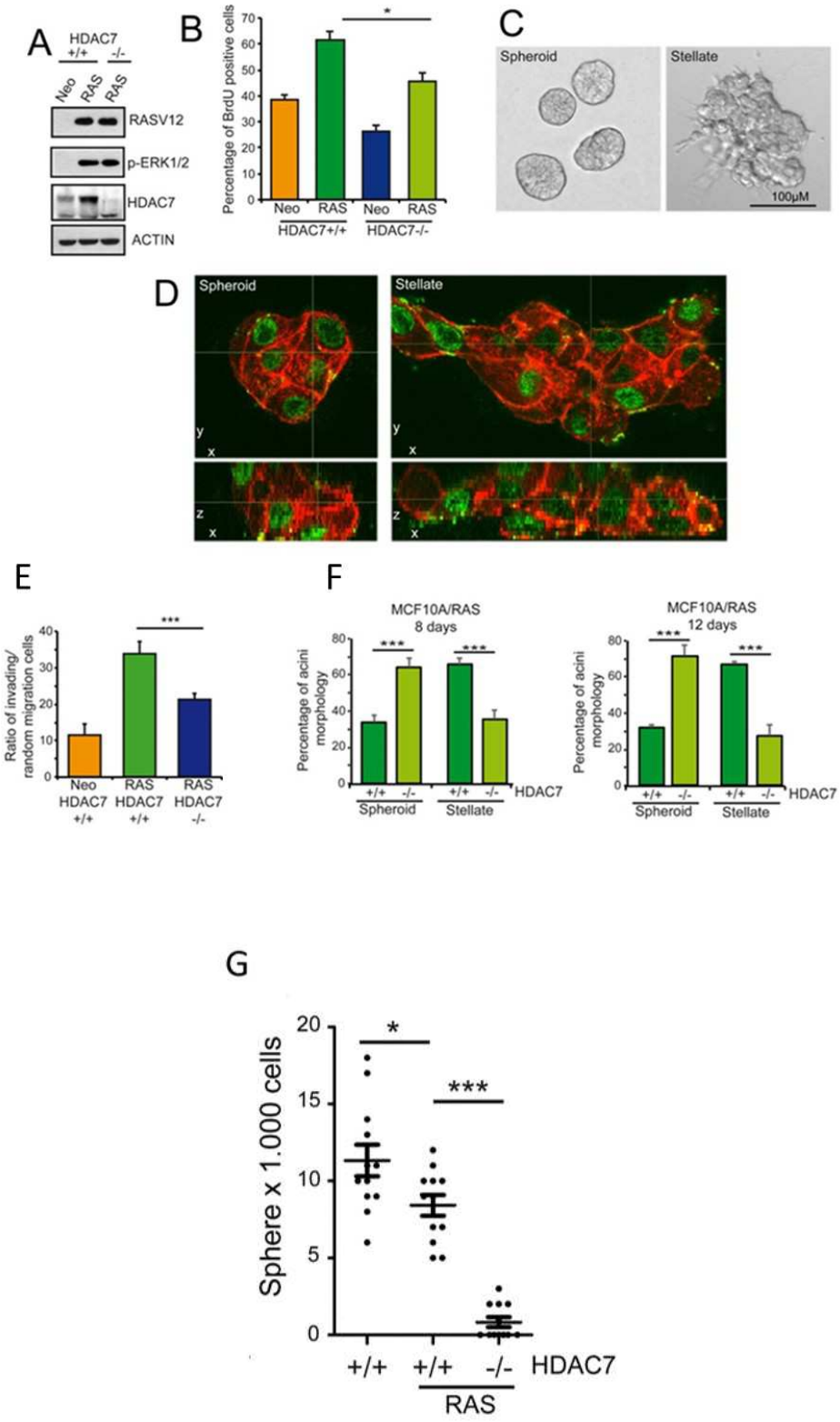

Figure 13: HDAC7 loss reduces the transformed phenotype of MCF10A HRAS cells.
A: Immunoblot analysis of HRASV12, pERK 1/2 and HDAC7 in MCF10A-WT; MCF10A-RASV12 and MCF10A-RASV12-HDAC7$^{-/-}$. Actin was used as loading control.
B: BrdU positive cells percentage of MCF-10A-WT, MCF10A-HDAC7$^{-/-}$. MCF10A-RASV12 and MCF10A- RASV12-HDAC7$^{-/-}$. Cells were seeded and after 24h BrdU was added for 3h then, cells were processed for immunofluorescence.

C: Images representing the difference between spheroid and stellate shaped acini in a 3D culture after 12 days of culture.
D: Confocal images showing the comparison of stellate acini with spheroid acini. AF546-phalloidin was used to stain F-actin and nuclei were stained with anti HMGA2 (green). In lower part, the Z-section is shown as indicated.
E: Transwell migration assay of MCF10A-WT; MCF10A-HRAS and MCF10A-HRAS-HDAC7$^{-/-}$. The percentage of migrating cells was calculated through the ratio between the number of invasive cells and the random migrating cells.
F: Percentage of spheroid and stellate acini in MCF10A-WT; MCF10A-RASV12 and MCF10A-RASV12-HDAC7$^{-/-}$, after 8 and 12 days in culture.
G: 3D sphere formation assay was used to demonstrate the role of HDAC7 role in cancer stem cells. Spheres were obtained from MCF10A-WT; MCF10A-RASV12 and MCF10A-RASV12-HDAC7$^{-/-}$.

4. DISCUSSION

During a woman's life, mammary glands are susceptible to different processes, which include pubertal development, pregnancy, lactation and involution. The mammary gland is represented principally by two different cell types: luminal epithelial cells and basal epithelial cells. The luminal cells are cells involved in ductal and acinar lumen formation of the mammary tree. They represent a heterogeneous population of cells where differentiated and progenitor cells can coexist. They are responsible for milk production, during lactation and they can be interested by the neoplastic transformation. The luminal cells are surrounded by a layer of myoepithelial cells. These cells have contractile properties and are responsible of the basal membrane production.

To investigate the morphogenetic process and the transformation of human mammary gland *in vitro*, a widely used cellular model is represented by the immortalised mammary human epithelial cells MCF10A grown under 3D conditions. (Schmeichel and Bissell, 2003).

Class IIa HDACs are important regulators of cell-fate decision by modulating epigenetic changes linked to gene transcription and silencing (Di Giorgio and Brancolini, 2016). Among the class IIa HDACs, HDAC7 is the most expressed in breast tissue and in particular in MCF10A cells. When ectopically expressed, HDAC7 can influence the proliferation of MCF10A cells (Clocchiatti et al., 2015). Knockout of the *Hdac7* gene in mice results in embryonic lethality due to the disaggregation of the cell-cell junctions and consequent rupture of blood vessels integrity (Chang et al., 2006). To date, the study of the HDAC7 functions in breast human cells was supported only by the shRNA technology (Witt et al., 2017) or by specific HDACs inhibitors (Duong et al., 2008).

The role of HDAC7 in the control of mammary cells proliferation

In this thesis, we took advantage from the CRISPR/Cas9 technology to knockout HDAC7 in MCF10A cells. The project was aimed to characterise the phenotype resulting from HDAC7 abrogation. The difficulty to obtain HDAC7$^{-/-}$ cells, compared with the higher amount of the WT and HDAC7$^{+/-}$ cells achieved, suggests a negative selection induced by the absence of HDAC7. In literature, some evidences describe that HDAC7, in DP thymocytes, is required to maintain normal thymocyte viability (Kasler et al., 2011; Kasler et al., 2017;Hart et al., 2015).

In literature, is well know that class IIa HDACs act on the *CDKN1A* expression (Liu et al., 2009; Mottet et al., 2009). In 2014 was published that MEF2–HDAC axis controls the cell cycle progression by modulating CDKN1A expression in MCF10A (Clocchiatti et al., 2015). In particular, the recruitment of HDAC7 on the *CDKN1A* promoter takes place at the +1.5 Kb region, which is under the MEF2s control (Ernst et al., 2011). This data can explain the up-

regulation of the CDKN1A expression in HDAC7$^{-/-}$ cells. The up regulation of p21 in HDAC7$^{-/-}$ clones, unequivocally supports the idea that HDAC7 influences the cell cycle progression of MCF10A cells, by acting as a repressor of the p21 expression. Further ChIP experiments need to be done in order to understand the regions bound by HDAC7 on the *CDKN1A* promoter.
Risks of off-target effects are the dark side of the CRISPR/Cas9 technique. The possibility of getting unwanted phenotypes by the deletion of different targets from the investigated one, must be taken into account (Zhang et al., 2015;Schaefer et al., 2017). Rescue experiments are considered the most straightforward approach to fight the off-targets effects (Graham and Root, 2015). A strategy is to re-express, in KO cells the target gene, which lack of the PAM sequence, in order to prevent the Cas9 editing (Kwart et al., 2017). Importantly, several evidences in literature describe that, through the time, the Cas9 activity is reduced (Anders and Jinek, 2016; Zhou et al., 2014; Anders and Jinek, 2016) and a rescue of the phenotype with a WT form of the gene is possible (Peng et al., 2016). In this work, the rescue of the phenotype with a WT form of HDAC7 indirectly proved the absence of Cas9 activity in the selected clones. Reintroduction of HDAC7 unambiguously demonstrated the role of HDAC7 in the control of proliferation and CDKN1A expression in MCF10A cells.

The role of HDAC7 in the control of the stem cell properties of MCF10A

Stem cells are necessary to sustain lobules and ducts growth during puberty and pregnancy (Petersen and Polyak, 2010; Zhao et al., 2017). Adult stem cells are distributed long the mammary gland among differentiated epithelial cells (Joshi et al., 2012). To date, evidences that illustrate a role of class IIa HDACs in stemness maintenance are limited. Zhuang et al., in 2013, explained for the first time, how class IIa HDACs can regulates cell reprogramming. It was described that in fibroblasts expressing the Yamanaka factors, class IIa HDACs, through the repression of MEF2, support the reprogramming of these cells from differentiated cells to iPSCs (Zhuang et al., 2013).
More recent data, proposed a relevant contribution of HDAC7 to breast stem maintenance. Knock-down of HDAC7, negatively impacts on stem cells growth (Witt et al., 2017). We proved that HDAC7 impacts on sphere formation of MCF10A-HDAC7$^{-/-}$ cells, an assay used to evaluate the number of stem cells (Eirew et al., 2008). HDAC7$^{-/-}$ cells generated less mammospheres and they were smaller compared to WT. Hence, HDAC7 not only controls cell proliferation (dimension of sphere) but also the number of cells capable of generating these structures.
CD44 and CD24 have been used extensively in combination or with other putative markers to identify stem cells in a cell population. We applied the cytometric analysis to compare the percentage of the CD44^{high}/CD24^{low} between MCF10A HDAC7$^{-/-}$ and HDAC7$^{+/+}$ cells. The small but significant reduced number of CD44^{high}/CD24^{low} cells in the HDAC7$^{-/-}$ population, compared to HDAC7$^{+/+}$ further suggests a role of HDAC7 in progenitors preservation. It was

proved that BMP4 treatment is sufficient to increase stemness in MCF10A cells (Clément et al., 2017). We confirmed this observation. However, although mammospheres were formed also in HDAC7$^{-/-}$ in response to BMP4 treatment, they were always less numerous compared to WT cells.

The microarray studies discovered an up-regulation of genes involved in the inflammatory response in HDAC7$^{-/-}$ cells. IL24, IL8 and CCL20 were among the highest up-regulated genes in MCF10A HDAC7$^{-/-}$ cells. Furthermore, also the interferon-γ was induced in HDAC7$^{-/-}$ cells, as proved by the up-regulation of ISG15. Future experiments will be conducted to better understand the role of HDAC7 in the repression of the inflammatory response.

Importantly, much of the pro-inflammatory response triggered in HDAC7 KO cells is blunted after BMP4 treatment, with exception of CCL20. Thus, the partial effect on spheres formation in HDAC7 KO cells could depend on the suppression of the inflammatory response (Chang et al., 2016; Yeh et al., 2016).

It was reported that class IIa HDACs promotes muscular atrophy by repressing Dach2, by activating the transcription of Myogenin and its targets, the E3-ligase Atrogin-1/FBOX32 and MURF1 (Tintignac et al., 2015). Our microarray analysis showed an up-regulation of the FBOX32 gene in HDAC7 KO cells.

Another gene significantly up-regulated in MCF10A HDAC7$^{-/-}$ cells was ERRFI1, a negative regulator of several EGFR family members. Interestingly, ERRFI1 expression was previously demonstrated being sensitive to SAHA treatment and HDAC4 expression (Clocchiatti et al., 2013; Dudakovic et al., 2013).

Members of the IGFBPs family (IGFBP3,6,7) were also significantly induced in HDAC7$^{-/-}$ cells. The IGFBPs are involved in the recruitment of free IGF-1 (Hwa et al., 1999). In literature the role of IGF-1 in stemness is well known (Le Coz et al., 2016; Farabaugh et al., 2015). As a matter of fact, it was discovered that IGFBP6, alters skeletal muscle differentiation of human mesenchymal stem cells (Aboalola and Han, 2017). Specifically, experimental evidences describe that IGFBP6 exposure activates the muscle lineage commitment by increasing the expression of muscle-specific markers such as MyoD, MyoG, and MHC.

In literature, the contribution of IGFBP7 in stem niche was recently reported. In *Drosophila melanogaster,* the homolog of IGFBP7 is called ImpL2. The down-regulation of ImpL2 prevents InR activation in somatic stem cells and most importantly it prevents differentiation by inhibiting PI3K/Tor pathway activity (Amoyel et al., 2016). Finally, the important contribution of IGF-1 network in stemness regulation found validation in IGF-1 itself. IGF-1 can be considered as a niche factor released by the stem niche cells to increase the stem cells renewal (Zhao et al., 2017).

The regulation of IGFBPs in HDAC7 KO cells unveils a new role of HDAC7 in the regulation of the stem niche factors release. In fact, we demonstrated that HDAC7 can down-regulate the

expression of IGFBPs, which are mandatory to sustain the IGF-1 signalling and thus recovering spheres formation potential.

As predicted, spheres that have been obtained from HDAC7$^{-/-}$ treated with IGF-1 were less than the control. A phenomenon that could be explained by the up-regulation of IGFBPs in HDAC7$^{-/-}$ cells.

All these data suggest two possible functions of HDAC7 in stem cell growth and self-renewal. On one side, we could hypothesize a role of HDAC7 in sustaining different pathways included the IGF-1 signalling pathway, contributing to stem cells fitness and spheres formation (Figure 14). This hypothesis points to an intrinsic role of HDAC7 as epigenetic regulators in the epithelial stem cells being part of the IGF-1 signalling pathway (but not only). This intrinsic role could also explain the partial rescue of the sphere formation in BMP4, IGF-1 and WT conditioned medium from HDAC7$^{-/-}$ cells. On the other side, HDAC7 can be undoubtedly be important for the IGF-1 availability within the microenvironment, through the suppression of IGFBPs and of an inflammatory response. The experiments performed with the conditioned medium confirmed this function of HDAC7. In fact, the medium conditioned from HDAC7$^{+/+}$ cells is richer of factors that influence the stem growth compared to medium conditioned from HDAC7$^{-/-}$ cells.

If we consider HDAC7 in the mammary gland context, we can suppose that this protein acts within stem cells by sustaining the growth of this tissue. In addition, through the influence on the microenvironment, HDAC7 can contribute to the release of niche factors (Figure 14). Further analysis will be necessary to investigate about the recruitment of HDAC7 on the promoters of the IGFBPs. We confirmed with the expression of a conditionally active form of MEF2D that the IGFBP6 and 7 expression is not directly regulated by MEF2D. Additional transcription factors such FOXA1 and RXRα could be involved in the *IGFB*Ps transcription and being under the supervision of HDAC7 to orchestrate the necessary epigenetic changes (Imamura et al., 2012).

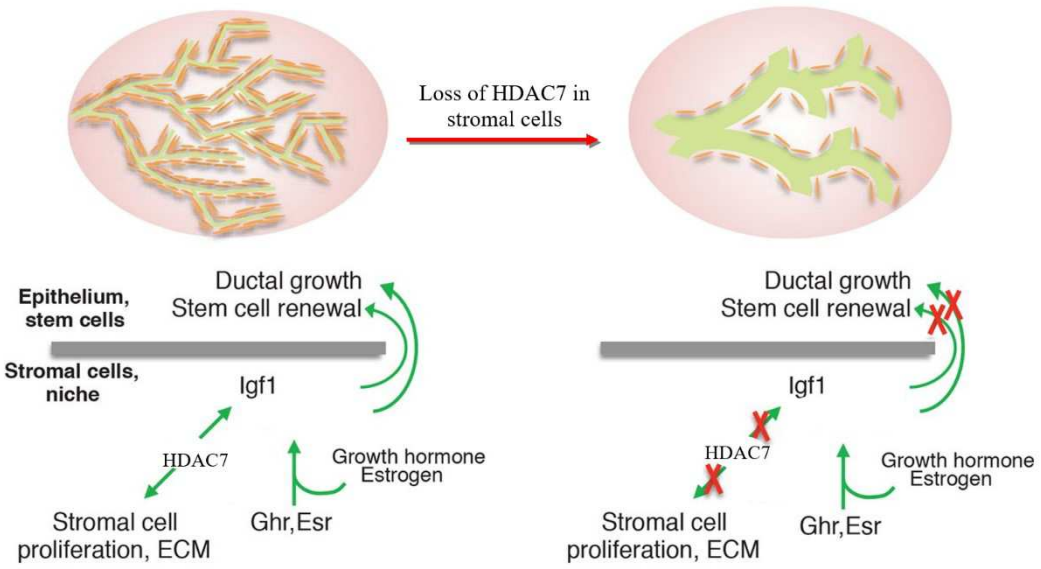

Figure 14: Rapresentation of the HDAC7 possible effect on the niche microenvironment.

HDAC7 and RAS-dependent transformation

The role of HDAC7 in neoplastic transformation is still controversial. Evidences describing HDAC7 as an oncogene (Ouaïssi et al., 2014; Zhu et al., 2011) are questioned by other data suggesting a role of HDAC7 as a tumour suppressor (Margariti et al., 2010). In 2015 the pro-growth effect of HDAC7 in epithelial cells was confirmed. In fact, a super-repressive version of HDAC7 induced the formation of acini with a higher number of nuclei per acinus in 3D culture (Clocchiatti et al., 2015). To better understand the function of HDAC7 in transformed cells and its contribution in the neoplastic transformation, we generated MCF10A WT and HDAC7$^{-/-}$ expressing HRAS oncogene.

Interestingly, the expression of RAS increased the expression of HDAC7 in MCF10A-HRAS. Past discoveries described a similar effect on HDAC7 expression induced by another oncogene, HER2 (Clocchiatti et al., 2015). Furthers analysis will clarify at which level the regulation of HDAC7 expression is operated by RAS. Importantly, the RAS transformed phenotype was influenced by the HDAC7 expression. This open new hypothesis on the cooperation between HDAC7 and oncogenes to promote proliferation, invasiveness and altered morphogenic processes. These funding make real the possibility to consider HDAC7 as a carrier of the transformed phenotype in malignant cells. Future generation of HDAC7 KO in breast cancer cell lines will help to clarify the role of the HDAC7 in breast cancer.

It is well known, in literature, that cancer stem cells are fundamental in the cancer progression and relapse after treatment (Chang, 2016; Li et al., 2015). Considering the involvement of HDAC7 in stemness, we asked if HDAC7 could be important not only in stem cells but also in

cancer stem cells development and self-renewal. Seeding in ULA conditions MCF10A-HRAS and MCF10A-HRAS-HDAC7$^{-/-}$ cells, we obtained a small number of spheres. This result demonstrates that: a) RAS boosts the proliferative and invasive feature of cells but not the stemness proprieties, b) HDAC7 loss impacts on the stemness also in transformed cells.

In conclusion, our results demonstrate an involvement of HDAC7 in the proliferation of mammary epithelial cells. Moreover, it was better investigated the contribution of HDAC7 to mammary epithelial stemness and in neoplastic transformation. Certainly, additional steps will be important to consolidate the idea of HDAC7 as a therapeutic target in breast cancer. Further studies will be necessary to define the HDAC7 role in neoplastic transformation, with the aim to generate HDAC7 specific inhibitors for anti-cancer therapy.

5. BIBLIOGRAPHY

Aboalola, D., and Han, V.K.M. (2017). Insulin-Like Growth Factor Binding Protein-6 Alters Skeletal Muscle Differentiation of Human Mesenchymal Stem Cells. *2017*.

Addis, R.C., Prasad, M.K., Yochem, R.L., Zhan, X., Sheets, T.P., Axelman, J., Patterson, E.S., and Shamblott, M.J. (2010). OCT3/4 regulates transcription of histone deacetylase 4 (Hdac4) in mouse embryonic stem cells. J. Cell. Biochem. *111*, 391–401.

Al-Hajj, M., Wicha, M.S., Benito-Hernandez, A., Morrison, S.J., and Clarke, M.F. (2003). Prospective identification of tumorigenic breast cancer cells. Proc. Natl. Acad. Sci. *100*, 3983–3988.

Amoyel, M., Hillion, K.-H., Margolis, S.R., and Bach, E.A. (2016). Somatic stem cell differentiation is regulated by PI3K/Tor signaling in response to local cues. Development *143*, 3914–3925.

Anders, C., and Jinek, M. (2016). Europe PMC Funders Group In vitro Enzymology of Cas9. 1–20.

Azagra, A., Román-González, L., Collazo, O., Rodríguez-Ubreva, J., de Yébenes, V.G., Barneda-Zahonero, B., Rodríguez, J., Castro de Moura, M., Grego-Bessa, J., Fernández-Duran, I., et al. (2016). In vivo conditional deletion of HDAC7 reveals its requirement to establish proper B lymphocyte identity and development. J. Exp. Med. jem.20150821.

Bakin, R.E., and Jung, M.O. (2004). Cytoplasmic sequestration of HDAC7 from mitochondrial and nuclear compartments upon initiation of apoptosis. J. Biol. Chem. *279*, 51218–51225.

Barneda-Zahonero, B., Collazo, O., Azagra, A., Fernández-Duran, I., Serra-Musach, J., Islam, A.B.M.M.K., Vega-García, N., Malatesta, R., Camós, M., Gómez, A., et al. (2015). The transcriptional repressor HDAC7 promotes apoptosis and c-Myc downregulation in particular types of leukemia and lymphoma. Cell Death Dis. *6*, e1635.

Besson, A., Dowdy, S.F., and Roberts, J.M. (2008). CDK Inhibitors: Cell Cycle Regulators and Beyond. Dev. Cell *14*, 159–169.

Black, B.L., and Olson, E.N. (1998). Transcriptional Control of Muscle Development By Myocyte Enhancer Factor-2 (Mef2) Proteins. Annu. Rev. Cell Dev. Biol *14*, 167–196.

Bolomsky, A., Hose, D., Schreder, M., Seckinger, A., Lipp, S., Klein, B., Heintel, D., Ludwig, H., and Zojer, N. (2015). Insulin like growth factor binding protein 7 (IGFBP7) expression is linked to poor prognosis but may protect from bone disease in multiple myeloma. J. Hematol. Oncol. *8*, 10.

Bonnet, D., and Dick, J.E. (1997). Human acute myeloid leukemia is organized as a hierarchy that originates from a primitive hematopoietic cell. Nat. Med. *3*, 730–737.

Bradley, E.W., Carpio, L.R., Olson, E.N., and Westendorf, J.J. (2015). Histone deacetylase 7 (Hdac7) suppresses chondrocyte proliferation and ??-catenin activity during endochondral ossification. J. Biol. Chem. *290*, 118–126.

Bradner, J.E., West, N., Grachan, M.L., Greenberg, E.F., Haggarty, S.J., Warnow, T., and Mazitschek, R. (2010). NIH Public Access. *6*, 238–243.

Campbell, J.J., and Watson, C.J. (2009). Three-dimensional culture models of mammary gland. Organogenesis *5*, 43–49.

Canté-Barrett, K., Pieters, R., and Meijerink, J.P.P. (2013). Myocyte enhancer factor 2C in hematopoiesis and leukemia. Oncogene 403–410.

Cernotta, N., Clocchiatti, A., Florean, C., and Brancolini, C. (2011). Ubiquitin-dependent degradation of HDAC4, a new regulator of random cell motility. Mol. Biol. Cell *22*, 278–289.

Chang, J.C. (2016). Cancer stem cells Role in tumor growth, recurrence, metastasis, and treatment resistance. *0*.

Chang, H.H., Bong, S.J., Kao, H.Y., and Jin, Z.G. (2008). VEGF stimulates HDAC7 phosphorylation and cytoplasmic accumulation modulating matrix metalloproteinase expression and angiogenesis. Arterioscler. Thromb. Vasc. Biol. *28*, 1782–1788.

Chang, S., Young, B.D., Li, S., Qi, X., Richardson, J.A., and Olson, E.N. (2006). Histone Deacetylase 7 Maintains Vascular Integrity by Repressing Matrix Metalloproteinase 10. Cell *126*, 321–334.

Clément, F., Xu, X., Donini, C.F., Clément, A., Omarjee, S., Delay, E., Treilleux, I., Fervers, B., Le Romancer, M., Cohen, P.A., et al. (2017). Long-term exposure to bisphenol A or benzo(a)pyrene alters the fate of human mammary epithelial stem cells in response to BMP2 and BMP4, by pre-activating BMP signaling. Cell Death Differ. *24*, 155–166.

Clocchiatti, A., Florean, C., and Brancolini, C. (2011). Class IIa HDACs: From important roles in differentiation to possible implications in tumourigenesis. J. Cell. Mol. Med. *15*, 1833–1846.

Clocchiatti, A., Di Giorgio, E., Ingrao, S., Meyer-Almes, F.J., Tripodo, C., and Brancolini, C. (2013). Class IIa HDACs repressive activities on MEF2-depedent transcription are associated with poor prognosis of ER+ breast tumors. FASEB J. *27*, 942–954.

Clocchiatti, A., Di Giorgio, E., Viviani, G., Streuli, C., Sgorbissa, A., Picco, R., Cutano, V., and Brancolini, C. (2015). The MEF2-HDAC axis controls proliferation of mammary epithelial cells and acini formation in vitro. J. Cell Sci. *128*, 3961–3976.

Compagnucci, C., Barresi, S., Petrini, S., Bertini, E., and Zanni, G. (2015). Rho-kinase signaling controls nucleocytoplasmic shuttling of class IIa Histone Deacetylase (HDAC7) and transcriptional activation of orphan nuclear receptor NR4A1. Biochem. Biophys. Res. Commun. *459*, 179–183.

Le Coz, V., Zhu, C., Devocelle, A., Vazquez, A., Boucheix, C., Azzi, S., Gallerne, C., Eid, P., Lecourt, S., and Giron-Michel, J. (2016). IGF-1 contributes to the expansion of melanoma-initiating cells through an epithelial-mesenchymal transition process. Oncotarget *7*, 82511–82527.

Dairkee, S., and Heid, H.W. (1993). Cytokeratin profile of immunomagnetically separated epithelial subsets of the human mammary gland. Vitr. Cell. Dev. Biol. - Anim. *29*, 427–432.

Debnath, J., Mills, K.R., Collins, N.L., Reginato, M.J., Muthuswamy, S.K., and Brugge, J.S. (2002). The role of apoptosis in creating and maintaining luminal space within normal and oncogeneexpressing mammary acini. Cell *111*, 29–40.

Delcuve, G.P., Khan, D.H., and Davie, J.R. (2012). Roles of histone deacetylases in epigenetic regulation: emerging paradigms from studies with inhibitors. Clin. Epigenetics *4*, 5.

Dequiedt, F., Kasler, H., Fischle, W., Kiermer, V., Weinstein, M., Herndier, B.G., and Verdin, E. (2003). HDAC7, a thymus-specific class II histone deacetylase, regulates Nur77 transcription and TCR-mediated apoptosis. Immunity *18*, 687–698.

Dequiedt, F., Van Lint, J., Lecomte, E., Van Duppen, V., Seufferlein, T., Vandenheede, J.R., Wattiez, R., and Kettmann, R. (2005). Phosphorylation of histone deacetylase 7 by protein kinase D mediates T cell receptor-induced Nur77 expression and apoptosis. J. Exp. Med. *201*, 793–804.

Dick, J.E. (2003). Breast cancer stem cells revealed. Proc. Natl. Acad. Sci. U. S. A. *100*, 3547–3549.

Dijkstra, J., France, J., Dhanoa, M.S., Maas, J.A., Hanigan, M.D., Rook, A.J., and Beever, D.E. (1997). A Model to Describe Growth Patterns of the Mammary Gland During Pregnancy and Lactation. J. Dairy Sci. *80*, 2340–2354.

Dressel, U., Bailey, P.J., Wang, S.C.M., Downes, M., Evans, R.M., and Muscat, G.E.O. (2001). A Dynamic Role for HDAC7 in MEF2-mediated Muscle Differentiation. J. Biol. Chem. *276*, 17007–17013.

Du, P., Kibbe, W.A., and Lin, S.M. (2008). lumi: A pipeline for processing Illumina microarray. Bioinformatics *24*, 1547–1548.

Duong, V., Bret, C., Altucci, L., Mai, A., Duraffourd, C., Loubersac, J., Harmand, P.-O., Bonnet, S., Valente, S., Maudelonde, T., et al. (2008). Specific activity of class II histone deacetylases in human breast cancer cells. Mol. Cancer Res. *6*, 1908–1919.

Duru, N., Gernapudi, R., Lo, P., Yao, Y., Zhang, Y., and Zhou, Q. (2016). Characterization of the CD49f / CD44 / CD24 single-cell derived stem cell population in basal-like DCIS cells. *7*.

Eirew, P., Stingl, J., Raouf, A., Turashvili, G., Aparicio, S., Emerman, J.T., and Eaves, C.J. (2008). A method for quantifying normal human mammary epithelial stem cells with in vivo regenerative ability. Nat. Med. *14*, 1384–1389.

Ernst, J., Kheradpour, P., Mikkelsen, T.S., Shoresh, N., Ward, L.D., Epstein, C.B., Zhang, X., Wang, L., Issner, R., Coyne, M., et al. (2011). Mapping and analysis of chromatin state dynamics in nine human cell types. Nature *473*, 43–49.

Fabregat, I., Malfettone, A., and Soukupova, J. (2016). New Insights into the Crossroads between EMT and Stemness in the Context of Cancer. J. Clin. Med. *5*, 37.

Farabaugh, S.M., Boone, D.N., and Lee, A. V. (2015). Role of IGF1R in breast cancer subtypes, stemness, and lineage differentiation. Front. Endocrinol. (Lausanne). *6*, 1–12.

Ferraro, F., Lo Celso, C., and Scadden, D. (2010). Adult Stem cells and their niches. Adv Exp Med Biol. *695*, 155–168.

Fischle, W., Dequiedt, F., Hendzel, M.J., Guenther, M.G., Lazar, M.A., Voelter, W., Verdin, E., Francisco, S., and Tg, A. (2002). Enzymatic Activity Associated with Class II HDACs Is Dependent on a Multiprotein Complex Containing HDAC3 and SMRT / N-CoR. Mol. Cell *9*, 45–57.

Flavell, S.W. (2006). Activity-Dependent Regulation of MEF2 Transcription Factors Suppresses Excitatory Synapse Number. Science (80-.). *311*, 1008–1012.

Fox, S.B., Fawcett, J., Jackson, D.G., Collins, I., Gatter, K.C., Harris, A.L., Gearing, A., and Simmons, D.L. (1994). Normal Human Tissues, in Addition to Some Tumors, Express Multiple Different CD44 Isoforms. Cancer Res. *54*, 4539–4546.

Fridriksdottir, Agla J.R., Petersen, O.W.. (2011). Mammary gland stem cells: current status and future challenges AGLA. Int J Dev Biol *55*, 719–729.

Fuchs, G.G. and E. (2005). Mice in the world of stem cell biology. Nat. Genet. *37*, 1201–1206.

G, P., M, M., and Brancolini, C. (2004). Caspase-dependent Regulation of Histone Deacetylase 4 Nuclear-Cytoplasmic Shuttling Promotes Apoptosis. Mol. Biol. Cell *15*, 3751–3737.

Gao, C., Li, X., Lam, M., Liu, Y., Chakraborty, S., and Kao, H.Y. (2006). CRM1 mediates nuclear export of HDAC7 independently of HDAC7 phosphorylation and association with 14-3-3s. FEBS Lett. *580*, 5096–5104.

Gao, L., Cueto, M.A., Asselbergs, F., and Atadja, P. (2002). Cloning and functional characterization of HDAC11, a novel member of the human histone deacetylase family. J. Biol. Chem. *277*, 25748–25755.

Gao, M.-Q., Choi, Y.-P., Kang, S., Youn, J.H., and Cho, N.-H. (2010). CD24+ cells from hierarchically organized ovarian cancer are enriched in cancer stem cells. Oncogene *29*, 2672–2680.

Ginestier, C., Hur, M.H., Charafe-Jauffret, E., Monville, F., Dutcher, J., Brown, M., Jacquemier, J., Viens, P., Kleer, C.G., Liu, S., et al. (2007). ALDH1 Is a Marker of Normal and Malignant Human Mammary Stem Cells and a Predictor of Poor Clinical Outcome. Cell Stem Cell *1*, 555–567.

Di Giorgio, E., and Brancolini, C. (2016). Regulation of class IIa HDAC activities: it is not only matter of subcellular localization. Epigenomics *8*, 251–269.

Di Giorgio, E., Gagliostro, E., Clocchiatti, A., and Brancolini, C. (2015). The control operated by the cell cycle machinery on MEF2 stability contributes to the downregulation of CDKN1A and entry into S phase. Mol. Cell. Biol. *35*, 1633–1647.

Di Giorgio, E., Franforte, E., Cefalù, S., Rossi, S., Dei Tos, A.P., Brenca, M., Polano, M., Maestro, R., Paluvai, H., Picco, R., et al. (2017). The co-existence of transcriptional activator and transcriptional repressor MEF2 complexes influences tumor aggressiveness. PLoS Genet. *13*, 1–29.

Glukhova, M., Koteliansky, V., Sastre, X., and Thiery, J.P. (1995). Adhesion systems in normal breast and in invasive breast carcinoma. Am. J. Pathol. *146*, 706–716.

Graham, D.B., and Root, D.E. (2015). Resources for the design of CRISPR gene editing experiments. Genome Biol. *16*, 260.

Gregoretti, I. V., Lee, Y.M., and Goodson, H. V. (2004). Molecular evolution of the histone deacetylase family: Functional implications of phylogenetic analysis. J. Mol. Biol. *338*, 17–31.

Grozinger, C.M., and Schreiber, S.L. (2000). Regulation of histone deacetylase 4 and 5 and transcriptional activity by 14-3-3-dependent cellular localization. Proc. Natl. Acad. Sci. U. S. A. *97*, 7835–7840.

Gudjonsson, T., Adriance, M.C., Sternlicht, M.D., Petersen, O.W., and Bissell, M.J. (2009). NIH Public Access. J. Mammary Gland Biol. Neoplasia *10*, 261–272.

Gusterson, B.A., Warburton, M.J., Mitchell, D., Ellison, M., Neville, A.M., and Rudland, P.S. (1982). Distribution of myoepithelial cells and basement membrane proteins in the normal breast and in benign and malignant breast diseases. Cancer Res *42*, 4763–4770.

Haaksma, C.J., Schwartz, R.J., and Tomasek, J.J. (2011). Myoepithelial Cell Contraction and Milk Ejection Are Impaired in Mammary Glands of Mice Lacking Smooth Muscle Alpha-Actin 1. Biol. Reprod. *85*, 13–21.

Haigis, M.C., and Guatente, L.P. (2006). Mammalian sirtuins-energing role in physiology, aging, and calorie restriction. Genes Dev. *20*, 2913–2921.

Hanks, S.K. (2003). Genomic analysis of the eukaryotic protein kinase superfamily: a perspective. Genome Biol. *4*, 111.

Hart, T., Chandrashekhar, M., Aregger, M., Steinhart, Z., Brown, K.R., MacLeod, G., Mis, M., Zimmermann, M., Fradet-Turcotte, A., Sun, S., et al. (2015). High-Resolution CRISPR Screens Reveal Fitness Genes and Genotype-Specific Cancer Liabilities. Cell *163*, 1515–1526.

Hennessy, B.T., Stemke-hale, K., Gilcrease, M.Z., Krishnamurthy, S., Lee, J., Fridlyand, J., Agarwal, R., Joy, C., Liu, W., Stivers, D., et al. (2010). NIH Public Access. *69*, 4116–4124.

Herschkowitz, J.I., Simin, K., Weigman, V.J., Mikaelian, I., Usary, J., Hu, Z., Rasmussen, K.E., Jones, L.P., Assefnia, S., Chandrasekharan, S., et al. (2007). Identification of conserved gene expression features between murine mammary carcinoma models and human breast tumors. Genome Biol. *8*, R76.

Houdebine, L.-M., Djiane, J., Dusanter-Fourt, I., Martel, P., Kelly, P.A., Devinoy, E., and Servely, J.-L. (1985). Hormonal Action Controlling Mammary Activity. J. Dairy Sci. *68*, 489–500.

Hu, M., Yao, J., Carroll, D.K., Weremowicz, S., Chen, H., Carrasco, D., Richardson, A., Violette, S., Nikolskaya, T., Bauerlein, E.L., et al. (2008). Regulation of In Situ to Invasive Breast Carcinoma Transition. Cancer Cell *13*, 394–406.

Hurley, W.L. (1989). Mammary gland function during involution. J. Dairy Sci. *72*, 1637–1646.

Hwa, V., Oh, Y., and Rosenfeld, R.G. (1999). The Insulin-Like Growth Factor-Binding Protein (IGFBP) Superfamily [1]. Endocr. Rev. *20*, 761–787.

Imamura, Y., Sakamoto, S., Endo, T., Utsumi, T., Fuse, M., Suyama, T., Kawamura, K., Imamoto, T., Yano, K., Uzawa, K., et al. (2012). FOXA1 promotes tumor progression in prostate cancer via the insulin-like growth factor binding protein 3 pathway. PLoS One *7*, 1–14.

Imbalzano, K.M., Tatarkova, I., Imbalzano, A.N., and Nickerson, J.A. (2009). Increasingly transformed MCF-10A cells have a progressively tumor-like phenotype in three-dimensional basement membrane culture. Cancer Cell Int. *9*, 7.

Javed, A., and Lteif, A. (2013). Development of the human breast. Semin. Plast. Surg. *27*, 5–12.

Jensen, E.D., Schroeder, T.M., Bailey, J., Gopalakrishnan, R., and Westendorf, J.J. (2008). Histone deacetylase 7 associates with Runx2 and represses its activity during osteoblast maturation in a deacetylation-independent manner. J. Bone Miner. Res. *23*, 361–372.

Jones, D.L., and Wagers, A.J. (2008). No place like home: anatomy and function of the stem cell niche. Nat. Rev. Mol. Cell Biol. *9*, 11–21.

Joshi, P.A., Di Grappa, M.A., and Khokha, R. (2012). Active allies: Hormones, stem cells and the niche in adult mammopoiesis. Trends Endocrinol. Metab. *23*, 299–309.

Kai, Y., Peng, W., Ling, W., Jiebing, H., and Zhuan, B. (2014). Reciprocal effects between microRNA-1405p and ADAM10 suppress migration and invasion of human tongue cancer cells. Biochem. Biophys. Res. Commun. *448*, 308–314.

Kao, H., Downes, M., Ordentlich, P., and Evans, R.M. (2000). Isolation of a novel histone deacetylase reveals that class I and class II deacetylases promote SMRT-mediated repression Isolation of a novel histone deacetylase reveals that class I and class II deacetylases promote SMRTmediated repression. Genes Dev. *14*, 55–66.

Kasler, H.G., Young, B.D., Mottet, D., Lim, H.W., Collins, A.M., Olson, E.N., and Verdin, E. (2011). Histone Deacetylase 7 Regulates Cell Survival and TCR Signaling in CD4/CD8 Double-Positive Thymocytes. J. Immunol. *186*, 4782–4793.

Kasler, H.G., Lee, I.S., Lim, H.W., Verdin, E., and Francisco, S. (2017). Histone Deacetylase 7 Mediates Tissue-Specific Autoimmunity via Control of Innate Effector Function in Invariant Natural Killer T-Cells. 1–49.

Kleinberg, D.L. (1997). Early mammary development: growth hormone and IGF-1. J. Mammary Gland Biol. Neoplasia *2*, 49–57.

Kobayashi, K., Tsugami, Y., Matsunaga, K., Oyama, S., Kuki, C., and Kumura, H. (2016). Prolactin and glucocorticoid signaling induces lactation-specific tight junctions concurrent with ??-casein expression in mammary epithelial cells. Biochim. Biophys. Acta - Mol. Cell Res. *1863*, 2006–2016.

Kristin A. Plichta, Jessica L. Mathers, Shelley A. Gestl, Adam B. Glick2,4, and, and Gunther, E.J. (2012). Basal but not luminal mammary epithelial cells require PI3K/ mTOR signaling for Ras-driven overgrowth. Cancer Res. *31*, 115–128.

Kuperwasser, C., Chavarria, T., Wu, M., Magrane, G., Gray, J.W., Carey, L., Richardson, A., and Weinberg, R.A. (2004). Reconstruction of functionally normal and malignant human breast tissues in mice. Proc. Natl. Acad. Sci. U. S. A. *101*, 4966–4971.

Kwart, D., Paquet, D., Teo, S., and Tessier-Lavigne, M. (2017). Precise and efficient scarless genome editing in stem cells using CORRECT. Nat. Protoc. *12*, 329–354.

Lahm, A., Paolini, C., Pallaoro, M., Nardi, M.C., Jones, P., Neddermann, P., Sambucini, S., Bottomley, M.J., Lo Surdo, P., Carfi, A., et al. (2007). Unraveling the hidden catalytic activity of vertebrate class IIa histone deacetylases. Proc. Natl. Acad. Sci. *104*, 17335–17340.

Lambert, A.W., Ozturk, S., and Thiagalingam, S. (2012). Integrin Signaling in Mammary Epithelial Cells and Breast Cancer. ISRN Oncol. *2012*, 1–9.

Lazard, D., Sastre, X., Frid, M.G., Glukhova, M.A., Thiery, J.P., and Koteliansky, V.E. (1993). Expression of smooth muscle-specific proteins in myoepithelium and stromal myofibroblasts of normal and malignant human breast tissue. Proc. Natl. Acad. Sci. U. S. A. *90*, 999–1003.

Li, H., Radford, J.C., Ragusa, M.J., Shea, K.L., McKercher, S.R., Zaremba, J.D., Soussou, W., Nie, Z., Kang, Y.J., Nakanishi, N., et al. (2008). Transcription factor MEF2C influences neural stem/progenitor cell differentiation and maturation in vivo. Proc. Natl. Acad. Sci. U. S. A. *105*, 9397–9402.

Li, Y., Rogoff, H.A., Keates, S., Gao, Y., Murikipudi, S., Mikule, K., Leggett, D., Li, W., Pardee, A.B., and Li, C.J. (2015). Suppression of cancer relapse and metastasis by inhibiting cancer stemness. Proc. Natl. Acad. Sci. *112*, 1839–1844.

Lim, S., and Kaldis, P. (2013). Cdks, cyclins and CKIs: roles beyond cell cycle regulation. Development *140*, 3079–3093.

Lim, J., Lee, K.M., Shim, J., and Shin, I. (2014). CD24 regulates stemness and the epithelial to mesenchymal transition through modulation of Notch1 mRNA stability by p38MAPK. Arch. Biochem. Biophys. *558*, 120–126.

Liu, R., Wang, L., Chen, G., Katoh, H., Chen, C., Liu, Y., and Zheng, P. (2009). F0XP3 Up-regulates p21 expression by site-specific inhibition of histone deacetylase 2/histone deacetylase 4 association to the locus. Cancer Res. *69*, 2252–2259.

Liu, Y., Nenutil, R., Appleyard, M. V, Murray, K., Boylan, M., Thompson, A.M., and Coates, P.J. (2014). Lack of correlation of stem cell markers in breast cancer stem cells. Br. J. Cancer *110*, 2063–2071.

Lobba, A.R.M., Forni, M.F., Carreira, A.C.O., and Sogayar, M.C. (2012). Differential expression of CD90 and CD14 stem cell markers in malignant breast cancer cell lines. Cytom. Part A *81 A*, 1084–1091.

Loeffler, M., and Roeder, I. (2002). Tissue stem cells: Definition, plasticity, heterogeneity, selforganization and models - A conceptual approach. Cells Tissues Organs *171*, 8–26.

Louderbough, J.M. V., and Schroeder, J.A. (2011). Understanding the Dual Nature of CD44 in Breast Cancer Progression. Mol. Cancer Res. *9*, 1573–1586.

Louderbough, J.M. V, Brown, J.A., Nagle, R.B., and Schroeder, J.A. (2011). CD44 Promotes Epithelial Mammary Gland Development and Exhibits Altered Localization during Cancer Progression. Genes Cancer *2*, 771–781.

Love, S.M., and Barsky, S.H. (2004). Anatomy of the nipple and breast ducts revisited. Cancer *101*, 1947–1957.

Lu, J., McKinsey, T.A., Nicol, R.L., and Olson, E.N. (2000). Signal-dependent activation of the MEF2 transcription factor by dissociation from histone deacetylases. Proc. Natl. Acad. Sci. U. S. A. *97*, 4070–4075.

Macias, H., and Hinck, L. (2013). Mammary Gland Development. Wiley Interdiscip. Rev. Dev. Biol. *1*, 533–557.

Mahele, A.-H. (2011). Ambiguous cells: the emergence of the stem cell concept in the nineteenth and twentieth centuries. R. Soc. 359–378.

Malhotra, G.K., Zhao, X., Band, H., and Band, V. (2010). Histological, molecular and functional subtypes of breast cancers. Cancer Biol. Ther. *10*, 955–960.

Marampon, F., Megiorni, F., Camero, S., Crescioli, C., McDowell, H.P., Sferra, R., Vetuschi, A., Pompili, S., Ventura, L., De Felice, F., et al. (2017). HDAC4 and HDAC6 sustain DNA double strand break repair and stem-like phenotype by promoting radioresistance in glioblastoma cells. Cancer Lett. *397*, 1–11.

Marcato, P., Dean C., P.D. (2011). Aldehyde Dehydrogenase Activity of Breast Cancer Stem Cells is Primarily Due to Isoform ALDH1A3 and Its Expression is Predictive of Metastasis. Stem Cells 263–273.

Margariti, A., Zampetaki, A., Xiao, Q., Zhou, B., Karamariti, E., Martin, D., Yin, X., Mayr, M., Li, H., Zhang, Z., et al. (2010). Histone deacetylase 7 controls endothelial cell growth through modulation of ??-Catenin. Circ. Res. *106*, 1202–1211.

Martin, M., Kettmann, R., and Dequiedt, F. (2007). Class IIa histone deacetylases: regulating the regulators. Oncogene *26*, 5450–5467.

Martin, M., Potente, M., Janssens, V., Vertommen, D., Twizere, J.-C., Rider, M.H., Goris, J., Dimmeler, S., Kettmann, R., and Dequiedt, F. (2008). Protein phosphatase 2A controls the activity of histone deacetylase 7 during T cell apoptosis and angiogenesis. Pnas *105*, 4727–4732.

McKinsey, T.A., Zhang, C.L., and Olson, E.N. (2002). MEF2: A calcium-dependent regulator of cell division, differentiation and death. Trends Biochem. Sci. *27*, 40–47.

McKinsey, T. a, Zhang, C.L., Lu, J., and Olson, E.N. (2000). Signal-dependent nuclear export of a histone deacetylase regulates muscle differentiation. Nature *408*, 106–111.

Miska, E.A., Karlsson, C., Langley, E., Nielsen, S.J., Pines, J., and Kouzarides, T. (1999). HDAC4 deacetylase associates with and represses the MEF2 transcription factor. EMBO J. *18*, 5099– 5107.

Morath, I., Hartmann, T.N., and Orian-Rousseau, V. (2016). CD44: More than a mere stem cell marker. Int. J. Biochem. Cell Biol. *81*, 166–173.

Mottet, D., Bellahcène, A., Pirotte, S., Waltregny, D., Deroanne, C., Lamour, V., Lidereau, R., and Castronovo, V. (2007). Histone deacetylase 7 silencing alters endothelial cell migration, a key step in angiogenesis. Circ. Res. *101*, 1237–1246.

Mottet, D., Pirotte, S., Lamour, V., Hagedorn, M., Javerzat, S., Bikfalvi, A., Bellahcène, A., Verdin, E., and Castronovo, V. (2009). HDAC4 represses p21WAF1/Cip1 expression in human cancer cells through a Sp1-dependent, p53-independent mechanism. Oncogene *28*, 243–256.

Murrell, T.G.C. (1995). The potential for oxytocin (OT) to prevent breast cancer: A hypothesis*. 225–229.

Oakes, S.R., Gallego-Ortega, D., and Ormandy, C.J. (2014). The mammary cellular hierarchy and breast cancer. Cell. Mol. Life Sci. *71*, 4301–4324.

Ouaïssi, M., Silvy, F., Loncle, C., Ferraz da Silva, D., Martins Abreu, C., Martinez, E., Berthézene, P., Cadra, S., Le Treut, Y.P. atrice, Hardwigsen, J., et al. (2014). Further characterization of HDAC and SIRT gene expression patterns in pancreatic cancer and their relation to disease outcome. PLoS One *9*, e108520.

Pardo-Saganta, A., Tata, P.R., Law, B.M., Saez, B., Chow, R.D.-W., Prabhu, M., Gridley, T., and Rajagopal, J. (2015). Parent stem cells can serve as niches for their daughter cells. Nature *523*, 597–601.

Paroni, G., Henderson, C., Schneider, C., and Brancolini, C. (2001). Caspase-2-induced Apoptosis is Dependent on Caspase-9, but Its Processing during UV- or Tumor Necrosis Factordependent Cell Death Requires Caspase-3. J. Biol. Chem. *276*, 21907–21915.

Parra, M. (2015). Class IIa HDACs - New insights into their functions in physiology and pathology. FEBS J. *282*, 1736–1744.

Parra, M., Kasler, H., McKinsey, T.A., Olson, E.N., and Verdin, E. (2005). Protein kinase D1 phosphorylates HDAC7 and induces its nuclear export after T-cell receptor activation. J. Biol. Chem. *280*, 13762–13770.

Parra, M., Mahmoudi, T., Verdin, E., Parra, M., Mahmoudi, T., and Verdin, E. (2007). Myosin phosphatase dephosphorylates HDAC7 , controls its nucleocytoplasmic shuttling , and inhibits apoptosis in thymocytes service Myosin phosphatase controls its nucleocytoplasmic shuttling , and inhibits apoptosis in thymocytes. 638–643.

Peixoto, P., Blomme, A., Costanza, B., Ronca, R., Rezzola, S., Palacios, A.P., Schoysman, L., Boutry, S., Goffart, N., Peulen, O., et al. (2016). HDAC7 inhibition resets STAT3 tumorigenic activity in human glioblastoma independently of EGFR and PTEN: new opportunities for selected targeted therapies. Oncogene 1–14.

Peng, R., Lin, G., and Li, J. (2016). Potential pitfalls of CRISPR/Cas9-mediated genome editing. FEBS J. *283*, 1218–1231.

Petersen, O.W., and van Deurs, B. (1988). Growth factor control of myoepithelial-cell differentiation in cultures of human mammary gland. Differentiation *39*, 197–215.

Petersen, O.W., and Polyak, K. (2010). Stem Cells in the Human Breast. *2*, 15.

Plaks, V., Kong, N., and Werb, Z. (2015). The cancer stem cell niche: How essential is the niche in regulating stemness of tumor cells? Cell Stem Cell *16*, 225–238.

Pon, J.R., and Marra, M.A. (2016). MEF2 transcription factors: developmental regulators and emerging cancer genes. Oncotarget *7*, 2297–2312.

Potthoff, M.J., and Olson, E.N. (2007). MEF2: a central regulator of diverse developmental programs. Development *134*, 4131–4140.

Qu, Y., Han, B., Yu, Y., Yao, W., Bose, S., Karlan, B.Y., Giuliano, A.E., and Cui, X. (2015). Evaluation of MCF10A as a reliable model for normal human mammary epithelial cells. PLoS One *10*, 1–16.

Ramakrishnan, R., Khan, S.A., and Badve, S. (2002). Morphological Changes in Breast Tissue with Menstrual Cycle. Mod. Pathol. *15*, 1348–1356.

Ramalho-Santos, M., and Willenbring, H. (2007). On the Origin of the Term “Stem Cell.” Cell Stem Cell *1*, 35–38.

Rena Callahan (2011). HER2-Positive Breast Cancer: Current Management of Early, Advanced, and Recurrent Disease. Curr Opin Obs. Gynecol *23*, 37–43.

Ritchie, M.E., Phipson, B., Wu, D., Hu, Y., Law, C.W., Shi, W., and Smyth, G.K. (2015). limma powers differential expression analyses for RNA-sequencing and microarray studies. Nucleic Acids Res. *43*, e47.

Roignot, J., Peng, X., Mostov, K., Stephenson, R.O., Rossant, J., and Tam, P.L. (2013). Polarity in Mammalian Epithelial Morphogenesis Polarity in Mammalian Epithelial Morphogenesis. 1–16.

Ruscetti, M., Dadashian, E.L., Guo, W., Quach, B., Mulholland, D.J., Park, J.W., Tran, L.M., Kobayashi, N., Bianchi-Frias, D., Xing, Y., et al. (2015). HDAC inhibition impedes epithelial-mesenchymal plasticity and suppresses metastatic, castration-resistant prostate cancer. Oncogene 1–15.

Ruscetti, M., Dadashian, E.L., and Guo, W. (2016). HDAC Inhibition Impedes Epithelial-Mesenchymal Plasticity and Suppresses Metastatic, Castration-Resistant Prostate Cancer Marcus. Oncogene *35*, 3781–3795.

Sasaki, H., Matsui, C., Furuse, K., Mimori-Kiyosue, Y., Furuse, M., and Tsukita, S. (2003). Dynamic behavior of paired claudin strands within apposing plasma membranes. Proc. Natl. Acad. Sci. U. S. A. *100*, 3971–3976.

Schaefer, K.A., Wu, W.-H., Colgan, D.F., Tsang, S.H., Bassuk, A.G., and Mahajan, V.B. (2017). Unexpected mutations after CRISPR–Cas9 editing in vivo. Nat. Methods *14*, 547–548.

Schnitt, S.J. (2010). Classification and prognosis of invasive breast cancer: from morphology to molecular taxonomy. Mod. Pathol. *23*, S60–S64.

Scott, F.L., Fuchs, G.J., Boyd, S.E., Denault, J.B., Hawkins, C.J., Dequiedt, F., and Salvesen, G.S. (2008). Caspase-8 cleaves histone deacetylase 7 and abolishes its transcription repressor function. J. Biol. Chem. *283*, 19499–19510.

Shackleton, M., Vaillant, F., Simpson, K.J., Stingl, J., Smyth, G.K., Asselin-Labat, M.-L., Wu, L., Lindeman, G.J., and Visvader, J.E. (2006). Generation of a functional mammary gland from a single stem cell. Nature *439*, 84–88.

Stingl, J., Eirew, P., Ricketson, I., Shackleton, M., Vaillant, F., Choi, D., Li, H.I., and Eaves, C.J. (2006). Purification and unique properties of mammary epithelial stem cells. Nature *439*, 993–997.

Subramanian, A., Tamayo, P., Mootha, V.K., Mukherjee, S., Ebert, B.L., Gillette, M.A., Paulovich, A., Pomeroy, S.L., Golub, T.R., Lander, E.S., et al. (2005). Gene set enrichment analysis: A knowledge-based approach for interpreting genome-wide expression profiles. Proc. Natl. Acad. Sci. *102*, 15545–15550.

Takahashi, K., and Yamanaka, S. (2006). Induction of Pluripotent Stem Cells from Mouse Embryonic and Adult Fibroblast Cultures by Defined Factors. Cell *126*, 663–676.

Taylor-Papadimitriou, J., Stampfer, M., Bartek, J., Lewis, a, Boshell, M., Lane, E.B., and Leigh, I.M. (1989). Keratin expression in human mammary epithelial cells cultured from normal and malignant tissue: relation to in vivo phenotypes and influence of medium. J. Cell Sci. *94 (Pt 3)*, 403–413.

Toft, D.J., and Cryns, V.L. (2011). Minireview: Basal-like breast cancer: from molecular profiles to targeted therapies. Mol. Endocrinol. *25*, 199–211.

Twigger, A.-J., Hepworth, A.R., Tat Lai, C., Chetwynd, E., Stuebe, A.M., Blancafort, P., Hartmann, P.E., Geddes, D.T., and Kakulas, F. (2015). Gene expression in breastmilk cells is associated with maternal and infant characteristics. Sci. Rep. *5*, 12933.

Tzivion, G., Shen, Y.H., and Zhu, J. (2001). 14-3-3 Proteins; Bringing New Definitions To Scaffolding. Oncogene *20*, 6331–6338.

Verdin, E., Dequiedt, F., and Kasler, H. (2004). HDAC7 regulates apoptosis in developing thymocytes. Novartis Found. Symp. *259*, 115-29-31, 163–169.

Visvader, J.E., and Stingl, J. (2014). Mammary stem cells and the differentiation hierarchy : current status and perspectives. 1143–1158.

Wang, a H., Bertos, N.R., Vezmar, M., Pelletier, N., Crosato, M., Heng, H.H., Th'ng, J., Han, J., and Yang, X.J. (1999). HDAC4, a human histone deacetylase related to yeast HDA1, is a transcriptional corepressor. Mol. Cell. Biol. *19*, 7816–7827.

Wang, S., Li, X., Parra, M., Verdin, E., Bassel-Duby, R., and Olson, E.N. (2008). Control of endothelial cell proliferation and migration by VEGF signaling to histone deacetylase 7. Proc. Natl. Acad. Sci. U. S. A. *105*, 7738–7743.

Weigelt, B., Mackay, A., Roger, A., Natrajan, R., Tan, D.S.P., Dowsett, M., Ashworth, A., and Reis-filho, J.S. Breast cancer molecular profi ling with single sample predictors : a retrospective analysis. Lancet Oncol. *11*, 339–349.

Weigelt, B., Geyer, F.C., and Reis-Filho, J.S. (2010). Histological types of breast cancer: How special are they? Mol. Oncol. *4*, 192–208.

Wels, J., Kaplan, R.N., Rafii, S., and Lyden, D. (2008). Migratory neighbors and distant invaders: Tumorassociated niche cells. Genes Dev. *22*, 559–574.

Williams, R.T., Den Besten, W., and Sherr, C.J. (2007). Cytokine-dependent imatinib resistance in mouse BCR-ABL+, Arf-null lymphoblastic leukemia. Genes Dev. *21*, 2283–2287.

Wilson, Byun, N. (2008). HDAC4 Promotes Growth of Colon Cancer Cells via Repression of p21. Mol. Biol. Cell *82*, 327–331.

Witt, A.E., Lee, C.-W., Lee, T.I., Azzam, D.J., Wang, B., Caslini, C., Petrocca, F., Grosso, J., Jones, M., Cohick, E.B., et al. (2017). Identification of a cancer stem cell-specific function for the histone deacetylases, HDAC1 and HDAC7, in breast and ovarian cancer. Oncogene *36*, 1707–1720.

Wu, M.Y., Fu, J., Xiao, X., Wu, J., and Wu, R.C. (2014). MiR-34a regulates therapy resistance by targeting HDAC1 and HDAC7 in breast cancer. Cancer Lett. *354*, 311–319.

Xie, T., and Spradling, A.C. (1998). decapentaplegic is essential for the maintenance and division of germline stem cells in the Drosophila ovary. Cell *94*, 251–260.

Yang, X.-J., and Seto, E. (2008). The Rpd3/Hda1 family of lysine deacetylases: from bacteria and yeast to mice and men. Nat. Rev. Mol. Cell Biol. *9*, 206–218.

Yang, X., and Gre, S. (2005). Class II Histone Deacetylases : from Sequence to Function , Regulation , and Clinical Implication MINIREVIEW Class II Histone Deacetylases : from Sequence to Function , Regulation , and Clinical Implication. Mol. Cell. Biol. *25*, 2873–2884.

Yang, X.R., Figueroa, J.D., Falk, R.T., Zhang, H., Pfeiffer, R.M., Hewitt, S.M., Lissowska, J., Peplonska, B., Brinton, L., Garcia-Closas, M., et al. (2012). Analysis of terminal duct lobular unit involution in luminal A and basal breast cancers. Breast Cancer Res. *14*, R64.

Youssef, A., Aboalola, D., and Han, V.K.M. (2017). The Roles of Insulin-Like Growth Factors in Mesenchymal Stem Cell Niche. Stem Cells Int. *2017*, 9453108.

Zhang, J., and Li, L. (2005). BMP signaling and stem cell regulation. Dev. Biol. *284*, 1–11.

Zhang, B., Cao, X., Chen, J., Chen, J., Fu, L., Hu, X., Jiang, Z., Liao, N., Liu, D., Tao, O., et al. (2012). Guidelines on the diagnosis and treatment of breast cancer (2011 edition). *1*, 39–61.

Zhang, C.L., McKinsey, T.A., Chang, S., Antos, C.L., Hill, J.A., and Olson, E.N. (2002). Class II histone deacetylases act as signal-responsive repressors of cardiac hypertrophy. Cell *110*, 479–488.

Zhang, L., Jin, M., Margariti, A., Wang, G., Luo, Z., Zampetaki, A., Zeng, L., Ye, S., Zhu, J., and Xiao, Q. (2010). Sp1-dependent activation of HDAC7 is required for platelet-derived growth factorBB-induced smooth muscle cell differentiation from stem cells. J. Biol. Chem. *285*, 38463– 38472.

Zhang, X.-H., Tee, L.Y., Wang, X.-G., Huang, Q.-S., and Yang, S.-H. (2015). Off-target Effects in CRISPR/Cas9-mediated Genome Engineering. Mol. Ther. - Nucleic Acids *4*, e264.

Zhao, C., Cai, S., Shin, K., Lim, A., Kalisky, T., Lu, W.-J., Clarke, M.F., and Beachy, P.A. (2017). Stromal *Gli2* activity coordinates a niche signaling program for mammary epithelial stem cells. Science (80-.). *356*, eaal3485.

Zhou, B., Margariti, A., Zeng, L., Habi, O., Xiao, Q., Martin, D., Wang, G., Hu, Y., Wang, X., and Xu, Q. (2011). Splicing of histone deacetylase 7 modulates smooth muscle cell proliferation and neointima formation through nuclear β-catenin translocation. Arterioscler. Thromb. Vasc. Biol. *31*, 2676–2684.

Zhou, Y., Zhu, S., Cai, C., Yuan, P., Li, C., Huang, Y., and Wei, W. (2014). High-throughput screening of a CRISPR/Cas9 library for functional genomics in human cells. Nature *509*, 487–491.

Zhu, C., Chen, Q., Xie, Z., Ai, J., Tong, L., Ding, J., and Geng, M. (2011). The role of histone deacetylase 7 (HDAC7) in cancer cell proliferation: Regulation on c-Myc. J. Mol. Med. *89*, 279–289.

Zhuang, Q., Qing, X., Ying, Y., Wu, H., Benda, C., Lin, J., Huang, Z., Liu, L., Xu, Y., Bao, X., et al. (2013). Class IIa histone deacetylases and myocyte enhancer factor 2 proteins regulate the mesenchymal-to-epithelial transition of somatic cell reprogramming. J. Biol. Chem. *288*, 12022–12031.

(2001). https://stemcells.nih.gov/info/2001report/chapter4.htm.

6. ACKNOWLEDGMENTS

At the end of this PhD, I would like to thank the people that share with me this amazing experience. First of all, I would like to say thanks to Professor Brancolini, that three years ago give me the possibility to work in his lab. Thanks boss for your passion and dedication to science. A big thanks is for my scientific mentor and friend Dott. Eros Di Giorgio. Eros your contribution to this work is priceless, you share with me joy and pain in and outside the laboratory. Probably a "thank you" is not sufficient, but you know that you can always count on me.

I would like to thank Sara Cabodi, my external reviewer that, from Turin, support and encourage my work.

I share funny moments with my colleagues Sonia, Elisa, Hari, Andrea and Enrico. The time spent with you alleviated the workload. Thank you for all.

A special thank is for the guys that share the PhD experience from the first day: Marco and Giulia. A number, XXX, represent our friendship and I am sure that wherever we will go, we will never be far.

Francesca Mion, you treat me like a mother with her daughter from the day I came in Udine. For this and for thousand other things, thank you!

Silvia Tonon, thank you for the contribution to the layout of this thesis. I cannot say thank you for the molarity calculation and you know why.

Finally, thanks to all that people that I met during this long walk to reach the top of a mountain which I dreamed of climbing from all my life. For this reason, the biggest THANK is for my father Franco, my mother Caterina and my brother Giuseppe that support me every day. This work is dedicated to us.

In conclusion, I want to say that this work is dedicated also to Simone and Franco, my labours, my successes and my weekends in lab they always had a thought turned to you.

© 2015. Published by The Company of Biologists Ltd | Journal of Cell Science (2015) 128, 3961-3976 doi:10.1242/jcs.170357

RESEARCH ARTICLE

The MEF2–HDAC axis controls proliferation of mammary epithelial cells and acini formation *in vitro*

Andrea Clocchiatti[1,*], Eros Di Giorgio[1], Giulia Viviani[1], Charles Streuli[2], Andrea Sgorbissa[1], Raffaella Picco[1], Valentina Cutano[1] and Claudio Brancolini[1,‡]

ABSTRACT

The myocyte enhancer factor 2 and histone deacetylase (MEF2–HDAC) axis is a master regulator of different developmental programs and adaptive responses in adults. In this paper, we have investigated the contribution of the axis to the regulation of epithelial morphogenesis, using 3D organotypic cultures of MCF10A cells as a model. We have demonstrated that MEF2 transcriptional activity is upregulated during acini formation, which coincides with exit from the proliferative phase. Upregulation of the transcription of MEF2 proteins is coupled to downregulation of HDAC7, which occurs independently from changes in mRNA levels, and proteasome- or autophagy-mediated degradation. During acini formation, the MEF2–HDAC axis contributes to the promotion of cell cycle exit, through the engagement of the CDK inhibitor CDKN1A. Only in proliferating cells can HDAC7 bind to the first intron of the CDKN1A gene, a region characterized by epigenetic markers of active promoters and enhancers. In cells transformed by the oncogene HER2 (ERBB2), acini morphogenesis is altered, MEF2 transcription is repressed and HDAC7 is continuously expressed. Importantly, reactivation of MEF2 transcriptional activity in these cells, through the use of a HER2 inhibitor or by enhancing MEF2 function, corrected the proliferative defect and re-established normal acini morphogenesis.

KEY WORDS: HDAC7, HDAC4, MEF2A, MEF2D, p21, CDKN1A, Cell cycle, Morphogenesis, Apoptosis, HDAC5, Breast cancer, HER2, ERBB2, Lapatinib, 3D culture, H3K27

INTRODUCTION

Mammary morphogenesis is characterized by the presence of several different instructive signals, which provide the correct gene expression network to generate the proper glandular architecture. These structures transit from a disorganized state to an ordered epithelial organization that modulates polarity, proliferation and luminal cell clearance (Debnath et al., 2002; Lewandowski and Piwnica-Worms, 2014). Mammary epithelial MCF10A cells that have been cultured on a reconstituted extracellular matrix [three dimensional (3D) culture] undergo a morphogenetic process that resembles events found *in vivo* to generate acinar-like spheroids (Debnath et al., 2002, 2003; Streuli et al., 1991). Initially, each single cell proliferates to generate a filled spheroid. During this morphogenetic process, cells of the outer layer enter G0 (proliferation arrest) and polarize (Debnath et al., 2002; Weaver et al., 2002; Whyte et al., 2010). The outer layer of cells that contact the extracellular matrix (ECM) survive, whereas the inner core of cells, lacking basement membrane contacts, die through both apoptotic and non-apoptotic processes (Debnath et al., 2002; Mills et al., 2004; Wang et al., 2003). Integrin signaling plays a key role at different steps of this morphogenetic process (Lee and Streuli, 2014; Reginato et al., 2003), and the absence of integrin-mediated pro-survival signals (anoikis) promotes the expression and activity of pro-apoptotic factors. Death of the inner cells is responsible for the formation of hollow lumen-containing acini.

Transcriptional nodes that are responsible for the genetic reprogramming that controls this complex morphogenetic process are not completely defined. The myocyte enhancer factor 2 (MEF2) family of transcription factors, including the MEF2A, MEF2B, MEF2C and MEF2D isoforms, plays important functions in tissue development and homeostasis (Potthoff and Olson, 2007). Genetic studies in mice have proved the essential contribution of *Mef2a* to the regulation of the cardiovascular system (Naya et al., 2002). Likewise, defects in *Mef2c* impact on heart development, causing mice to die at embryonic day (E)9.5 (Lin et al., 1998, 1997). By contrast, mice with homozygous mutations in *Mef2d* are viable, probably because of overlapping expression patterns with other MEF2 members (Arnold et al., 2007). Conditional cell-lineage-specific deletions of MEF2s have shown that there are additional roles for these transcription factors during B-cell development (Debnath et al., 2013) and bone homeostasis (Collette et al., 2012; Kramer et al., 2012).

MEF2s influence the expression of numerous genes, depending on and in cooperation with other transcription factors (Potthoff and Olson, 2007). They can also operate as transcriptional repressors, when in complex with class-IIa histone deacetylases (HDACs) (Gregoire et al., 2006; Lu et al., 2000). HDAC4, HDAC5, HDAC7 and HDAC9 belong to the class-IIa subfamily, and they are distinguished by (i) the presence of an N-terminal regulatory region that is involved in binding to transcription factors and additional co-repressors, (ii) a C-terminal region that includes the catalytic domain, which in vertebrates exhibits an impaired Lys-deacetylase activity and (iii) nuclear–cytoplasmic shuttling in a signal-responsive fashion (Clocchiatti et al., 2013a, 2011; Yang and Seto, 2008). The intimate relationships between MEF2s and these repressors support the concept of a MEF2–HDAC axis.

Deregulated MEF2 transcriptional activities can impact on tumorigenesis, and recent results have demonstrated alterations in MEF2 levels and transcription in breast tumors (Clocchiatti et al., 2013b; Ma et al., 2014; Schuetz et al., 2006). In estrogen receptor (ER)-positive tumors, repression of putative MEF2-target genes

[1]Dipartiment of Medical and Biological Sciences, Università degli Studi di Udine, P.le Kolbe 4, Udine 33100, Italy. [2]Wellcome Trust Centre for Cell-Matrix Research, Faculty of Life Sciences, University of Manchester, Oxford Road, Manchester M13 9PT, UK.
*Present address: Cutaneous Biology Research Center, Massachusetts General Hospital, Boston, MA, USA.

‡Author for correspondence (claudio.brancolini@uniud.it)

Received 18 February 2015; Accepted 15 September 2015

Journal of Cell Science (2015) 128, 3961-3976 doi:10.1242/jcs.170357

correlates with aggressiveness, and high class-IIa HDAC expression is associated with reduced survival (Clocchiatti et al., 2013b). By contrast, in recurrent ER-positive mammary cancers, expression of MEF2s correlates with NOTCH1 protein levels (Pallavi et al., 2012). Although some reports point to a contribution of MEF2-dependent transcription to mammary gland neoplastic pathogenesis, data on the role of the MEF2–HDAC axis during normal gland development and homeostasis are lacking, and only little information is available on the role of the axis in epithelial cells (Ishikawa et al., 2010). Based on this evidence, we hypothesized that the MEF2–HDAC axis plays a role in the regulation of breast epithelial cell proliferation and/or differentiation. In this work, we have investigated the contribution of the axis to acini morphogenesis using an experimental model of MCF10A cells cultured in three dimensions.

RESULTS

Regulation of the MEF2–HDAC axis during acini morphogenesis

The first indication that the MEF2–HDAC axis contributes to mammary breast epithelial homeostasis resulted from the association of MEF2D expression with a better overall survival of individuals with breast cancer (Fig. 1A). Furthermore, MEF2D expression was significantly higher in normal samples compared to that in aggressive grade three cancers (Fig. 1B). Because high grading is associated with compromised glandular architecture and differentiation (Elston and Ellis, 2002), we decided to investigate the contribution of the MEF2–HDAC axis to mammary epithelial morphogenesis and maintenance. To gain insight into which members are expressed in this context, we compared expressed sequence tag (EST) profiles between skeletal muscle and breast tissue for class-IIa HDACs and MEF2A, MEF2C and MEF2D (Fig. 1C). As expected, in skeletal muscle, MEF2C, HDAC4 and HDAC5 were the most expressed members of each family. By contrast, in breast tissue, MEF2A, MEF2D and HDAC7 were the most expressed isoforms. Furthermore, Gene Set Enrichment Analysis (GSEA), using a signature of putative MEF2-target genes, suggested that MEF2-dependent transcription was positively modulated during MCF10A acinar morphogenesis (Fig. 1D). Hence, we selected MCF10A cells to investigate the role of the MEF2–HDAC axis during epithelial morphogenesis. When plated onto laminin-rich ECM (for 3D culture), MCF10A cells transited from an initial proliferative disorganized state (Fig. 1E, day 4), evidenced by the presence of several mitotic figures per acinus (Fig. 1F) and by the random orientation of the Golgi, to a quiescent polarized condition, marked by Golgi re-orientation, formation of a hollow lumen and the absence of mitotic figures (Fig. 1E, day 16 and 1F).

The bioinformatics analysis prompted us to evaluate the transcriptional activity of MEF2s during acini development. Quantitative real-time (qRT)-PCR experiments showed that the mRNA levels of some MEF2-target genes – *KLF2*, *KLF4*, *NR4A1*, *END1* and *RHOB* – were augmented, although with different magnitudes, when acinar morphogenesis was completed at day 16 (Fig. 2A). Together with MEF2-target genes, *MEF2D* mRNA levels rose, similar to that described previously during muscle differentiation (Nebbioso et al., 2009; Sebastian et al., 2013) (Fig. 2B). The expression of *HDAC5* and *HDAC9* also increased during the acinar developmental process, whereas that of *HDAC4* and *HDAC7* remained constant (Fig. 2B). The upregulation of *CDKN1A* was selected as a marker of growth arrest (Besson et al., 2008), whereas *BMF* and *BIM* were selected as markers of apoptosis (Mailleux, et al., 2008).

To clarify the apparent paradox of the MEF2-dependent transcriptional stimulation coupled to the upregulation of *HDAC5* and *HDAC9* mRNA levels, we performed an absolute quantification of class-IIa HDAC expression (Fig. 2C). This analysis suggested that, in MCF10A cells, *HDAC7* and *HDAC4* levels are largely dominant over those of other class-IIa deacetylases and that, therefore, even a sixfold increase in *HDAC5* mRNA could be irrelevant in the context of MEF2-dependent transcription. The immunoblot analysis confirmed the upregulation of MEF2D and HDAC5 during acini morphogenesis and exposed a dramatic downregulation of HDAC7 levels (Fig. 2D). This drastic reduction of HDAC7 could explain the upregulation of MEF2-dependent transcription. Because HDAC7 downregulation did not result from a decrease of mRNA levels, to gain insight into the mechanism, MCF10A cells that had been grown for 4 or 16 days under 3D culture conditions were treated with bortezomib to block proteasome-mediated degradation or with chloroquine to block lysosome- and autophagy-mediated degradation, or with a combination of both drugs. Although class-IIa proteins can be targets of the proteasome (Cernotta et al., 2011; Potthoff et al., 2007), HDAC7 downregulation was unaffected by both drugs (Fig. 2E), thus indicating that other proteolytic events or mechanisms control HDAC7 protein levels during acini formation.

Class-IIa HDAC nuclear–cytoplasmic shuttling is under the influence of multiple signaling pathways (Clocchiatti et al., 2011). We therefore investigated the subcellular localization of MEF2D, HDAC4 (Fig. 2F) and HDAC7 (Fig. 2G) in cells that had been grown for 4 or 16 days under 3D culture conditions. MEF2D localized in the nucleus, and both deacetylases showed both nuclear and cytoplasmic distributions. Treatment of MCF10A cells with leptomycin-B, an inhibitor of CRM1-mediated nuclear export, promoted the nuclear accumulation of HDAC7, thus indicating that the deacetylase undergoes nuclear–cytoplasmic shuttling. Similar results were observed at day 16 and for HDAC4 (data not shown). In conclusion, we have demonstrated that the MEF2–HDAC axis is regulated during acinar morphogenesis and that the upregulation of MEF2 transcriptional activity could be the consequence of HDAC7 downregulation.

MEF2D downregulation does not affect acinar morphogenesis but elicits different compensatory mechanisms

MEF2 transcriptional activities could play roles during acinar morphogenesis. To comprehend this role, we silenced MEF2D expression by using lentiviral infection with small hairpin (sh) RNAs. We selected MEF2D because (i) MEF2D is the most expressed isoform in breast tissue (Fig. 1A) and (ii) its expression is upregulated during morphogenesis (Fig. 2B,D). Despite an evident downregulation of MEF2D at the mRNA and protein levels, MCF10A cells expressing two different shRNAs against MEF2D (Fig. S1A,B) did not show any evidence that the expression of the MEF2-target genes had been negatively altered. Instead, unexpectedly, *END1* mRNA levels were augmented (Fig. S1B). In cells with downregulated MEF2D, acinar morphogenesis appeared to be normal, as proved by scoring the luminal filling per structure and Golgi orientation (Fig. S1C). We also evaluated whether the absence of MEF2D could influence the initial proliferation phase by measuring the acinar size. Here, again MEF2D seemed to be dispensable (Fig. S1D). The absence of evident phenotypes in cells that had been silenced for MEF2D could be the consequence of redundancy and/or of compensatory

Journal of Cell Science (2015) 128, 3961-3976 doi:10.1242/jcs.170357

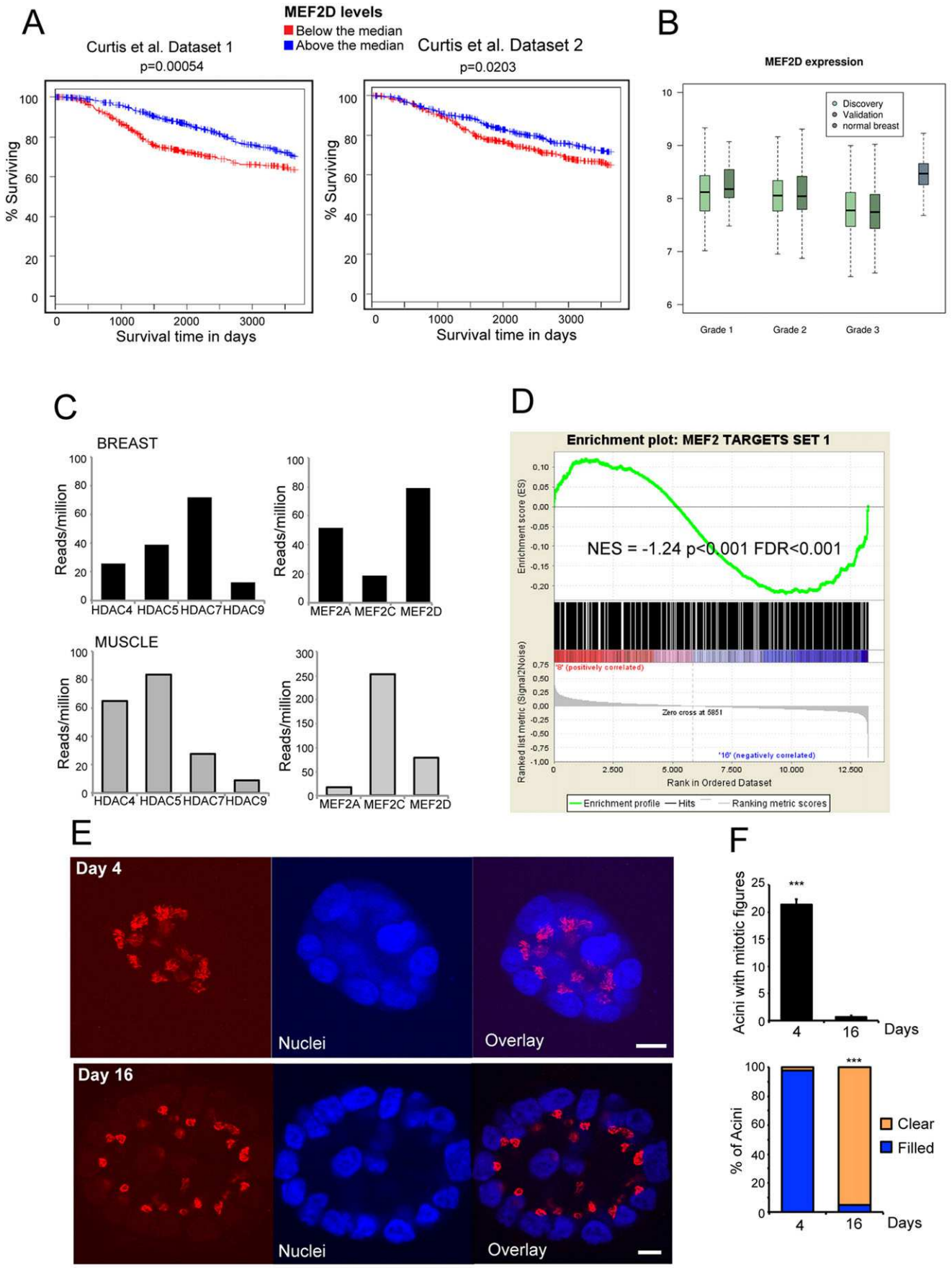

Fig. 1. See next page for legend.

Journal of Cell Science (2015) 128, 3961-3976 doi:10.1242/jcs.170357

Fig. 1. The MEF2–HDAC axis in mammary gland. (A) Kaplan–Meier analysis based on the expression levels of MEF2D. Data were from 2136 arrays including 997 for discovery, 995 for validation and 144 of normal breast. The associated genotype and expression data are deposited at the European Genome-Phenome Archive (EGA, http://www.ebi.ac.uk/ega/), which is hosted by the European Bioinformatics Institute, under accession number EGAS00000000083. (B) Box plots illustrating *MEF2D* mRNA levels in normal breast and cancer counterparts. Expression levels of MEF2D were significantly reduced in tumor samples and particularly in grade (G)3 tumors. Statistical significance was calculated using the Wilcoxon rank-sum test. Grade3 discovery vs normal, 3.88×10^{-41}; Grade3 validation vs normal, 4.47×10^{-41}. Data were from 2136 arrays including 997 for discovery, 995 for validation and 144 of normal breast. The associated genotype and expression data are deposited at the European Genome-Phenome Archive (EGA, http://www.ebi.ac.uk/ega/), which is hosted by the European Bioinformatics Institute, under accession number EGAS00000000083. Boxes represent the first and the third quartile, the middle line represents the median, and whiskers represent the minimum and the maximum. (C) Plots illustrating the frequency of EST tags for class-IIa HDACs and MEF2-family members in skeletal muscle and breast tissues. Data were retrieved from http://www.ncbi.nlm.nih.gov/nucest/. (D) GSEA analysis of a list of 900 putative MEF2-target genes in expression data from MCF10A cells cultured under 3D conditions comparing day 8 with 16. Dataset was obtained from GEO (http://www.ncbi.nlm.nih.gov/geo/) GSE26148 (Simpson et al., 2011). (E) Confocal images comparing MCF10A cells grown in 3D culture for 4 or 16 days to evaluate the distribution of the Golgi using the GM130 marker (red) and nuclei (blue) using TOPRO-3. Images are shown in pseudocolors. Scale bars: 10 µm. (F) Quantification of luminal filling and mitotic figures in acini generated by MCF10A cells grown in 3D for 4 or 16 days. ***P<0.005 (t-test).

mechanisms, as observed in other contexts (Liu et al., 2014). In fact, MCF10A cells with downregulated MEF2D exhibited an increase in MEF2A protein levels, in concert with HDAC4 and HDAC5 downregulation (Fig. S1A).

Unscheduled expression of MEF2 compromises cell proliferation and reduces acini size

To understand the contribution of the MEF2–HDAC axis, we decided to use an alternative strategy. We introduced into MCF10A cells a conditionally active form of MEF2C fused to the VP16 activation domain of herpes simplex and to the ligand binding domain of the estrogen receptor (Flavell et al., 2006), as a control, a DNA-binding defective mutant (ΔDBD) was used (Fig. 3A). In 2D culture, activation of MEF2–VP16 with 4-hydroxytamoxifen (4-OHT), but not the control construct, efficiently promoted transcription of MEF2-target genes (Fig. 3B). Importantly, the magnitude of induction perfectly mirrored the changes observed during acini morphogenesis in 3D culture (compare Figs 2B and 3B). Induction of MEF2 transcriptional program in 2D-cultured MCF10A cells had a profound effect on proliferation (Fig. 3C). This anti-proliferative effect was also observed when cells were grown in 3D. Timecourse analysis indicated that stimulation of MEF2 activity within the first four days constrained acinar size (Fig. 3D). At day 4, in the presence of unscheduled MEF2 transcriptional activity, acinar structures were smaller and populated by a reduced number of cells (Fig. 3E and F). To understand whether MEF2 elicits a growth-repressive effect during different phases of acinar morphogenesis, we selectively stimulated its activity for 4 days, starting from day 4, 8 or 12. Boosting MEF2 transcriptional activity from day 4 to day 8 still interfered with the proliferation of MCF10A cells, as evidenced by the reduced acini size (Fig. 3G), the number of cells (Fig. 3H) and the dramatic decrease of mitotic activity (Fig. 3I). It is noteworthy that activation of MEF2 at the next time intervals (at day 8 or 12) did not exert any effect on acinar diameter (Fig. 3J and K), cell numbers or luminal cell death (data not shown), thus indicating that MEF2 perturbations are principally linked to the proliferative phase of the morphogenetic process. Overall, these data suggest that, in order to proceed with the normal morphogenetic process in the mammary epithelial cells, MEF2 transcriptional activity must be restrained during the initial proliferative phase.

Sustained HDAC7 activity promotes cell proliferation and affects acinar morphogenesis

The demonstration of a role for MEF2-dependent transcription in limiting the proliferation of mammary epithelial cells indicates that the downregulation of HDAC7, which is observed during the morphogenetic process, could be instrumental to drive the exit from the cell cycle. To verify this hypothesis, we generated MCF10A cells expressing a conditionally active form of HDAC7, fused to the ligand-binding domain of the estrogen receptor (Fig. 4A). This mutant, named HDAC7/SA-ER, presents the replacement of four serine residues with alanine residues, in the amino-terminal region (Dequiedt et al., 2003). In the wild-type protein, these serine residues, once phosphorylated by various kinases, become binding sites for 14-3-3 proteins and are required for the efficient nuclear export of the deacetylase (Yang and Seto, 2008). Hence, upon treatment with 4-OHT, this chimera should promptly accumulate in the nucleus and repress MEF2-dependent transcription. Fig. 4A shows that the fused protein is expressed at the expected size and, after 4-OHT addition, it efficiently accumulates in the nucleus of MCF10A cells (Fig. 4B). Moreover, HDAC7/SA-ER effectively repressed MEF2-dependent transcription, as evidenced by the decrease in *RHOB* mRNA levels after 8 days in 3D culture (Fig. 4C). To determine the effect of unscheduled HDAC7 repressive activity during morphogenesis, we observed the acinar size at 4, 8 and 12 days after induction with 4-OHT. Acini that had been generated by MCF10A cells expressing HDAC7/SA-ER were bigger at all time points analyzed (Fig. 4D). This increase in size depended on an increase in the number of nuclei per acinus (Fig. 4E). The increased number of acini presenting a partially filled lumen (Fig. 4F and the quantitative analysis in Fig. 4G) confirmed the pro-growth effect of HDAC7. However, HDAC7/SA-ER acini were also characterized by higher numbers of picnotic and fragmented nuclei (Fig. 4E, arrows, and quantitative analysis in Fig. 4H) pointing to an increase in the apoptotic activity as a counterbalance in order to restrain excessive proliferation. These data indicate that although HDAC7 can stimulate epithelial cell growth, compensatory mechanisms are engaged that limit this potentially harmful effect. When the MEF2-binding sequence (amino acids 78–93) was removed, HDAC7/SA-ER was incapable of sustaining cell proliferation (Fig. S2A–E). These results further strengthen the evidence for the importance of the MEF2–HDAC axis in the control of mammary epithelial cell proliferation.

MEF2-dependent transcription and HDAC7 levels are regulated during growth arrest in mammary epithelial cells

The discovery that MEF2 activity influences cell cycle progression encouraged us to address whether this response can also be observed independently from the morphogenetic process. As alternative conditions for G0 induction, exit from the cell cycle was promoted by density-dependent inhibition and by growth factor starvation. Under contact inhibition, MEF2A and MEF2D protein levels increased in the absence of appreciable rises of the relative mRNAs (Fig. 5A and B). As described above under 3D culture conditions, HDAC7 protein levels decreased and HDAC5

Journal of Cell Science (2015) 128, 3961-3976 doi:10.1242/jcs.170357

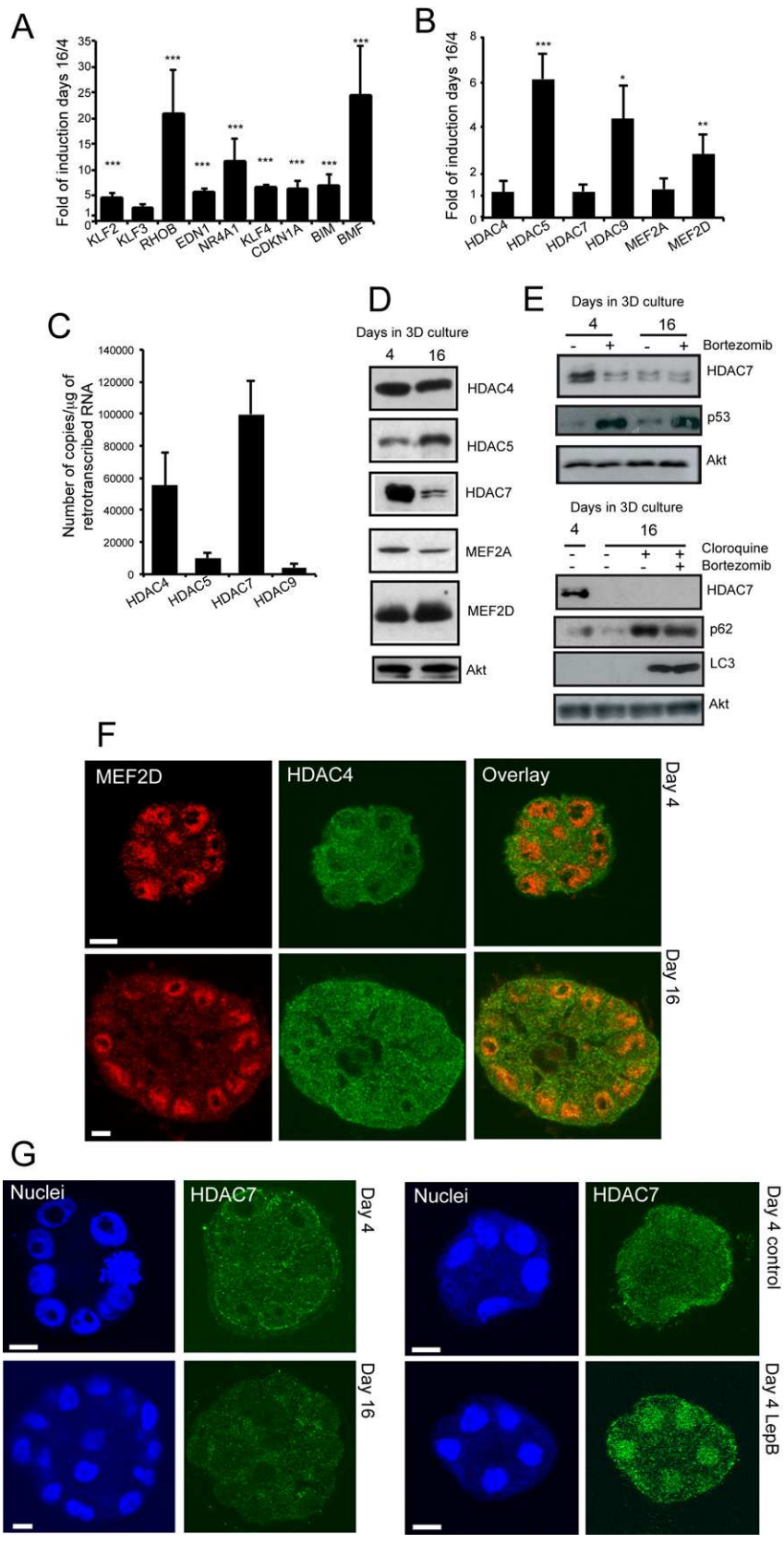

Fig. 2. Analysis of MEF2-dependent transcription and class-IIa HDAC expression in MCF10A breast epithelial cells during acini morphogenesis. (A) qRT-PCR analysis was performed to quantify the mRNA levels of MEF2-target genes, of the cell cycle inhibitor CDKN1A and of the apoptotic genes *BIM* and *BMF* in MCF10A cells grown in 3D culture for 4 and 16 days. The fold induction was calculated as the ratio relative to expression at 4 days of culture. (B) qRT-PCR was performed to quantify the mRNA levels of the most abundant class-IIa members (HDAC4, HDAC5 and HDAC7) as well as of MEF2 members (MEF2A, MEF2C, and MEF2D) in MCF10A cells grown in 3D for 4 or 16 days. Fold induction was calculated as the ratio relative to expression at 4 days of culture. (C) qRT-PCR analysis was performed to quantify the mRNA levels of all class-IIa members (HDAC4, HDAC5, HDAC7 and HDAC9) in MCF10A cells. The expression was calculated as number of copies relative to the µg of retro-transcribed RNA. (D) Immunoblot analysis of MEF2-family members and class-IIa HDACs in MCF10A cells grown in 3D for 4 and 16 days. Cell lysates of MCF10A cells were subjected to immunoblot analysis using the indicated antibodies. AKT1 was used as loading control. (E) Immunoblot analysis of HDAC7 levels in 3D cultures of MCF10A cells at 4 and 16 days treated or not with bortezomib or bortezomib in association with chloroquine for 8 h, as indicated. p53 was used as positive control for proteasome-mediated degradation inhibition. p62 and LC3 were used as positive controls for the blocking of lysosome- and autophagy-mediated degradation. AKT1 was used as loading control. (F) Confocal images illustrating the subcellular localization of MEF2D (red) and HDAC4 (green) in MCF10A cells grown in 3D culture for 4 and 16 days. Images are shown in pseudocolors. Scale bars: 10 µm. (G) Confocal pictures exemplifying the subcellular localization of HDAC7 in MCF10A cells cultured in 3D for 4 and 16 days, and for 4 days treated or not with leptomycin-B for 1 h. Nuclei (blue) were stained with TOPRO-3. Images are shown in pseudocolors. Scale bars: 50 µm. Mean±s.d.; **P*<0.05, ***P*<0.01, ****P*<0.005 (*t*-test).

levels increased (Fig. 5A). Expression of *KLF2*, *RHOB* and *HDAC5* augmented, whereas *HDAC7* mRNA levels were unchanged (Fig. 5B). Similar results were obtained when G0 was elicited through serum and growth factor deprivation (Fig. 5C and D). Serum starvation triggered the downregulation of HDAC4, as previously observed (Cernotta et al., 2011). Induction of HDAC7 repressive activity using the HDAC7/SA-ER chimera in cells that had been subjected to growth factor deprivation limited the

Journal of Cell Science (2015) 128, 3961-3976 doi:10.1242/jcs.170357

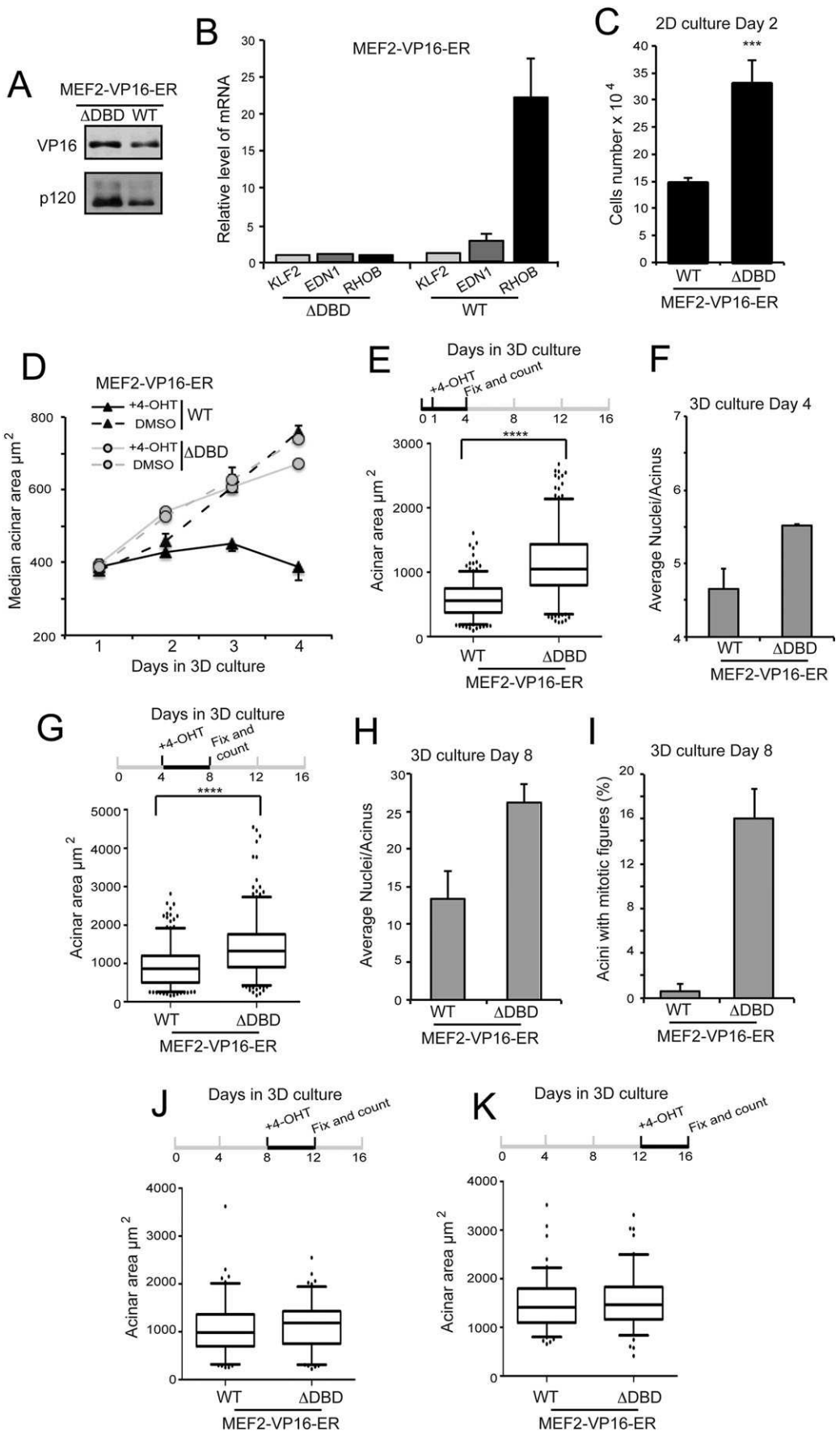

Fig. 3. See next page for legend.

Journal of Cell Science (2015) 128, 3961-3976 doi:10.1242/jcs.170357

Fig. 3. MEF2 transcriptional activity can compromise cell proliferation and acini size during the normal morphogenetic process in mammary epithelial cells. (A) Immunoblot analysis of MEF2-VP16-ER levels in MCF10A cells expressing the MEF2-VP16-ER chimera (WT) or its mutant that was defective in DNA binding MEF2ΔDBD-VP16-ER (ΔDBD). MEF2-VP16-ER-dependent transcription was induced by treating cells with 4-OHT for 24 h. Cell lysates were generated and subjected to immunoblot analysis with an antibody against VP16. p120 (also known as CTNND1) was used as a loading control. (B) mRNA levels of selected MEF2-target genes were measured by using qRT-PCR analysis of MCF10A cells expressing MEF2-VP16-ER or the mutant MEF2ΔDBD-VP16-ER following 4-OHT treatment in 2D culture. (C) Quantitative analysis of cell proliferation of MCF10A cells expressing the two MEF2 constructs. The day after seeding, 4-OHT was added to the culture medium, and cell numbers scored 24 h later. (D) Time-course analysis of acinar area at the indicated times, as generated by MCF10A cells expressing the two MEF2 inducible constructs. The day after seeding, 4-OHT was added to the culture medium. (E) The acinar size of MCF10A cells, expressing the two MEF2 chimeras, grown in 3D culture for 4 days was analyzed. The day after seeding, 4-OHT was added to the culture medium. Data are from a representative set of three independent experiments in which ∼250 acini per condition were measured. (F) Number of nuclei per acinus as generated by the different transgenic MCF10A cells after 4 days in 3D culture. (G) The acinar size of MCF10A cells, expressing the two MEF2 chimeras, grown 3D culture for 8 days were analyzed. On the fourth day in culture, 4-OHT was added to culture medium. Data are from a representative set of three independent experiments in which ∼250 acini per condition were measured. (H) Number of nuclei per acinus generated from the different transgenic MCF10A cells after 8 days in 3D culture. (I) Number of acini with mitotic figures, as generated by the different transgenic MCF10A cells after 8 days in 3D culture. (J) Acinar size of MCF10A cells, expressing the two MEF2 inducible constructs, in 3D culture for 12 days were analyzed. 4-OHT was added to culture medium as indicated. Data are from a representative set of three independent experiments in which ∼250 acini per condition were measured. (K) The acinar size of MCF10A cells, expressing the two MEF2 inducible constructs, in 3D culture for 16 days were analyzed. 4-OHT was added to culture medium as indicated. Data are from a representative set of three independent experiments in which ∼250 acini per condition were measured. E,G,J,K, boxes represents the first and the third quartile, the middle line represents the median, whiskers represent the 10th and the 90th percentile, and dots represents the outliers. Mean±s.d.; ***P<0.005, ****P<0.001 (Mann–Whitney test).

upregulation of RHOB expression (Fig. S3A), sustained cell proliferation (Fig. S3B) and DNA synthesis (Fig. S3C). An increase of cells in S-phase could also be achieved using a conditionally active mutant form of HDAC4 (Fig. S3B). Compared to EGF, the HDAC7/SA-ER chimera was less capable of repressing *RHOB* and sustaining DNA synthesis. This partial effect could be a result of the dramatic decrease in its expression that is observed when cells were deprived of serum and growth factors (Fig. S3D,E).

The most prominent effect of cell cycle exit on the MEF2–HDAC axis, in both 3D and 2D culture models, was the downregulation of HDAC7 levels. To verify whether the upregulation of MEF2-target genes depends on the reduced recruitment of HDAC7 on the promoter of such genes, we performed chromatin immunoprecipitation (ChIP) analysis. The *RHOB* promoter was selected as a prototype of the MEF2-target genes. Fig. 5E illustrates that HDAC7 bound to the *RHOB* proximal promoter during the proliferative phase, whereas this binding was clearly reduced upon growth arrest, as induced by either serum starvation or density-dependent inhibition.

HDAC7 binds to the p21 promoter

Cyclin-dependent kinases (CDKs) are master regulators of cell cycle progression and cell proliferation. The CDK inhibitor p21 (CDKN1A) is a well-known negative regulator of proliferation, under the control of multiple signals, including growth factors and differentiation (Besson et al., 2008). Some reports have suggested that class-IIa HDACs are involved in the regulation of transcription of *CDKN1A* (Liu et al., 2009; Mottet et al., 2009; Wilson et al., 2008). To explore whether MEF2s and class-IIa HDACs control p21 expression during acinar morphogenesis, we initially interrogated the ENCODE database to map the epigenetic status of the *CDKN1A* promoter in human mammary epithelial cells (HMECs) (Ernst et al., 2011; Rosenbloom et al., 2013). We investigated the genomic region that is situated between two insulators (CTCF). Trimethylated Lys4 of histone 3 (H3K4me3) and acetylated Lys27 of histone 3 (H3K27ac), well-known markers of open chromatin status and characteristics of active promoter and enhancer regions, outline the first intron as an important element that is involved in *CDKN1A* transcription (Fig. 6A). A similar pattern can be observed in lymphoblastoid GM12878 cells (Fig. S4) and in the leukemia cells K562 (data not shown). Interestingly, the available ENCODE data for GM12878 and K562 cell lines highlighted the conserved binding of MEF2 factors to the promoter and enhancer elements, although with slight variations in the position of binding.

Next we screened for potential MEF2-binding sites a 20-kb genomic region of *CDKN1A*, comprising the first intron, which contains the active chromatin markers above described. The enlargement in Fig. 6A illustrates the presence of several potential MEF2 binding sites in the analyzed genomic region and particularly in the first intron.

To evaluate the involvement of HDAC7 in the regulation of *CDKN1A* transcription, we decided to investigate its ability to bind to the regions highlighted in Fig. 6A. ChIP experiments proved that HDAC7 bound preferentially to the region containing the MEF2-binding site at +1.5 kb from the transcription start site (TSS). Importantly, this binding was abolished or dramatically reduced when growth arrest was induced by growth factor starvation or high confluence (Fig. 6B).

Class-IIa HDACs are recruited to specific genomic regions following interactions with DNA-binding transcription factors. Hence, we assessed the binding of MEF2D to the same genomic regions. In proliferating cells, MEF2D bound to the *RHOB* and the *CDKN1A* promoters at +1.5 and +2.1 kb from the TSS, respectively (Fig. 7A). Surprisingly, a different behavior was observed in starved cells in contrast to confluent cells. MEF2D binding was maintained under starvation on both promoters in the same regions (slightly increased in the case of *CDKN1A*), whereas it was dramatically decreased in confluent cells. For *CDKN1A*, a new binding of MEF2D at the −5.7 kb region was observed only when cells were arrested through confluence.

ChIP experiments using an antibody against H3K27ac (Fig. 7B) confirmed the ENCODE data. Enrichment for H3K27 acetylation could be observed from +1.5 kb up to +3.6 kb from the TSS of the *CDKN1A* promoter (compare Fig. 6A). Concerning *RHOB*, H3K27ac was not pronounced, probably because this region is very close to the TSS, as reported in the ENCODE project. Under starvation, a consistent increase in H3K27ac was observed for the *RHOB* promoter, and this increase was much less pronounced at confluence. Overall, changes in this epigenetic modification are in agreement with MEF2D and HDAC7 binding to promoters.

Growth arrest through starvation elicits an overt increase of H3K27ac around the +2.1-kb region of the *CDKN1A* promoter. A small but significant increase can be appreciated also in the region +1.5 kb, in accordance with MEF2D binding and HDAC7 release. When growth arrest was induced through high confluence, the most

Journal of Cell Science (2015) 128, 3961-3976 doi:10.1242/jcs.170357

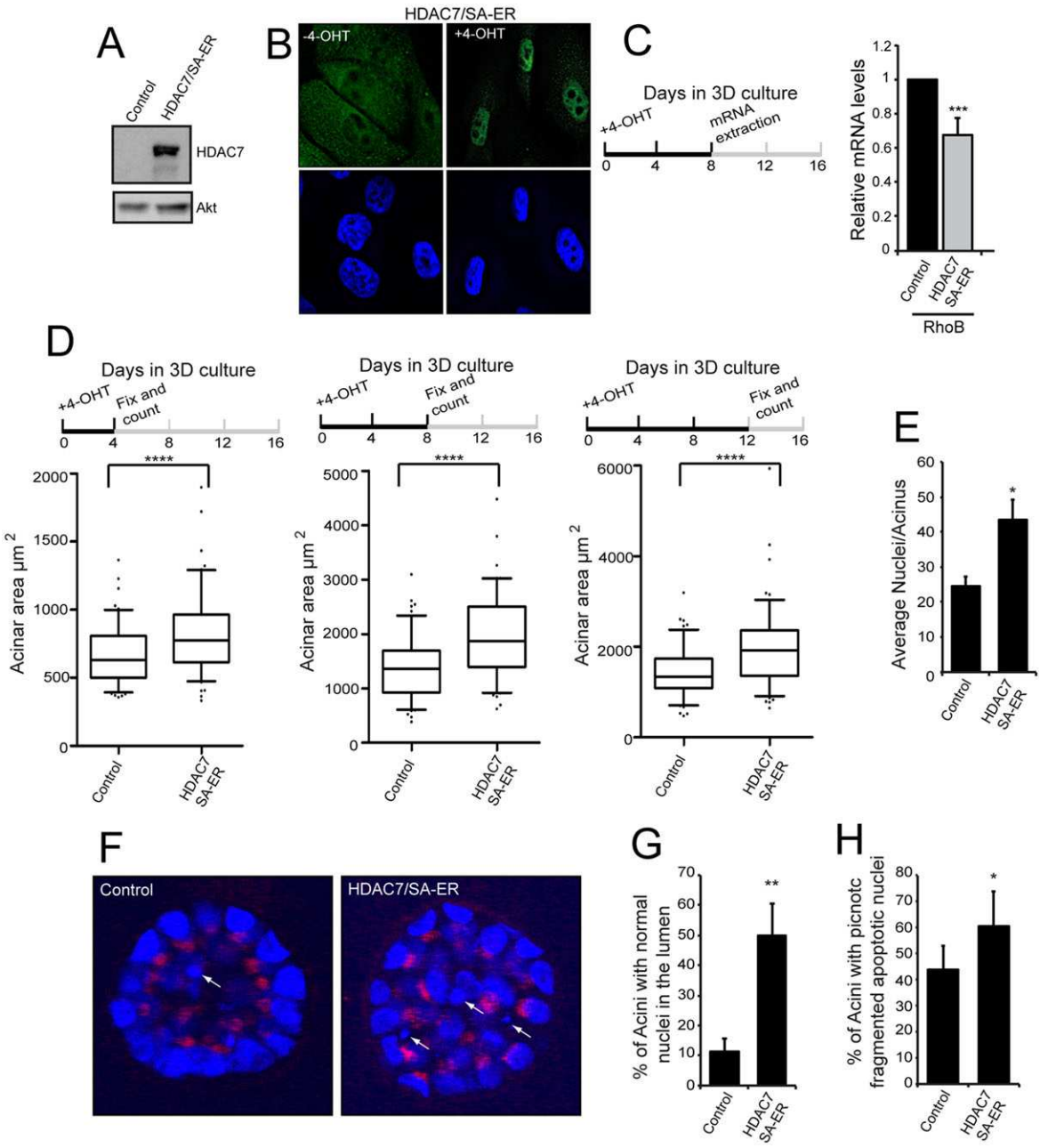

Fig. 4. Sustained HDAC7 activity promotes cell proliferation and affects acinar morphogenesis. (A) Immunoblot analysis of HDAC7 levels in MCF10A cells expressing a mutant form of HDAC7 in which four serine residues were mutated (normally the binding sites for 14-3-3 proteins) (HDAC7/SA-ER) or the control empty vector. HDAC7/SA-ER activity was induced by treating cells with 4-OHT for 24 h. Cellular lysates were generated and subjected to immunoblot analysis to verify the molecular size of the transgene using an anti-HDAC7 antibody. AKT1 was used as a loading control. (B) Confocal pictures of MCF10A cells showing HDAC7/SA-ER nuclear accumulation after the induction with 4-OHT. Nuclei were stained with TOPRO-3. Images are shown in pseudocolors. (C) mRNA expression levels of the MEF2-target gene *RHOB* were measured by using qRT-PCR analysis of MCF10A cells expressing HDAC7/SA-ER or control cells grown in 3D culture for 8 days. 4-OHT was added to culture medium on the day of seeding and the fourth day of culture. (D) Acinar size of MCF10A cells, expressing HDAC7/SA-ER, in 3D culture for 4, 8 and 12 days. When cells were seeded, 4-OHT was added to culture medium as well as on every fourth day in culture. Data are from a representative set of three independent experiments in which ~250 acini per condition were measured. Boxes represents the first and the third quartile, the middle line represents the median, whiskers represent the 10th and the 90th percentile, and dots represents the outliers. (E) Number of nuclei per acinus, as generated from MCF10A cells expressing HDAC7/SA-ER or the control, after 12 days in 3D culture. (F) Confocal images comparing the presence of picnotic fragmented apoptotic nuclei in the lumen of acini generated from MCF10A cells, expressing HDAC7/SA-ER or the control, grown in 3D culture for 12 days. Nuclei were stained with Hoechst 33258. Images are shown in pseudocolors. Arrowheads point to picnotic apoptotic nuclei. (G) Quantification of the number of acini with normal nuclei in the lumen, as generated by MCF10A expressing the different transgenes after 12 days of culture in 3D. (H) Quantification of the number of apoptotic cells per acini, as generated by MCF10A expressing the different transgenes after 12 days in 3D culture. Mean±s.d.; **P*<0.05, ***P*<0.01, ****P*<0.005, *****P*<0.001 (*t*-test).

evident relative increase in H3K27ac regarded the overall poorly acetylated region at −5.7 kb. This is the same region bound by MEF2D in confluent cells (Fig. 7A).

The involvement of the MEF2–HDAC axis in the regulation of *CDKN1A* transcription was confirmed after induction of the MEF2-VP16 chimera in 2D conditions at both mRNA and protein levels

Journal of Cell Science (2015) 128, 3961-3976 doi:10.1242/jcs.170357

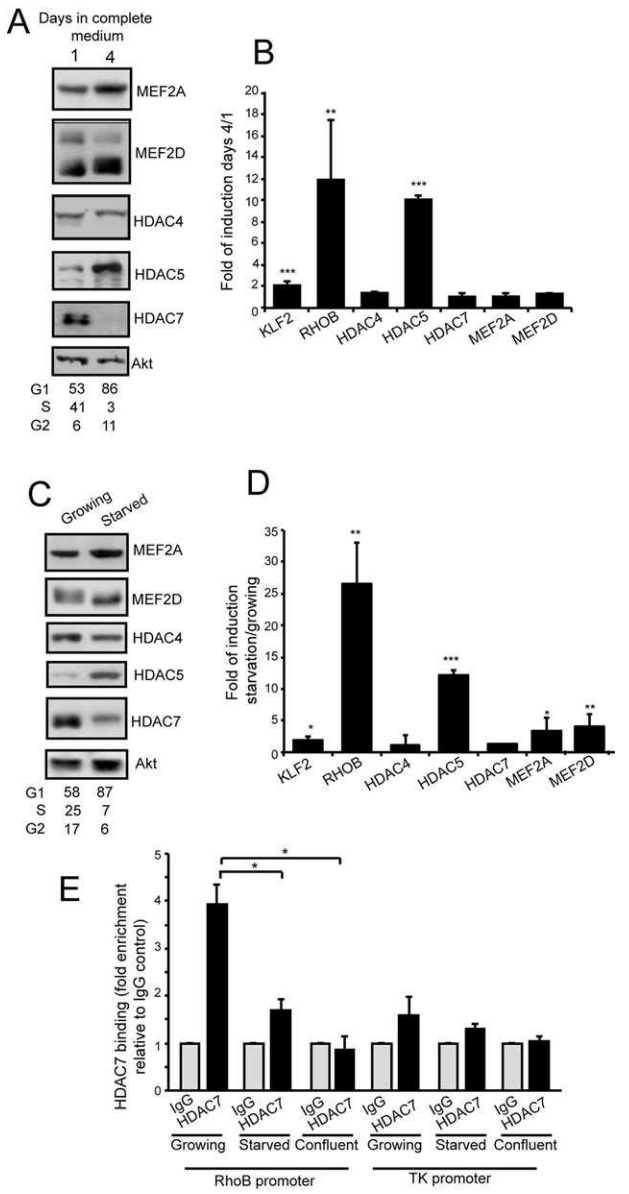

Fig. 5. MEF2-dependent transcription and HDAC7 levels are regulated during growth arrest in mammary epithelial cells. (A) Immunoblot analysis of MEFs and class-IIa HDAC-family member levels in MCF10A cells. Cellular lysates were obtained at the indicated time points after seeding in complete medium and subjected to immunoblot analysis using the specific antibodies. AKT1 was used as loading control. Cell cycle analysis is provided underneath the blots as percentage of cells. (B) qRT-PCR analysis was performed to quantify mRNA levels of class-IIa members (*HDAC4*, *HDAC5* and *HDAC7*) and of MEF2s (*MEF2A* and *MEF2D*), as well as of MEF2-taget genes (*KLF2* and *RHOB*) in MCF10A cells. The fold induction was calculated as the ratio relative to expression at 1 day of culture in complete medium. Data are from three independent experiments. (C) Immunoblot analysis of MEF2- and class-IIa-HDAC-family member levels in MCF10A cells. Cellular lysates were obtained at the different growing conditions and subjected to immunoblot analysis using the specific antibodies. AKT1 was used as loading control. Cell cycle analysis is provided underneath the blots as percentage of cells. (D) qRT-PCR analysis was performed to quantify the mRNA levels of the most expressed class-IIa members (*HDAC4*, *HDAC5* and HDAC7) as well as of MEF2 members (*MEF2A* and *MEF2D*) and MEF2-target genes (*KLF2* and *RHOB*) in MCF10A cells. Fold induction was calculated as the ratio between starvation and growing conditions. Data are from three independent experiments. (E) qRT-PCR analysis on chromatin that had been immunoprecipitated with the indicated antibodies in the different conditions shown. Mean±s.d.; **P*<0.05, ***P*<0.01, ****P*<0.005 (one-way ANOVA test coupled to Tukey's HSD post-hoc test).

(Fig. 7C,D), and in 3D conditions at the mRNA level (Fig. 7E). Finally, the repression that was mediated by the HDAC7/SA-ER chimera in 2D (Fig. S2F) and 3D conditions (Fig. 7F) further supports such involvement.

The MEF2–HDAC axis is regulated during HER2-mediated transformation of mammary epithelial cells

The contribution of the MEF2–HDAC axis to the regulation of mammary epithelial cell proliferation prompted us to determine whether oncogenic lesions that alter mammary epithelial morphogenesis provoke dysregulation of the axis. The tyrosine kinase receptor HER2 (also known as ERBB2) is the key determinant of a subclass of breast tumors, and overexpression of HER2 profoundly alters the normal mammary epithelial morphogenetic process (Leung and Brugge, 2012). Hence, we generated MCF10A cells that overexpressed HER2 to assess dysregulation of the MEF2–HDAC axis. After 16 days in 3D culture, HER2-overexpressing cells showed an elevated proliferative index, as proved by the development of larger acini (Fig. 8A) that comprised higher numbers of cells per structure and that were marked by the presence of mitotic figures even at day 16 (Fig. 8B). Moreover, the compromised epithelial organization was apparent because of the alterations in polarity and the presence of cells in the luminal cavity (Fig. 8B). Accordingly, HER2 significantly reduced the expression of epithelial morphogenesis markers (*BIM* and *BMF*). Similarly, the expression of certain MEF2 targets (*KLF2*, *RHOB* and *CDKN1A*) was reduced (Fig. 8C). Importantly, the decrease in MEF2-dependent transcription was coupled to the rescue of HDAC7 levels at day 16 (Fig. 8D). Curiously, MEF2D levels seem to increase in HER2-expressing cells. Conversely, the inhibition of HER2 tyrosine kinase activity with lapatinib, a quinazoline derivative, dramatically impacted on epithelial growth, thus limiting acinar size (Fig. 8E). Acinar cellularity and mitotic figures were also reduced in lapatinib-treated cells (Fig. 8F). Lapatinib also restored the appearance of acini with hollow lumens (Fig. 8F). Interestingly, the effect of this inhibitor seemed to be cell cycle dependent, without interference through the induction of apoptosis, as supported by the unchanged rate of picnotic nuclei per acini (Fig. 8F).

In agreement with our studies, treatment of MCF10A HER2-expressing cells that had been grown for 8 days in 3D culture with lapatinib upregulated MEF2-dependent gene transcription, the expression of *BIM* and *BMF* morphogenetic markers (Fig. 8G) and elicited the downregulation of HDAC7 (Fig. 8H). HDAC7 downregulation showed the same features during growth arrest as described above. It occurred in the absence of changes in mRNA levels (Fig. 8G) and was lysosome and proteasome independent (Fig. S4C). Interestingly, HDAC4 levels seemed to be reduced after HER2 inhibition.

Importantly, induction of MEF2 transcription in MCF10A cells that expressed HER2 restored normal epithelial morphogenesis to an extent that was comparable to that with lapatinib. All of the proliferative parameters (average number of nuclei per acinus, the percentage of acini with mitotic figures and of acini with normal nuclei in the lumen) were reduced following MEF2 activation in HER2-overexpressing cells (Fig. 8I).

DISCUSSION

The mammary gland undergoes complex remodeling during different stages – i.e. puberty, pregnancy, lactation and involution (Gjorevski and Nelson, 2011). 3D cultures have significantly helped in understanding how some of these processes take place.

Journal of Cell Science (2015) 128, 3961-3976 doi:10.1242/jcs.170357

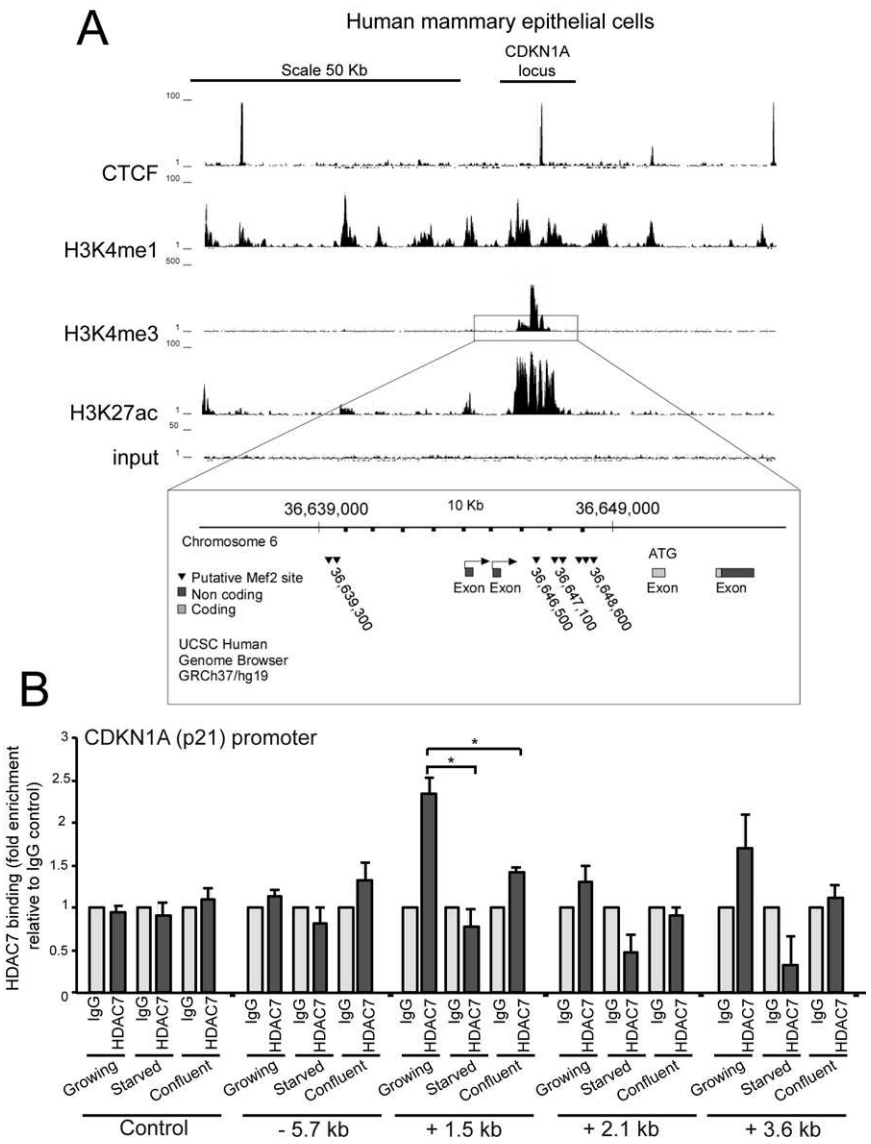

Fig. 6. HDAC7 binds to the promoter region of *CDKN1A*. (A) Schematic representation of the epigenetic status of the *CDKN1A* locus in human mammary epithelial cells as mapped with the ENCODE project. Two insulator CTCF peaks comprise the analyzed region, and the promoter was identified through H3K4me3 and H3K27ac signals. A region of 20 kb, highlighted in the black box, including the promoter, was selected and scanned for putative MEF2-binding sites. (B) qRT-PCR analysis on chromatin immunoprecipitated with the indicated antibodies in different growth conditions as shown. The different genomic regions of *CDKN1A* containing putative MEF2-binding sites are indicated starting from the transcription start site. An internal region (+4.7 kb) of the *CDKN1A* gene was used as a negative control (Control). Mean± s.e.m.; **P*<0.05 (one-way ANOVA test coupled to Tukey's HSD post-hoc test).

Particularly, although MCF10A cells grown under 3D conditions do not enter terminal differentiation (Muthuswamy et al., 2001) with milk protein production, the imposed 3D environment influences cell behavior and mimics the steps required for proper developmental and homeostatic cues (Leung and Brugge, 2012; Lo et al., 2012; Shaw et al., 2004). Complex cellular decisions take place during the 16-day interval that is necessary for acini formation. After the initial proliferation phase, cells begin to polarize and gradually exit from the cell cycle. The process terminates with the death of the cells in the lumen and with cavity formation (Frisch et al., 2013).

In this context, we have studied the regulation of the MEF2–HDAC axis and have dissected its contribution to the epithelial morphogenetic program. Quantitative and qualitative changes in gene expression profiles characterize the morphogenetic process of MCF10A cells grown under 3D condition (Yu et al., 2012). However, few studies have addressed the contribution of specific transcription factors and of the relative transcriptional gene networks to this morphogenetic process. We have initially demonstrated that the expression of MEF2-target genes is augmented during acini formation. This behavior resembles that under other differentiation contexts, as in skeletal muscle, where the contribution of the axis has been previously studied (McKinsey et al., 2000; Sebastian et al., 2013). Activation of MEF2 transcription is parallel to a dramatic downregulation of HDAC7 protein. In MCF10A cells, in contrast to other cellular models, anti-proliferative signals unleash MEF2-dependent transcription by impacting on HDAC7 levels, rather than by controlling its nuclear–cytoplasmic shuttling (McKinsey et al., 2000; Paroni et al., 2008). HDAC7 downregulation is linked to growth arrest, and it can also be observed in 2D conditions, after growth factor starvation or density inhibition. At the moment, the mechanism that is responsible for HDAC7 downregulation is unknown. We can only exclude changes in mRNA levels, in proteasomal degradation and in autophagy.

HDAC5 and HDAC9 expression increases during acini formation. Being both MEF2-target genes, it is possible that such induction is part of the well-known negative feedback loop that is activated by MEF2 itself (Haberland et al., 2007). Nevertheless, because HDAC7 is the most expressed class-IIa deacetylase in breast tissue and in MCF10A cells, its withdrawal can justify the upregulation of MEF2 transcription. Furthermore, some reports indicate a differential repressive capability of class-IIa HDACs towards MEF2 proteins, with HDAC5 being the enzyme that is least prone to such repression (Dressel et al., 2001).

Journal of Cell Science (2015) 128, 3961-3976 doi:10.1242/jcs.170357

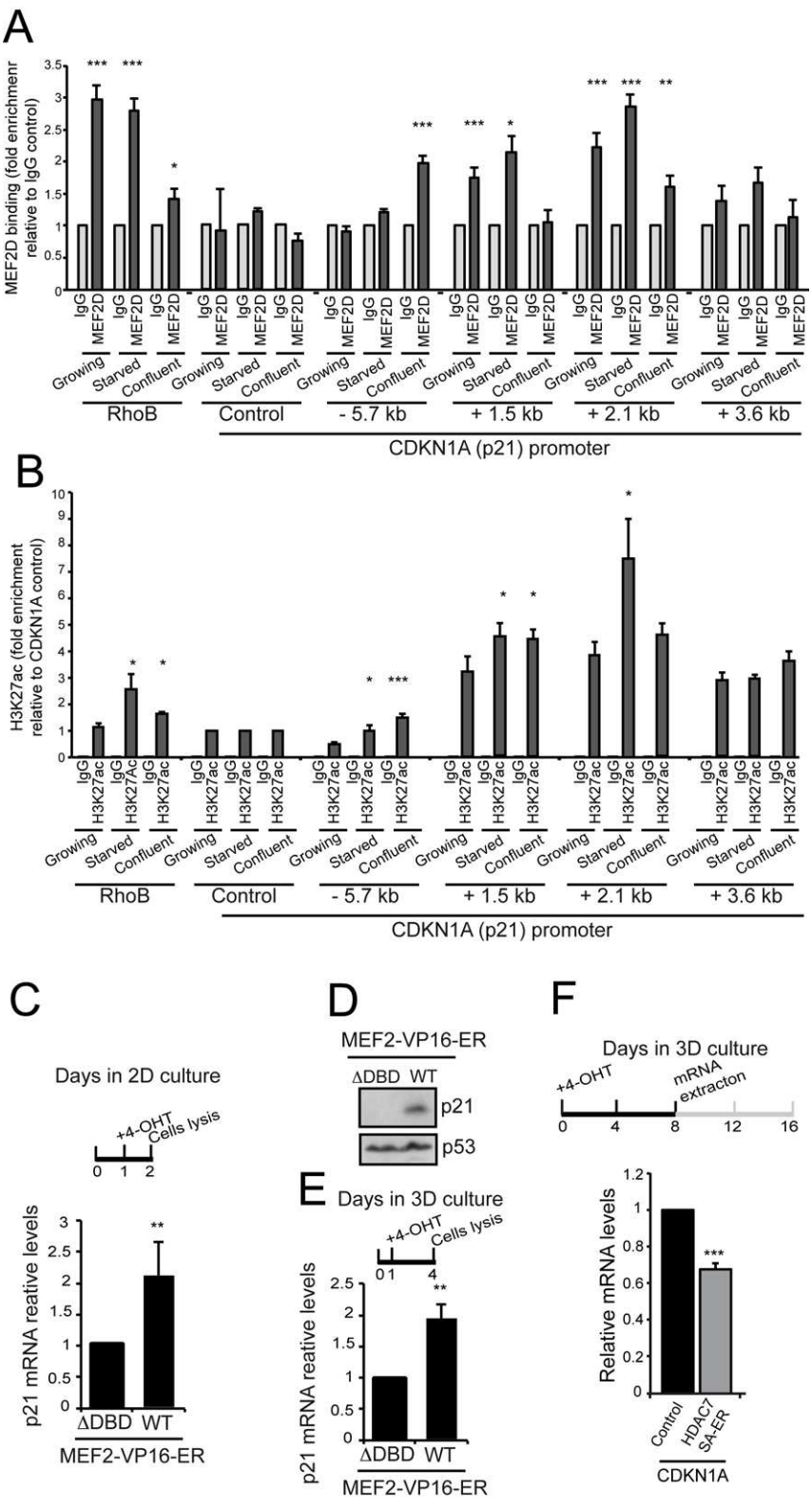

Fig. 7. MEF2D binding and H3K27 acetylation at the promoter regions of *CDKN1A* and *RHOB*. (A) qRT-PCR analysis on chromatin immunoprecipitated with the indicated antibodies in the different growth conditions shown. The different genomic regions of *CDKN1A* containing putative MEF2-binding sites are indicated, starting from the transcription start site. An internal region (+4.7 kb) of the *CDKN1A* gene was used as a negative control (Control). (B) qRT-PCR analysis on chromatin immunoprecipitated with the indicated antibodies in the different growth conditions shown. The different genomic regions of *CDKN1A* containing putative MEF2-binding sites are indicated starting from the transcription start site. An internal region (+4.7 kb) of the *CDKN1A* gene was used as a negative control (Control). (C) qRT-PCR analysis was performed to quantify *CDKN1A* mRNA levels in cells in which MEF2 transcription had been induced after treatment with 4-OHT. Fold induction was calculated as the ratio relative to expression in cells in which the expression of MEF2 defective in DNA (ΔDBD) binding was induced by 4-OHT treatment, as indicated. (D) Immunoblot analysis of MCF10A cells expressing the indicated transgene for p21/CDKN1A levels. Induction of the transgenes was performed as described in C. (E) mRNA expression levels of *CDKN1A* were measured by using qRT-PCR analysis in MCF10A cells grown for 8 days in 3D culture. MEF2 transcription was induced after treatment with 4-OHT. The fold induction was calculated as the ratio of expression relative to that of cells expressing MEF2 defective in DNA binding. 4-OHT was added to the culture medium on the day of seeding and on the fourth day of culture. (F) mRNA expression levels of *CDKN1A* were measured by using qRT-PCR in MCF10A cells expressing HDAC7/SA-ER or the control construct that had been grown in 3D culture for 8 days. 4-OHT was added to the culture medium the day of seeding and on the fourth day of culture. WT, non-mutated construct. Mean±s.e.m.; **P*<0.05, ***P*<0.01, ****P*<0.005 (*t*-test, and one-way ANOVA test coupled to Tukey's HSD post-hoc test in B).

We exploited different approaches to interfere with the MEF2 transcriptional activity. In all instances, the effect was an impediment of the proliferative phase. Increasing MEF2-dependent transcription reduced cell division, whereas increasing HDAC7 repressive activity favored cell proliferation. The polarization process and the induction of cell death were unaffected after modulation of the MEF2–HDAC axis.

Although MEF2 proteins are the best-characterized class-IIa HDAC partners, these deacetylases can influence the activity of additional transcriptional regulators (Clocchiatti et al., 2103a). In this study, we have found logical correlations between MEF2 and class-IIa HDACs in the regulation of proliferation and gene expression during acini formation. Furthermore, deletion of the MEF2-binding sequence abrogated the pro-growth effect of

Journal of Cell Science (2015) 128, 3961-3976 doi:10.1242/jcs.170357

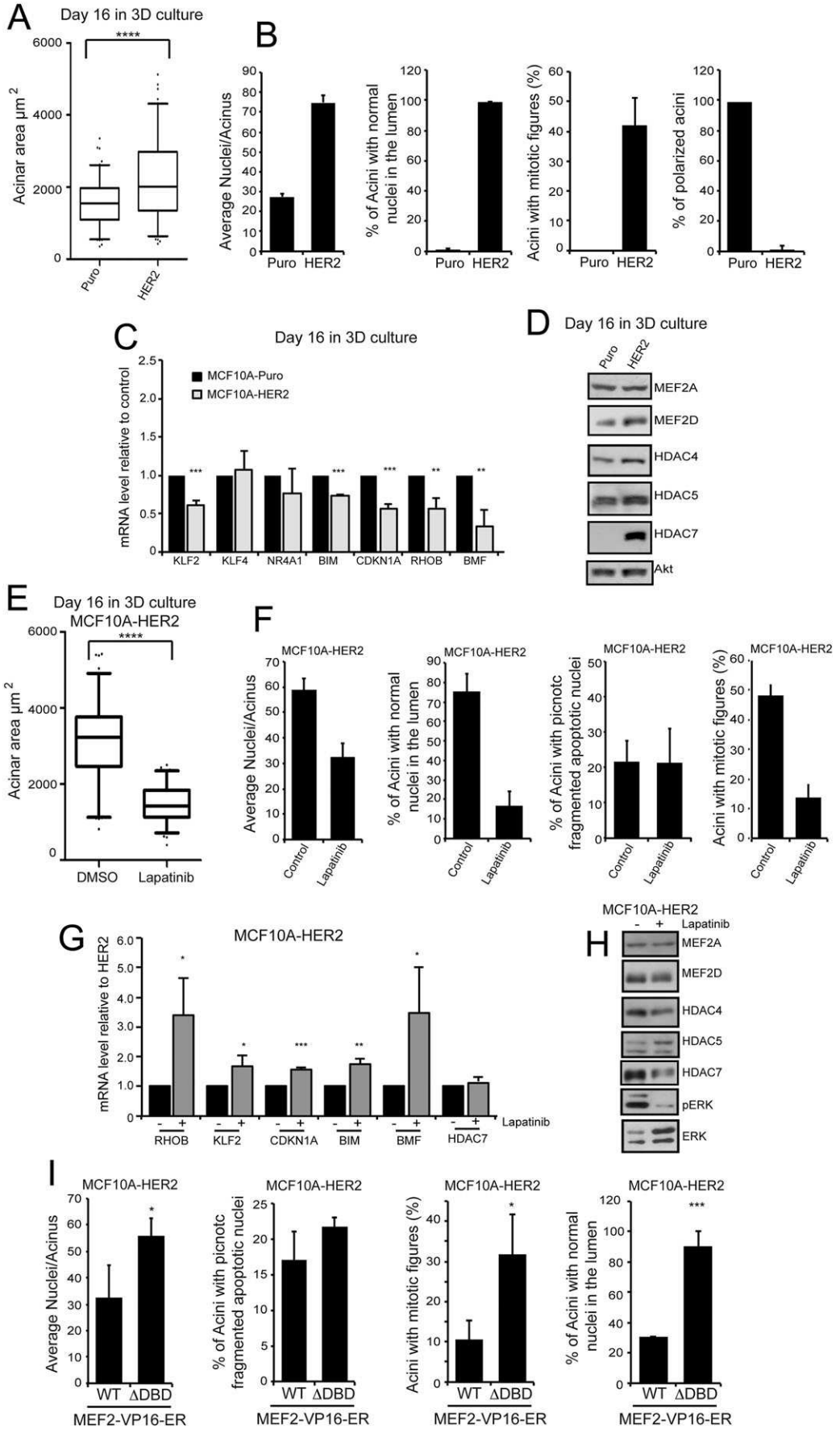

Fig. 8. See next page for legend.

Journal of Cell Science (2015) 128, 3961-3976 doi:10.1242/jcs.170357

Fig. 8. The MEF2–HDAC axis is regulated during HER2-mediated transformation of mammary epithelial cells. (A) The acinar size of MCF10A cells expressing HER2 that had been grown in 3D culture for 16 days was analyzed. Data are from three independent experiments in which ∼250 acini per condition were measured. (B) The number of nuclei per acinus, number of acini with normal nuclei in the lumen, number of acini with mitotic figures and number of polarized acini in acini generated from MCF10A cells expressing HER2 after 16 days in 3D culture. Puro, indicates the cells that express the resistence to Puromycin as control. (C) qRT-PCR analysis was performed to evaluate mRNA levels of MEF2-target genes in MCF10A cells expressing HER2 that had been cultured in 3D for 16 days. (D) Immunoblot analysis of MEF2s and class-IIa-HDAC-family member levels in MCF10A cells expressing HER2 that had been grown in 3D for 16 days. Cell lysates were subjected to immunoblot analysis using the indicated antibodies. AKT1 was used as loading control. (E) The acinar size of MCF10A cells expressing HER2 that had been grown in 3D culture for 16 days and treated or not with lapatinib was analyzed. Data are from three independent experiments in which ∼250 acini per condition were measured. (F) The number of nuclei per acinus, number of acini with normal nuclei in the lumen, number of acini with picnotic and fragmented apoptotic nuclei and number of acini with mitotic figures in acini generated from MCF10A cells expressing HER2 that had been treated or not with lapatinib, after 16 days in 3D culture. (G) qRT-PCR analysis was performed to evaluate the mRNA levels of MEF2-target genes in MCF10A cells expressing HER2 that had been treated or not with lapatinib and cultured in 3D for 8 days. (H) Immunoblot analysis of MEFs and class-IIa-HDAC-family member levels in MCF10A cells expressing HER2 that had been treated or not with lapatinib and grown in 2D culture. Cell lysates were subjected to immunoblot analysis using the indicated antibodies. Total ERK1/2 was used as loading control. (I) The number of nuclei per acinus, number of acini with picnotic and fragmented apoptotic nuclei, number of acini with mitotic figures and number of acini with normal nuclei in the lumen in acini generated from MCF10A cells expressing HER2 and the MEF2-VP16-ER chimera (WT) or its mutant defective in DNA binding (MEF2ΔDBD-VP16-ER, ΔDBD) after 8 days in 3D culture. MEF2-VP16-ER activation was induced by adding 4-OHT to growth medium after 4 days in 3D culture. A,E, Boxes represent the first and the third quartile, the middle line represents the median, whiskers represent the 10th and the 90th percentile, and dots represent the outliers. Mean±s.d.; **P*<0.05, ***P*<0.01, ****P*<0.005, *****P*<0.001, Mann–Whitney test.

the nuclear resident HDAC7. Overall, our data strongly support that the described HDAC7 action is explicated through MEF2s.

We propose that the influence of the axis on cell proliferation could be operated through the regulation of the CDK inhibitor p21/CDKN1A. Previous results have shown that class-IIa HDACs can control CDKN1A expression (Liu et al., 2009; Mottet et al., 2009; Saramaki et al., 2009; Wilson et al., 2008); however, the mechanisms involved are debated. MEF2-binding sites are present in the genomic regions surrounding *CDKN1A*. In particular, several MEF2-binding sites lie within the first intron. This intron is characterized by the presence of open chromatin markers (Ernst et al., 2011). Our results suggest that the MEF2–HDAC axis imposes a control on the cell cycle by modulating CDKN1A expression. Recruitment of HDAC7 onto the *CDKN1A* promoter is confined in a region (+1.5 kb) that is also under the control of MEF2 factors in other cell lineages scrutinized by the ENCODE project (Ernst et al., 2011). We have also proved that, in MCF10A cells, MEF2D binds to this region. However, MEF2D can also tether to additional regions, such as that at +2.1 kb, which are not bound by HDAC7, as we have recently observed in fibroblasts (Di Giorgio et al., 2015b). Whether specific MEF2–HDAC complexes exist bound to different chromatin regions deserves further studies.

At the +1.5 kb position, HDAC7 binding is dramatically reduced under conditions that stimulate cell cycle arrest, and this reduction is associated only with a modest increase in H3K27ac. Even though class-IIa HDACs do not exhibit catalytic activity, they can act as platforms to recruit class-I enzymes (Lahm et al., 2007; Di Giorgio et al., 2015a). Hence, HDAC7 could influence epigenetic changes at the *CDKN1A* promoter both by recruiting co-repressors and by competing with co-activators for binding to MEF2 proteins. Certainly, it is possible that different growth conditions influence additional epigenetic changes within this genomic region.

The most evident increase in H3K27ac was observed as occurring at the +2.1 kb position when growth arrest was induced by starvation, pointing to the existence of additional mechanisms of regulation. Finally, our analysis of the binding of MEF2D to the *CDKN1A* promoter indicates the existence of specific chromatin changes in response to different conditions of growth arrest.

The effect of MEF2 on the regulation of *CDKN1A* transcription seems to be a general phenomenon that is not limited to MCF10A cells. Also, in fibroblasts, MEF2C and MEF2D bind to the CDKN1A promoter. Importantly, in these cells, the downregulation of MEF2D is sufficient to increase cell proliferation and efficiently impacts on the expression of MEF2-target genes, including *CDKN1A* (Di Giorgio et al., 2015b).

HER2 overexpression, a frequent oncogenic event in breast tumors, is able to maintain HDAC7 levels and decrease MEF2 transcription during the morphogenetic process, which might be an additional and powerful way to control p21 function beyond regulating its localization (Xia et al., 2004). Interestingly, forcing MEF2 activity in MCF10A HER2-overexpressing cells reverses the transformed phenotype, mainly by restraining proliferation, thus ensuring correct epithelial organization. Furthermore, treatment with the receptor tyrosine kinase (RTK) inhibitor lapatinib rescued HDAC7 downregulation and acini formation in 3D cultured cells. In conclusion, our studies unveil a role for the MEF2–HDAC axis in the control of epithelial cell proliferation and suggest that targeting class-IIa HDACs with inhibitors could be an interesting therapeutic strategy, in addition to or in combination with treatment with RTK inhibitors, for the treatment of breast cancer.

MATERIALS AND METHODS

Cell culture and reagents

Human normal immortalized epithelial breast cells (MCF10A) (Whyte et al., 2010) and MCF10A cells expressing HER2 were maintained in Ham's F12: Dulbecco's modified Eagle's medium (DMEM) 1:1 medium (Sigma-Aldrich) supplemented with 5% horse serum (Gibco), penicillin (100 U/ml), streptomycin (100 µg/ml), L-glutamine (2 mM) (Lonza), insulin (0.01 mg/ml), hydrocortisone (500 ng/ml), cholera toxin (100 ng/ml) (Sigma-Aldrich) and epithelial growth factor (20 ng/ml) (Peprotech). HEK-293T cells were grown in DMEM supplemented with 10% fetal bovine serum (FBS), L-glutamine (2 mM), penicillin (100 U/ml), and streptomycin (100 µg/ml) (Lonza). Cells expressing inducible forms of MEF2 and HDAC7 were grown in complete F12/DMEM medium without phenol red (Sigma-Aldrich) and with 5% charcoal-stripped horse serum. The proteasome inhibitor bortezomib (LC Laboratories) was used at 250 nM for 8 h. The lysosome and autophagy inhibitor chloroquine (Sigma-Aldrich) was used at 10 µM for 8 h. The CRM1 inhibitor leptomycin-B (LC Laboratories) was used at 5 ng/ml. 4-OHT (Sigma-Aldrich) was used at 1 µM. The inhibitor of HER2 lapatinib (LC Laboratories) was used at 1 µM for 2 h.

3D morphogenetic assay

3D morphogenetic assays were conducted as previously described (Debnath et al., 2003). Briefly, to obtain mammospheres, cells (3×10^4) were plated in a thick layer of ∼1–2 mm of laminin-rich extracellular matrix (Cultrex-Trevigen), under these conditions each acinus derives from a single cell. Cultrex was overlaid with cells grown in medium containing 5 ng/ml EGF along with 2% (v/v) cultrex. Cells were maintained at 37°C and 5% CO_2 and the culture medium was changed every 4 days. Images of mammospheres were collected by using a Leica AF 6000LX microscope. Acinar area measurements were determined using Volocity 3D image analysis software.

Journal of Cell Science (2015) 128, 3961-3976 doi:10.1242/jcs.170357

Plasmid construction, transfection, retroviral and lentiviral infection, and silencing

The pWZL-Hygro-MEF2C-VP16-ER construct comprising the first 119 amino acids of MEF2C has been previously described (Di Giorgio et al., 2013). The ligand-binding domain of the estrogen receptor was PCR amplified from pcDNA MEF2-VP16-ER (Flavell et al., 2006) and cloned into pWZLHygro. To generate pWZL-Hygro-HDAC7/SA-ER, an *EcoR*I-digested fragment of the HDAC7/SA point mutant (Di Giorgio et al., 2013) was cloned into pWZL-Hygro-ER. MCF10A cells expressing the MEF2-VP16-ER or HDAC7/SA-ER transgenes were generated by using retroviral infection, as described previously (Cernotta et al., 2011). The HDAC7/SA-ER construct that comprised deletion of the MEF2-binding domain, lacking amino acids 78–93 was generated by using PCR and subsequent two steps cloning into pWZL-Hygro-ER. HEK-293T packaging cells were transfected 24 h after plating by using calcium-phosphate precipitation. After 48–72 h, the virus-containing medium was filtered and added to target cells. Recombinant lentiviruses (Sigma-Aldrich) were produced through transfection of HEK-293T cells. Briefly, subconfluent HEK-293T packaging cells were co-transfected with 20 µg of lentiviral vector plasmids, 15 µg of pCMV-ΔR8.91 and 5 µg of VSVG envelope plasmid by using calcium-phosphate precipitation. After 24 h, medium was changed, and recombinant lentiviruses vectors were harvested 24–36 h later.

Immunofluorescence, antibody production and immunoblotting

Cells were fixed in 3% paraformaldehyde and permeabilized with 1% Triton-X100. Next, coverslips were incubated with the following primary antibodies: anti-HDAC4 (Paroni et al., 2004), anti-HDAC7 (sc-74563; Santa Cruz Biotechnology), anti-MEF2D (610774; BD Transduction Laboratories) and anti-GM130 (610822; BD Transduction Laboratories). Then, they were incubated with 488- or 546-Alexa-Fluor-conjugated secondary antibodies (Life Technologies). Finally, coverslips were incubated for 15 min with 5 µM TOPRO-3 (610822; Life Technologies) to label nuclei. Cells were imaged with a Leica confocal scanner SP instrument that was equipped with a 488-λ argon laser and a 543–633-λ helium-neon laser. Representative confocal images are shown as equatorial cross sections through the middle of acini.

Rabbits were immunized with a recombinant histidine-tagged HDAC5 fragment (amino acids 1132–2040) that had been purified from *Escherichia coli*. For purification of the anti-HDAC5 antibody from antiserum, HDAC5 was fused to glutathione S-transferase (GST) and cross-linked to glutathione–Sepharose, as described previously (Paroni et al., 2001).

Cell lysates after SDS-PAGE and immunoblotting were incubated with the following primary antibodies against: HDAC4 (Paroni et al., 2004), HDAC7 (sc-74563; Santa Cruz Biotechnology), MEF2A (sc-10794; Santa Cruz Biotechnology), MEF2D (610774; BD Transduction Laboratories), AKT (#9272; Cell Signaling Technology), p53 (sc-126; Santa Cruz Biotechnology), p62 (610497; BD Transduction Laboratories), LC3 (Demarchi et al., 2006), VP16 (sc-7545; Santa Cruz Biotechnology), p120 (610134; BD Transduction Laboratories), ERK (#4695; Cell Signaling Technology), phosphorylated ERK (#9101; Cell Signaling Technology). Secondary antibodies were obtained from Sigma-Aldrich, and blots were developed with Super West Dura (Pierce). To strip antibodies, blots were incubated for 30 min at 60°C in stripping solution containing 100 mM β-mercaptoethanol. DNA staining was performed as described previously (Cernotta et al., 2011). For S-phase analysis, cells were grown for 3 h with 100 µM bromodeoxyuridine (BrdU). After fixation, coverslips were treated with 1 N HCl (10 min, in ice), followed by 20 min with 2 N HCl at room temperature. Mouse anti-BrdU (B8434; Sigma-Aldrich) was used as primary antibody. Nuclei were stained with Hoechst 33258 (Sigma-Aldrich).

RNA extraction and qRT-PCR

Cells were lysed using RiboEx (GeneAll Biotechnology). 1 µg of total RNA was retro-transcribed by using 100 units of M-MLV reverse transcriptase (Life Technologies). qRT-PCR analyses were performed using the Bio-Rad CFX96 apparatus and SYBR Green technology (Kapa). Data were analyzed with the ΔΔCt method, using glyceraldehyde 3-phosphate dehydrogenase (GAPDH) and hypoxanthine phosphor-ribosyltransferase (HPRT) as normalizer genes. All reactions were performed in triplicate. To evaluate the mRNA copies per µg of retro-transcribed RNA for each class-IIa HDAC, standard curves of the qRT-PCR amplification were obtained using defined concentrations of the relative cDNAs.

Chromatin immunoprecipitation

For immunoprecipitations, DNA–protein complexes were cross-linked with 1% formaldehyde (Sigma-Aldrich) in PBS for 15 min at room temperature. After quenching and two washes in PBS, cells were collected and then lysed for 10 min with lysis buffer (5 mM PIPES, 85 mM KCl, 0.5% NP-40) containing protease inhibitor cocktail (Sigma-Aldrich). The pellets were re-suspended in RIPA-100 and sonicated using Bioruptor UCD-200 (Diagenode) with pulses of 30 s for 15 min, resulting in an average size of ∼500 bp for genomic DNA fragments. Samples were pre-cleared and immunoprecipitated overnight with 1 µg of anti-HDAC7 (sc-74563, Santa Cruz Biotechnology), 1.5 µM of anti-H3K27Ac (ab4729; Abcam) and 2 µM of anti-MEF2D antibodies followed by incubation with protein-A beads (GE Healthcare Bio-Sciences) blocked with BSA and salmon sperm DNA (1 µg/µl) at 4°C for 2 h. As control IgGs, we used IgGs purified from normal rabbit serum or anti-FLAG M2 (Sigma-Aldrich) mouse monoclonal antibody. Beads and inputs were treated with proteinase K overnight at 68°C to degrade proteins and reverse cross-linking. Genomic DNA was finally purified with Qiagen QIAquick PCR purification kit and eluted in 100 µl of water.

The graphic representation of the *CDKN1A* locus and its chromatin organization in human mammary epithelial cells was obtained from USCS Genome browser (http://genome.ucsc.edu/). Analysis of the putative binding site for MEF2D was performed using JASPAR (jaspar.genereg.net/).

Gene set enrichment analysis

Analyses were performed using the GSEA software (http://www.broadinstitute.org/gsea/index.jsp). The list of MEF2 target genes was obtained from the Molecular Signature Database (http://www.broadinstitute.org/gsea/msigdb/index.jsp). The dataset for MCF10A cells was obtained from GEO (http://www.ncbi.nlm.nih.gov/geo/) GSE26148 (Simpson et al., 2011). Human normal and breast tumor samples were taken from Curtis et al. (2012) with accession number EGAS00000000083, deposited at the European Genome-Phenome Archive (EGA; http://www.ebi.ac.uk/ega/).

Statistics

Results were expressed as the average±s.d. of at least three independent experiments, except for ChIP experiments where the s.e.m. was calculated. Results were expressed as the mean or median±s.d. of at least three independent experiments, except for ChIP experiments where the s.e.m. was calculated. Statistical analyses were performed using a Student's *t*-test with the level of significance set at $P<0.05$. Data from 3D acinar area measurements were analyzed using the non-parametric Mann–Whitney test (Prism GraphPad Software). Data were from at least three independent experiments. *$P<0.05$; **$P<0.01$; ***$P<0.005$.

Acknowledgements

We thank Oreste Segatto (Regina Elena National Cancer Institute, Rome, Italy) for the pBABE-Puro-ErbB2 plasmid; Finian Martin (University College Dublin, Dublin, Ireland) and Sara Cabodi (Università di Torino, Italy) for cell lines and reagents; and Antonio Beltrami and Daniela Cesselli (Università di Udine, Italy) for the use of the confocal microscope equipped with a laser UV.

Competing interests

The authors declare no competing or financial interests.

Author contributions

A.C. co-designed and performed most of the experiments, aided in the design of the study and reviewed the paper prior to submission. C.B. co-designed most of the experiments was responsible for the conception and design of the study, wrote, edited and submitted the manuscript. E.D.G. performed most of the experiments for the rebuttal and reviewed the paper prior to re-submission. G.V. performed experiments and reviewed the paper prior to submission; C.S. provided reagents, aided in the 3D cell cultures, reviewed the paper prior to submission. A.S. and R.P. performed the bioinformatics analysis. V.C. performed experiments for the rebuttal.

Funding
This work was supported by Research Projects of National Interest (PRIN) [grant number Progetto 2010W4J4RM_002] to C.B. A.C. received the 'Gemma del Cornò' fellowship from Associazione Italiana per la Ricerca sul Cancro (AIRC).

Supplementary information
Supplementary information available online at
http://jcs.biologists.org/lookup/suppl/doi:10.1242/jcs.170357/-/DC1

References

Arnold, M. A., Kim, Y., Czubryt, M. P., Phan, D., McAnally, J., Qi, X., Shelton, J. M., Richardson, J. A., Bassel-Duby, R. and Olson, E. N. (2007). MEF2C transcription factor controls chondrocyte hypertrophy and bone development. *Dev. Cell* **12**, 377-389.

Besson, A., Dowdy, S. F. and Roberts, J. M. (2008). CDK inhibitors: cell cycle regulators and beyond. *Dev. Cell* **14**, 159-169.

Cernotta, N., Clocchiatti, A., Florean, C. and Brancolini, C. (2011). Ubiquitin-dependent degradation of HDAC4, a new regulator of random cell motility. *Mol. Biol. Cell* **22**, 278-289.

Clocchiatti, A., Florean, C. and Brancolini, C. (2011). Class IIa HDACs: from important roles in differentiation to possible implications in tumourigenesis. *J. Cell. Mol. Med.* **15**, 1833-1846.

Clocchiatti, A., Di Giorgio, E., Demarchi, F. and Brancolini, C. (2013a). Beside the MEF2 axis: unconventional functions of HDAC4. *Cell. Signal.* **25**, 269-276.

Clocchiatti, A., Di Giorgio, E., Ingrao, S., Meyer-Almes, F.-J., Tripodo, C. and Brancolini, C. (2013b). Class IIa HDACs repressive activities on MEF2-depedent transcription are associated with poor prognosis of ER(+) breast tumors. *FASEB J.* **27**, 942-954.

Collette, N. M., Genetos, D. C., Economides, A. N., Xie, L., Shahnazari, M., Yao, W., Lane, N. E., Harland, R. M. and Loots, G. G. (2012). Targeted deletion of Sost distal enhancer increases bone formation and bone mass. *Proc. Natl. Acad. Sci. USA* **109**, 14092-14097.

Curtis, C., Shah, S. P., Chin, S.-F., Turashvili, G., Rueda, O. M., Dunning, M. J., Speed, D., Lynch, A. G., Samarajiwa, S., Yuan, Y. et al. (2012). The genomic and transcriptomic architecture of 2,000 breast tumours reveals novel subgroups. *Nature* **486**, 346-352.

Debnath, J., Mills, K. R., Collins, N. L., Reginato, M. J., Muthuswamy, S. K. and Brugge, J. S. (2002). The role of apoptosis in creating and maintaining luminal space within normal and oncogene-expressing mammary acini. *Cell* **111**, 29-40.

Debnath, J., Muthuswamy, S. K. and Brugge, J. S. (2003). Morphogenesis and oncogenesis of MCF10A mammary epithelial acini grown in three-dimensional basement membrane cultures. *Methods* **30**, 256-268.

Debnath, I., Roundy, K. M., Pioli, P. D., Weis, J. J. and Weis, J. H. (2013). Bone marrow-induced Mef2c deficiency delays B-cell development and alters the expression of key B-cell regulatory proteins. *Int. Immunol.* **25**, 99-115.

Demarchi, F., Bertoli, C., Copetti, T., Tanida, I., Brancolini, C., Eskelinen, E.-L. and Schneider, C. (2006). Calpain is required for macroautophagy in mammalian cells. *J. Cell Biol.* **175**, 595-605.

Dequiedt, F., Kasler, H., Fischle, W., Kiermer, V., Weinstein, M., Herndier, B. G. and Verdin, E. (2003). HDAC7, a thymus-specific class II histone deacetylase, regulates Nur77 transcription and TCR-mediated apoptosis. *Immunity* **18**, 687-698.

Di Giorgio, E., Clocchiatti, A., Piccinin, S., Sgorbissa, A., Viviani, G., Peruzzo, P., Romeo, S., Rossi, S., Dei Tos, A. P., Maestro, R. et al. (2013). MEF2 is a converging hub for histone deacetylase 4 and phosphatidylinositol 3-kinase/Akt-induced transformation. *Mol. Cell. Biol.* **33**, 4473-4491.

Di Giorgio, E., Gagliostro, E. and Brancolini, C. (2015a). Selective class IIa HDAC inhibitors: myth or reality. *Cell. Mol. Life Sci.* **72**, 73-86.

Di Giorgio, E., Gagliostro, E., Clocchiatti, A. and Brancolini, C. (2015b). The control operated by the cell cycle machinery on MEF2 stability contributes to the downregulation of CDKN1A and entry into S phase. *Mol. Cell. Biol.* **35**, 1633-1647.

Dressel, U., Bailey, P. J., Wang, S.-C. M., Downes, M., Evans, R. M. and Muscat, G. E. O. (2001). A dynamic role for HDAC7 in MEF2-mediated muscle differentiation. *J. Biol. Chem.* **276**, 17007-17013.

Elston, C. W. and Ellis, I. O. (2002). Pathological prognostic factors in breast cancer. I. The value of histological grade in breast cancer: experience from a large study with long-term follow-up. C. W. Elston & I. O. Ellis. Histopathology 1991; 19; 403-410. *Histopathology* **41**, 151, discussion 152-153.

Ernst, J., Kheradpour, P., Mikkelsen, T. S., Shoresh, N., Ward, L. D., Epstein, C. B., Zhang, X., Wang, L., Issner, R., Coyne, M. et al. (2011). Mapping and analysis of chromatin state dynamics in nine human cell types. *Nature* **473**, 43-49.

Flavell, S. W., Cowan, C. W., Kim, T.-K., Greer, P. L., Lin, Y., Paradis, S., Griffith, E. C., Hu, L. S., Chen, C. and Greenberg, M. E. (2006). Activity-dependent regulation of MEF2 transcription factors suppresses excitatory synapse number. *Science* **311**, 1008-1012.

Frisch, S. M., Schaller, M. and Cieply, B. (2013). Mechanisms that link the oncogenic epithelial–mesenchymal transition to suppression of anoikis. *J. Cell Sci.* **126**, 21-29.

Gjorevski, N. and Nelson, C. M. (2011). Integrated morphodynamic signalling of the mammary gland. *Nat. Rev. Mol. Cell Biol.* **12**, 581-593.

Gregoire, S., Tremblay, A. M., Xiao, L., Yang, Q., Ma, K., Nie, J., Mao, Z., Wu, Z., Giguere, V. and Yang, X.-J. (2006). Control of MEF2 transcriptional activity by coordinated phosphorylation and sumoylation. *J. Biol. Chem.* **281**, 4423-4433.

Haberland, M., Arnold, M. A., McAnally, J., Phan, D., Kim, Y. and Olson, E. N. (2007). Regulation of HDAC9 gene expression by MEF2 establishes a negative-feedback loop in the transcriptional circuitry of muscle differentiation. *Mol. Cell. Biol.* **27**, 518-525.

Ishikawa, F., Miyoshi, H., Nose, K. and Shibanuma, M. (2010). Transcriptional induction of MMP-10 by TGF-beta, mediated by activation of MEF2A and downregulation of class IIa HDACs. *Oncogene* **29**, 909-919.

Kramer, I., Baertschi, S., Halleux, C., Keller, H. and Kneissel, M. (2012). Mef2c deletion in osteocytes results in increased bone mass. *J. Bone Miner. Res.* **27**, 360-373.

Lahm, A., Paolini, C., Pallaoro, M., Nardi, M. C., Jones, P., Neddermann, P., Sambucini, S., Bottomley, M. J., Lo Surdo, P., Carfi, A. et al. (2007). Unraveling the hidden catalytic activity of vertebrate class IIa histone deacetylases. *Proc. Natl. Acad. Sci. USA* **104**, 17335-17340.

Lee, J. L. and Streuli, C. H. (2014). Integrins and epithelial cell polarity. *J. Cell Sci.* **127**, 3217-3225.

Leung, C. T. and Brugge, J. S. (2012). Outgrowth of single oncogene-expressing cells from suppressive epithelial environments. *Nature* **482**, 410-413.

Lewandowski, K. T. and Piwnica-Worms, H. (2014). Phosphorylation of the E3 ubiquitin ligase RNF41 by the kinase Par-1b is required for epithelial cell polarity. *J. Cell Sci.* **127**, 315-327.

Lin, Q., Schwarz, J., Bucana, C. and Olson, E. N. (1997). Control of mouse cardiac morphogenesis and myogenesis by transcription factor MEF2C. *Science* **276**, 1404-1407.

Lin, Q., Lu, J., Yanagisawa, H., Webb, R., Lyons, G. E., Richardson, J. A. and Olson, E. N. (1998). Requirement of the MADS-box transcription factor MEF2C for vascular development. *Development* **125**, 4565-4574.

Liu, R., Wang, L., Chen, G., Katoh, H., Chen, C., Liu, Y. and Zheng, P. (2009). FOXP3 up-regulates p21 expression by site-specific inhibition of histone deacetylase 2/histone deacetylase 4 association to the locus. *Cancer Res.* **69**, 2252-2259.

Liu, N., Nelson, B. R., Bezprozvannaya, S., Shelton, J. M., Richardson, J. A., Bassel-Duby, R. and Olson, E. N. (2014). Requirement of MEF2A, C, and D for skeletal muscle regeneration. *Proc. Natl. Acad. Sci. USA* **111**, 4109-4114.

Lo, A. T., Mori, H., Mott, J. and Bissell, M. J. (2012). Constructing three-dimensional models to study mammary gland branching morphogenesis and functional differentiation. *J. Mammary Gland Biol. Neoplasia* **17**, 103-110.

Lu, J., McKinsey, T. A., Nicol, R. L. and Olson, E. N. (2000). Signal-dependent activation of the MEF2 transcription factor by dissociation from histone deacetylases. *Proc. Natl. Acad. Sci. USA* **97**, 4070-4075.

Ma, L., Liu, J., Liu, L., Duan, G., Wang, Q., Xu, Y., Xia, F., Shan, J., Shen, J., Yang, Z. et al. (2014). Overexpression of the transcription factor MEF2D in hepatocellular carcinoma sustains malignant character by suppressing G2-M transition genes. *Cancer Res.* **74**, 1452-1462.

Mailleux, A. A., Overholtzer, M. and Brugge, J. S. (2008). Lumen formation during mammary epithelial morphogenesis: insights from in vitro and in vivo models. *Cell Cycle* **7**, 57-62.

McKinsey, T. A., Zhang, C.-L., Lu, J. and Olson, E. N. (2000). Signal-dependent nuclear export of a histone deacetylase regulates muscle differentiation. *Nature* **408**, 106-111.

Mills, K. R., Reginato, M., Debnath, J., Queenan, B. and Brugge, J. S. (2004). Tumor necrosis factor-related apoptosis-inducing ligand (TRAIL) is required for induction of autophagy during lumen formation in vitro. *Proc. Natl. Acad. Sci. USA* **101**, 3438-3443.

Mottet, D., Pirotte, S., Lamour, V., Hagedorn, M., Javerzat, S., Bikfalvi, A., Bellahcene, A., Verdin, E. and Castronovo, V. (2009). HDAC4 represses p21 (WAF1/Cip1) expression in human cancer cells through a Sp1-dependent, p53-independent mechanism. *Oncogene* **28**, 243-256.

Muthuswamy, S. K., Li, D., Lelievre, S., Bissell, M. J. and Brugge, J. S. (2001). ErbB2, but not ErbB1, reinitiates proliferation and induces luminal repopulation in epithelial acini. *Nat. Cell Biol.* **3**, 785-792.

Naya, F. J., Black, B. L., Wu, H., Bassel-Duby, R., Richardson, J. A., Hill, J. A. and Olson, E. N. (2002). Mitochondrial deficiency and cardiac sudden death in mice lacking the MEF2A transcription factor. *Nat. Med.* **8**, 1303-1309.

Nebbioso, A., Manzo, F., Miceli, M., Conte, M., Manente, L., Baldi, A., De Luca, A., Rotili, D., Valente, S., Mai, A. et al. (2009). Selective class II HDAC inhibitors impair myogenesis by modulating the stability and activity of HDAC-MEF2 complexes. *EMBO Rep.* **10**, 776-782.

Pallavi, S. K., Ho, D. M., Hicks, C., Miele, L. and Artavanis-Tsakonas, S. (2012). Notch and Mef2 synergize to promote proliferation and metastasis through JNK signal activation in Drosophila. *EMBO J.* **31**, 2895-2907.

Paroni, G., Henderson, C., Schneider, C. and Brancolini, C. (2001). Caspase-2-induced apoptosis is dependent on caspase-9, but its processing during UV- or tumor necrosis factor-dependent cell death requires caspase-3. *J. Biol. Chem.* **276**, 21907-21915.

Paroni, G., Mizzau, M., Henderson, C., Del Sal, G., Schneider, C. and Brancolini, C. (2004). Caspase-dependent regulation of histone deacetylase 4 nuclear-cytoplasmic shuttling promotes apoptosis. *Mol. Biol. Cell* **15**, 2804-2818.

Paroni, G., Cernotta, N., Dello Russo, C., Gallinari, P., Pallaoro, M., Foti, C., Talamo, F., Orsatti, L., Steinkuhler, C. and Brancolini, C. (2008). PP2A regulates HDAC4 nuclear import. *Mol. Biol. Cell* **19**, 655-667.

Potthoff, M. J. and Olson, E. N. (2007). MEF2: a central regulator of diverse developmental programs. *Development* **134**, 4131-4140.

Potthoff, M. J., Wu, H., Arnold, M. A., Shelton, J. M., Backs, J., McAnally, J., Richardson, J. A., Bassel-Duby, R. and Olson, E. N. (2007). Histone deacetylase degradation and MEF2 activation promote the formation of slow-twitch myofibers. *J. Clin. Invest.* **117**, 2459-2467.

Reginato, M. J., Mills, K. R., Paulus, J. K., Lynch, D. K., Sgroi, D. C., Debnath, J., Muthuswamy, S. K. and Brugge, J. S. (2003). Integrins and EGFR coordinately regulate the pro-apoptotic protein Bim to prevent anoikis. *Nat. Cell Biol.* **5**, 733-740.

Rosenbloom, K. R., Sloan, C. A., Malladi, V. S., Dreszer, T. R., Learned, K., Kirkup, V. M., Wong, M. C., Maddren, M., Fang, R., Heitner, S. G. et al. (2013). ENCODE data in the UCSC Genome Browser: year 5 update. *Nucleic Acids Res.* **41**, D56-D63.

Saramaki, A., Diermeier, S., Kellner, R., Laitinen, H., Vaisanen, S. and Carlberg, C. (2009). Cyclical chromatin looping and transcription factor association on the regulatory regions of the p21 (CDKN1A) gene in response to 1alpha,25-dihydroxyvitamin D3. *J. Biol. Chem.* **284**, 8073-8082.

Schuetz, C. S., Bonin, M., Clare, S. E., Nieselt, K., Sotlar, K., Walter, M., Fehm, T., Solomayer, E., Riess, O., Wallwiener, D. et al. (2006). Progression-specific genes identified by expression profiling of matched ductal carcinomas in situ and invasive breast tumors, combining laser capture microdissection and oligonucleotide microarray analysis. *Cancer Res.* **66**, 5278-5286.

Sebastian, S., Faralli, H., Yao, Z., Rakopoulos, P., Palii, C., Cao, Y., Singh, K., Liu, Q.-C., Chu, A., Aziz, A. et al. (2013). Tissue-specific splicing of a ubiquitously expressed transcription factor is essential for muscle differentiation. *Genes Dev.* **27**, 1247-1259.

Shaw, K. R. M., Wrobel, C. N. and Brugge, J. S. (2004). Use of three-dimensional basement membrane cultures to model oncogene-induced changes in mammary epithelial morphogenesis. *J. Mammary Gland Biol. Neoplasia* **9**, 297-310.

Simpson, D. R., Yu, M., Zheng, S., Zhao, Z., Muthuswamy, S. K. and Tansey, W. P. (2011). Epithelial cell organization suppresses Myc function by attenuating Myc expression. *Cancer Res.* **71**, 3822-3830.

Streuli, C. H., Bailey, N. and Bissell, M. J. (1991). Control of mammary epithelial differentiation: basement membrane induces tissue-specific gene expression in the absence of cell-cell interaction and morphological polarity. *J. Cell Biol.* **115**, 1383-1395.

Wang, P., Valentijn, A. J., Gilmore, A. P. and Streuli, C. H. (2003). Early events in the anoikis program occur in the absence of caspase activation. *J. Biol. Chem.* **278**, 19917-19925.

Weaver, V. M., Lelièvre, S., Lakins, J. N., Chrenek, M. A., Jones, J. C. R., Giancotti, F., Werb, Z. and Bissell, M. J. (2002). beta4 integrin-dependent formation of polarized three-dimensional architecture confers resistance to apoptosis in normal and malignant mammary epithelium. *Cancer Cell* **2**, 205-216.

Whyte, J., Thornton, L., McNally, S., McCarthy, S., Lanigan, F., Gallagher, W. M., Stein, T. and Martin, F. (2010). PKCzeta regulates cell polarisation and proliferation restriction during mammary acinus formation. *J. Cell Sci.* **123**, 3316-3328.

Wilson, A. J., Byun, D.-S., Nasser, S., Murray, L. B., Ayyanar, K., Arango, D., Figueroa, M., Melnick, A., Kao, G. D., Augenlicht, L. H. et al. (2008). HDAC4 promotes growth of colon cancer cells via repression of p21. *Mol. Biol. Cell* **19**, 4062-4075.

Xia, W., Chen, J.-S., Zhou, X., Sun, P.-R., Lee, D.-F., Liao, Y., Zhou, B. P. and Hung, M.-C. (2004). Phosphorylation/cytoplasmic localization of p21Cip1/WAF1 is associated with HER2/neu overexpression and provides a novel combination predictor for poor prognosis in breast cancer patients. *Clin. Cancer Res.* **10**, 3815-3824.

Yang, X.-J. and Seto, E. (2008). The Rpd3/Hda1 family of lysine deacetylases: from bacteria and yeast to mice and men. *Nat. Rev. Mol. Cell Biol.* **9**, 206-218.

Yu, M., Lin, G., Arshadi, N., Kalatskaya, I., Xue, B., Haider, S., Nguyen, F., Boutros, P. C., Elson, A., Muthuswamy, L. B. et al. (2012). Expression profiling during mammary epithelial cell three-dimensional morphogenesis identifies PTPRO as a novel regulator of morphogenesis and ErbB2-mediated transformation. *Mol. Cell. Biol.* **32**, 3913-3924.